Local Approach to Quantum Entanglement

Ho-Chih Lin

A thesis submitted in partial fulfillment

of the requirements for the degree of

Doctor of Philosophy

of the

University College London.

Department of Physics and Astronomy

University College London

August 2008

Declaration

The studies presented in this thesis were performed by the author whilst a member of the London Centre for Nanotechnology, Department of Physics and Astronomy, University College London, London, United Kingdom.

I, Ho-Chih Lin, confirm that the work presented in this thesis is my own. Where information has been derived from other sources, I confirm that this has been indicated in the thesis.

To my parents

Abstract

Quantum entanglement is the key property that makes quantum information theory different from its classical counterpart and is also a valuable physical resource with massive potential for technological applications. However, our understanding of entanglement is still far from complete despite intense research activities. Like other physical resources, the first step towards exploiting them fully is to know how to quantify. There are many reasons to focus on the entanglement of continuous-variable states since the underlying degrees of freedom of physical systems carrying quantum information are frequently continuous, rather than discrete. Much of the effort has been concentrated on Gaussian states, because these are common as the ground or thermal states of optical modes. Within this framework, many interesting topics have been studied and some significant progress made. Nevertheless, non-Gaussian states are also extremely important; this is especially so in condensed-phase systems, where harmonic behaviour in any degree of freedom is likely to be only an approximation. So far, there is little knowledge about the quantification of entanglement in non-Gaussian states.

This thesis aims to contribute to the active field of research in quantum entanglement by introducing a new approach to the analysis of entanglement, especially in continuous-variable states, and shows that it leads to the first systematic quantification of the (local) entanglement in arbitrary bipartite non-Gaussian states. By applying this local approach, many new insights can be gained. Notably, local entanglements of systems with smooth wavefunctions are fully characterised by the derived simple expressions, provided the wavefunction is known. The local (logarithmic) negativity of any two-mode mixed states can be directly computed from the closed-form formulae given. For multi-mode mixed states, this approach provides a scheme that permits much simpler numerical computation for quantifying entanglement than is generally possible from directly computing the full entanglement of the system.

Acknowledgements

I would like to begin by expressing my gratitude to my supervisor, Prof. Andrew Fisher. I truly enjoy his wonderful guidance and have benefited greatly from the breadth and depth of his knowledge. With his enthusiasm, inspiration, and excellent efforts to explain things clearly and simply, he made this research such a stimulating experience for me. Without his encouragement, advice and many great ideas, this thesis would never have been completed.

I wish to thank my entire extended family for providing a loving environment for me. My grandparents, some uncles, some aunts, my brother and sister were particularly supportive.

I would like to give my special thanks to my wife whose love, patience and considerate support enabled me to complete this work.

Lastly, and most importantly, I wish to thank my parents. They provided me with all their resources to let me overcome my past failures and to fulfil my selfish demands so I can get this far. To them I dedicate this thesis.

Contents

List of Figures

List of Tables

List of Abbreviations

EPR	Einstein-Podolsky-Rosen
LOCC	local operations and classical communication
POVM	positive operator-valued measure
PPT	positive partial transpose
WKB	Wentzel-Kramers-Brillouin-Jeffreys

List of Symbols

Some symbols may have multiple uses but the most important meaning will be listed here for easy reference. The page number of a symbol's first appearance in displayed on the right-hand side.

A	Alice	28
$\hat{A}$	$\hat{A}$ and $\hat{B}$ are arbitrary one-particle operators	115
$\mathcal{A}$	the region where Alice localise her subsystem inside	46
A_i	an operator acting on Alice's subsystem	32
a	the width of region $\mathcal{A}$	60
α	the coupling strength between harmonic oscillators	59
B	Bob	28
$\mathcal{B}$	the region where Bob localise his subsystem inside	49
B_i	an operator acting on Bob's subsystem	32
b	the width of region $\mathcal{B}$	63
$\mathcal{C}$	the concurrence	38
c	the concurrence density	79
C_1	the two-mode local negativity is zero if $C_1 = 0$	80
C_2	the two-mode local negativity is C_2 if $C_1 < 0$ and $C_2 < 0$	80
$\chi(\mathbf{R})$	the centre-of-mass wavefunction with a distance vector $\mathbf{R}$	104
$\chi(\xi)$	the characteristic function for the $2N$-dimensional vector ξ	41
D_1	D_1 and D_2 are coefficients of the a^2 and b^2 terms respectively in the two-mode local negativity	80
d	the displacement vector	42
$\mathcal{E}$	quantum entanglement; an entanglement measure	36
$\mathbb{E}$	a quantum operation	30
$\mathcal{E}_C$	the entanglement cost	37
$\mathcal{E}_D$	the entanglement in the discarding ensemble	47

$\bar{\mathcal{E}}_D$	the average of the entanglements in the discarding ensemble over all the partitions	50
$\mathcal{E}_\mathcal{D}$	the entanglement of distillation	38
ϵ	$S_v = h(\epsilon)$ for any ρ^A that (effectively) only has two non-zero eigenvalues	62
$\mathcal{E}_F$	the entanglement of formation	37
$\mathcal{E}_F^\infty$	the regularised entanglement of formation	37
E_i	a Kraus operator	30
$\mathcal{E}_\mathcal{N}$	the logarithmic negativity	40
$\mathcal{E}_{ND}$	the entanglement in the nondiscarding ensemble	47
F	degree of mixedness of a Werner state	34
γ	the covariance matrix	42
$h(\epsilon)$	$h(\epsilon) \equiv -\epsilon \log_2(\epsilon) - (1-\epsilon)\log_2(1-\epsilon)$	38
$H(X)$	the Shannon entropy of a random variable X	25
$H(X \parallel Y)$	the relative entropy of two random variables X and Y	25
$H(X,Y)$	the joint entropy of two random variables X and Y	25
$H(X \mid Y)$	the conditional entropy of two random variables X and Y	25
$\mathcal{H}$	the Hilbert space	28
I	information	24
$I(X:Y)$	the mutual information of two random variables X and Y	26
K	a Hooke's-law spring constant	59
$\mathbf{K}$	the phase matrix	58
$\mathbf{L}$	the intensity matrix	58
$\mathbf{M}$	the coherence matrix	58
m	mass	58
M_i	a measurement operator	27
M_s	total magnetic spin quantum number	51
$\mathcal{N}$	the negativity	39
μ	reduced mass	104
$\mathcal{N}_{\max}$	the maximised negativity	81
n	the negativity density	82
N	a number	42
ω	the natural frequency of uncoupled oscillators	58
$\mathbb{1}$	the identity operator	27
P_i	a projective measurement operator	26

P	the momentum variable	41
p_i	a probability	27
$\|\Phi^{\pm}\rangle$	Bell states	34
$\varphi(\mathbf{r})$	the relative-motion wavefunction with a distance vector $\mathbf{r}$	104
$\|\Psi^{\pm}\rangle$	Bell states	34
$\mathbf{q}$	a coordinate vector with components $\{q_i\}$	46
R	the canonical coordinate operators	41
ρ	a density operator of a mixture of states	27
ϱ	for a symmetrised density operator ρ, ϱ is its auxiliary asymmetric density operator	115
ρ_{ijkl}	a derivative of ρ with respect to Alice's and Bob's coordinates	79
ρ^A	the (Alice's) reduced density operator	28
ρ^{AB}	a composite quantum state shared by Alice and Bob	28
ρ_D	a density operator in the discarding ensemble	46
ρ_{ND}	a density operator in the nondiscarding ensemble	47
$\rho_{\mathcal{P}}$	a density operator in the discarding ensemble after precise measurements	48
ρ^{T_B}	the partial transposition of the state ρ with respect to Bob's subsystem	39
$\tilde{\rho}$	the spin-flipped state	38
ρ_W	a Werner state	34
S_v	the von Neumann entropy; the entropy of entanglement	31
σ	the Gaussian characteristic length	59
σ_x	the Pauli X-matrix	35
σ_y	the Pauli Y-matrix	35
σ_z	the Pauli Z-matrix	35
σ	a symplectic matrix	41
τ	the tangle	78
Tr_B	the partial trace over Bob's subsystem	28
U	an unitary operation	26
$\mathbf{V}$	the matrix contains the coupling coefficients among the positions in a hamonic system.	58
$\mathcal{W}$	the Wigner function	41
W	the displacement operator; the Weyl operator	41
X	the position variable	41
v_1	v_1 and v_2 are coefficients of the one-particle reduced density matrix of a	

	two-oscillator harmonic system	59
w	a coefficient that determines the ground-state entanglement of a two-oscillator harmonic system	60

Chapter 1

Introduction

Despite the recognition of quantum entanglement as the most profound feature of quantum mechanics in the early 20th century, it is only in the last dozen years that scientists started to recognise the possibility of exploitation of quantum entanglement for practical purposes [BBPS96, BDSW96, BBP$^+$96]. The various proposals of technological applications, such as quantum computing [Deu85], quantum cryptography [Eke91] and quantum teleportation [BBC$^+$93], have fuelled the rapidly growing interest of quantum entanglement as a topic of research. Partial but significant progress has been made, amid the intense research activities, in our knowledge of this intriguing and immensely deep phenomena of Nature but a complete theory of quantum entanglement is still years away, and far more questions and puzzles still wait to be answered.

Entanglement is the capacity of quantum states to exhibit correlations that cannot be accounted for classically. A pure state of a pair of quantum systems is called entangled if it is unfactorizable (inseparable) into a product of states of its subsystems. A mixed state is entangled if it cannot be represented as a mixture of factorizable (separable) pure states. For practical purposes, it is not enough to only know if quantum states are entangled, one of the main tasks of quantum information theory [NC00, Ved06] is therefore to quantify the amount of entanglement that quantum states possess.

For pure bipartite states, the extent of entanglement is simply given by the von Neumann entropy of the reduced state [DHR02, Vid00, PR97]. As for mixed states, the entanglement become much more complicated and is still not completely understood. Much work still needs to be done in order to characterise and quantify entanglement of bipartite systems, not to mention the extention of these investigations to multipartite systems, where even less is known (for example, necessary and sufficient criteria for separability are still lacking).

Apart from the key role that quantum entanglement plays in the advancement of quantum technology, the research of entanglement merits particular attention for the sake of purely

scientific curiosity. Most interacting systems exhibit the natural occurrence of entanglement, and their ground states are generally entangled [Nie98, Woo02a, Woo02b, OW01, ON02, OAFF02, BR01]. Although no one has yet proposed a universal and easy-to-compute entanglement measure which can quantify entanglement of any quantum system in any context, by using suitable entanglement measures, the study of entanglement properties of a number of physical models, including spin chains, coupled fermions and harmonic oscillators [ON02, OAFF02, VLRK03, LRV04, JK04, ZW02, MD, AEPW02, PHE04, Ved03] has not only uncovered many interesting aspects of entanglement in spatially extended many-body systems but also often lead us to a much deeper insight of the fundamental properties and behaviour of these systems. Therefore, studying quantum entanglement is not only interesting in its own right but also important for its usefulness to other fields of physics.

1.1 Motivation

Quantum information can be carried by either a discrete (finite-dimensional) system like a two-level atom or an electron spin, or by a continuous-variable (infinite-dimensional) systems such as harmonic oscillators or light modes. The underlying degrees of freedom of physical systems carrying quantum information are often continuous, rather than discrete, this justifies the focus on continuous-variable states. The research of quantum information theory and applications with continuous variables is a flourishing field that brings us new and exciting perspective [BP03, BvL05, CLP07].

The special class of Gaussian states (i.e., states whose Wigner function is a Gaussian; examples of Gaussian states include coherent, thermal and squeezed states of a optical mode) plays a very important role, especially in quantum optics. These Gaussian states can easily be produced and manipulated experimentally. Moreover, without the need of a description that is complicated by the overly complex technicalities of infinite-dimensional Hilbert spaces, their useful properties (for example, entanglement) can be completely determined by the (relatively small) finite-dimensional covariance matrix of two-point correlations between the canonically conjugated quadrature operators (position and momentum) [EP03]. Within this framework, many interesting topics have been studied; for example, entanglement distillation for Gaussian states [DGCZ00, ESP02a, Fiu02, GC02], multipartite entangled Gaussian states [vLB00, GKLC01, ASI04, ASI06] and entanglement measures, such as entanglement of formation [GWK$^+$03, WGK$^+$04, Shi04] and logarithmic negativity [AEPW02, APE03, VW02].

However, many physical realisations of quantum information processing, for example, electron charge qubits and superconducting charge (or flux) qubits, are based on continuous-

variable states in condensed matter systems, where states are generally non-Gaussian. Much less is known about the entanglement of these non-Gaussian states in view of the fact that the lack of knowledge about how to quantify it has proved to be a major obstacle.

1.2 Overview

I therefore present a new approach to the analysis of quantum entanglement of general quantum states, especially continuous-variable non-Gaussian states. The focus is on entanglement localised near particular regions in configuration space (the local entanglement), which we analyse via a thought experiment in which the entangled state is first measured to localise it. This corresponds to a particular type of projective filtering, used to identify the distribution of entanglement in a state which has a pre-existing bipartite structure. I will demonstrate that this local approach leads to, among other results, variable-resolution mapping of entanglement distributions and to our knowledge, the first efficient method to quantify aspects of quantum entanglement in arbitrary bipartite continuous-variable (non-Gaussian) states.

The thesis is organised as follows: the theoretical background is briefly sketched out in Chapter 2 and Chapter 3. A brief but just sufficient introduction of the fundamentals of the quantum information theory is presented in Chapter 2, and then in Chapter 3, the essential knowledge of quantum entanglement that forms the basis of the research is provided. A mathematical formalism of the local approach to quantum entanglement is laid out in detail in Chapter 4 while examples of its application to the analysis of entanglement in discrete-variable systems are also given. Next, the attention is fully turned to continuous-variable states. First, the question "how is quantum entanglement distributed in configuration-space" is addressed in Chapter 5, and the results are then compared with the classical correlations [LF07a]. In the limit of the size of the preliminary projective measurement being very small, surprisingly many interesting results can be derived, and the rest of the thesis will be made up of discussions of these . Chapter 6 is concerned with arbitrary smooth two-mode continuous-variable states, and it is shown how by using our local approach, the (local) entanglement can be analytically quantified from simple expressions, whether the state is pure or mixed [LF07b]. The results are then generalised to arbitrary smooth bipartite multimode pure states in Chapter 7, and again the (local) entanglement can be computed directly and explicitly via simple expressions, without the time-consuming numerical evaluation of the full entanglement generally inevitable for high-dimensional continuous-variable states [LF08]. Many particles in interacting systems are indistinguishable; the problem of indistinguishability has so far been ignored in the thesis but will now be worked out in Chapter 8. Finally, a brief summary of significant results of each

chapter is given in Chapter 9, and conclusions are drawn.

Chapter 2

Fundamentals of Quantum Information

2.1 Classical Information

The rapid development of computer science in the twentieth century has provided us an entirely new way of thinking about physics that physical systems are simply computers. A physical system evolves from a initial state to some final state just like a computer, after given an input, performs computations to give out an output. In other words, the evolution of a physical system is equivalent to information processing of a computer and that the values of the physical attributes of the system can be thought of as information held by the system at a given moment in time. Consequently, the laws of physics completely govern the laws of information processing.

As its name suggests, classical information theory assumes that information evolves according to the laws of classical physics. The cornerstone of classical information theory is the formulation of the Shannon entropy.

2.1.1 Shannon entropy

Shannon developed his theory of information in 1948, which answered an important question of information processing: How can information be quantified?

He proposed that any measure of information I should satisfy the following three requirements:

1. The amount of information I in an event i must depend only on its probability p.

2. I is a continuous function of the probability.

3. I is additive.

These lead to a unique measure of information, called the Shannon entropy. For a random variable X that has a probability distribution, $p_1, \ldots, p_n$, of the different possible values the

random variable takes, the *Shannon entropy* is defined as

$$H(X) \equiv -\sum_i p_i \log_2(p_i). \tag{2.1}$$

The Shannon entropy of X can be viewed as quantifying either the amount of uncertainty *before* we learn the value of X or how much information gained *after* we learn the value of X.

The importance of the Shannon entropy to classical information theory can not be overstated but the discussion of this will be beyond the scope of this thesis. However, we will introduce here some relevant measures of information that can be defined through the Shannon entropy.

2.1.1.1 Relative entropy

The *relative entropy* measures the difference in information between two random variables X and Y, and is defined as follows:

$$\begin{aligned} H(X \parallel Y) &\equiv -\sum_i p_i \log_2(q_i) - H(X) && (2.2)\\ &= \sum_i p_i \log_2\left(\frac{p_i}{q_i}\right), && (2.3) \end{aligned}$$

where p_i and q_i are probability function for random variables X and Y respectively. The relative entropy is always positive, and when $X = Y$, the relative entropy between X and Y vanishes.

The Shannon entropy is a special case of the relative entropy since the Shannon entropy of a random variable is the entropy relative to a definitely known state, i.e. $q_i = 1$ so that $H(X) = H(X \parallel Y)$.

2.1.1.2 Joint entropy

The *joint entropy* measures the combined information in two random variables X and Y, and is defined as the entropy of the joint distribution of X and Y:

$$H(X,Y) \equiv -\sum_{i,j} p_{i,j} \log_2(p_{i,j}), \tag{2.4}$$

where the events of X and Y are labeled by i and j respectively. The additive property of the Shannon entropy gives that

$$H(X,Y) = H(X) + H(Y) \tag{2.5}$$

only if X and Y are independent events.

2.1.1.3 Conditional entropy

The *conditional entropy* measures the information contained in one random variable given that the outcome of another random variable is known, and is defined as

$$H(X \mid Y) \equiv -\sum_{i,j} p_{i,j} \log_2\left(\frac{p_{i,j}}{p_j}\right). \tag{2.6}$$

The conditional and joint entropies are related by

$$H(X,Y) = H(X) + H(Y \mid X). \tag{2.7}$$

2.1.1.4 Mutual information

The *mutual information* between two random variables X and Y is the differences between the amount of information required to express X and Y separately and as a joint distribution:

$$I(X:Y) = H(X) + H(Y) - H(X,Y). \tag{2.8}$$

If X and Y are independent, the mutual information between them is zero. On the other hand, if X and Y are completely correlated, then the mutual information between them is the same as the information contained in X (or Y).

2.2 Quantum Information

2.2.1 Quantum mechanics

The theory of quantum mechanics developed in the early 20th century gives us a complete new understanding of Nature (in contrast to the classical Newtonian physics), and provides the foundation for the latest developments in quantum information and computation.

2.2.1.1 The postulates of quantum mechanics

There are four postulates of quantum mechanics, which are all we need in order to describe any quantum system, expressed here in terms of pure states for simplicity:

1. *States* of physical systems are represented by vectors in Hilbert spaces.

2. *Observables* are represented by Hermitian operators, which have real eigenvalues.

3. If $|\phi_1\rangle, \ldots, |\phi_n\rangle$ are orthogonal states, then a *measurement* of a quantum state $|\psi\rangle$ can be made by use of a projective measurement operator $P_i = |\phi_i\rangle\langle\phi_i|$ so that the state $|\psi\rangle$ collapses into the state $|\phi_i\rangle$ with a probability $|\langle\phi_i \mid \psi\rangle|^2$.

4. When no measurement is made, a *closed* quantum system evolves according to a *unitary transformation* so any change can be expressed by the action of an unitary operation. A operation U is unitary if it can be written as

$$U = \sum_i |\psi_i\rangle\langle\phi_i|, \tag{2.9}$$

where both ψ_i and ϕ_i form orthonormal bases.

2.2.1.2 Quantum measurements

Quantum measurement are described by a set of measurement operators M_i, that act on the state space of the measured system and satisfy the completeness relation,

$$\sum_i M_i^\dagger M_i = \mathbb{1}, \tag{2.10}$$

where $\mathbb{1}$ is the identity operator. The probability of the outcome "i" occurs after measuring the initial state of the quantum system $|\psi\rangle$ is given by

$$p_i = \langle\psi|M_i^\dagger M_i|\psi\rangle, \tag{2.11}$$

and the state of the system after the measurement is

$$\frac{M_i|\psi\rangle}{\sqrt{\langle\psi|M_i^\dagger M_i|\psi\rangle}}. \tag{2.12}$$

The projective measurements described in Postulate 3 are a special class of measurements. Projective operators P_i not only satisfy the completeness relation but also are orthogonal projectors so that they are Hermitian and $P_i P_{i'} = \delta_{ii'} P_i$.

Measurements are irreversible processes because the quantum system "loses" the information that we gained from the measurements whereas a unitary evolution of a quantum system is fully reversible, which means that the dynamics of an isolated system is reversible in the same way as classical Newtonian dynamics, since no information about the system is gained or lost.

2.2.1.3 The density operator

The *density operator* ρ of a mixture of states, in which a state ϕ_i, not necessarily orthonormal with respect to the other ϕ_i's, occurs with probability p_i, is expressed as

$$\rho = \sum_i p_i|\phi_i\rangle\langle\phi_i|, \tag{2.13}$$

and we call ρ a *mixed* state. When a state $|\psi\rangle$ occurs with certainty, i.e. $\rho = |\psi\rangle\langle\psi|$, it is called a *pure* state.

There are infinitely many equivalent ways of writing down the same density operator, and given any mixture of states, we can always diagonalise the density operator of the mixture as

$$\rho = \sum_i p_i|i\rangle\langle i|, \tag{2.14}$$

where the p_i's are positive eigenvalues and the $|i\rangle$'s are orthonormal.

2.2.1.4 The trace operation

The trace of a density operator ρ is

$$\mathrm{Tr}(\rho) = \sum_n \langle n|\rho|n\rangle \tag{2.15}$$

and is independent of the choice of the basis set $|n\rangle$. The trace of a pure state $|\psi\rangle$ is always 1 if the state is normalised. It follows the trace of a density operator $\rho = \sum_i p_i|i\rangle\langle i|$ is also always 1, provided all the states and corresponding probabilities are normalised; this simply arises from the fact that all the probabilities for various outcomes should add up to 1.

The trace operator can also be used to distinguish between pure and mixed states. Because the square of the density matrix ρ is

$$\rho^2 = \sum_i p_i|i\rangle\langle i| \sum_j p_j|j\rangle\langle j| \tag{2.16}$$

$$= \sum_i p_i^2|i\rangle\langle i|, \tag{2.17}$$

where $|i\rangle$ and $|j\rangle$ are orthonormal, the trace of the density operator squared is given by

$$\mathrm{Tr}(\rho^2) = \sum_i p_i^2. \tag{2.18}$$

$\sum_i p_i^2 = 1$ if and only if ρ is a pure state. For mixed states, $\mathrm{Tr}(\rho^2) < 1$.

2.2.1.5 The reduced density operator

Suppose Alice and Bob share a composite quantum state ρ^{AB} with the joint orthonormal basis $|i^A\rangle|j^B\rangle$ in the Hilbert space $\mathcal{H}_A \otimes \mathcal{H}_B$, where A and B indicate the subsystems belonging to Alice and Bob respectively, Alice's *reduced density operator* (also called the *reduced density matrix*) is defined by

$$\rho^A \equiv \mathrm{Tr}_B(\rho^{AB}), \tag{2.19}$$

where Tr_B represents the *partial trace* over Bob's subsystem and is defined as

$$\mathrm{Tr}_B(\rho^{AB}) \equiv \sum_j \langle j^B|\rho^{AB}|j^B\rangle. \tag{2.20}$$

The reduced density operator describes a subsystem of a composite quantum system, and its importance draws from the fact that many important properties of a quantum system are completely determined by the eigenvalues of the reduced density operator of the system. Additionally, it also completely determines the outcome of any measurement performed by Alice only. These points will become clear in the later analysis of quantum entanglement.

2.2.1.6 The Schmidt decomposition

A pure bipartite quantum state ψ^{AB} can be written as

$$\psi^{AB} = \sum_{i,j} \alpha_{ij} |i^A\rangle |j^B\rangle, \tag{2.21}$$

where $|i^A\rangle$ and $|j^B\rangle$ are any fixed orthonormal bases for systems A and B respectively, for some complex number α_{ij}. There exist orthonormal states $|\psi_i^A\rangle$ for system A and $|\psi_j^B\rangle$ for system B such that we can find the *Schmidt decomposition* of ψ^{AB} written as

$$\psi^{AB} = \sum_i \lambda_i |\psi_i^A\rangle |\psi_i^B\rangle, \tag{2.22}$$

where λ_i are non-negative real numbers satisfying $\sum_i \lambda_i^2 = 1$ known as the *Schmidt coefficients*. Note that the sum now goes over only the i's rather than both the i's and j's. There is no analogue of Schmidt decomposition for mixed states, however.

By the Schmidt decomposition, we can immediately trace out each subsystem separately to obtain reduced density operators ρ^A and ρ^B:

$$\rho^A = \sum_i \lambda_i^2 |\psi_i^A\rangle\langle\psi_i^A| \tag{2.23}$$

and

$$\rho^B = \sum_i \lambda_i^2 |\psi_i^B\rangle\langle\psi_i^B|. \tag{2.24}$$

The eigenvalues of ρ^A and ρ^B are identical so many of the properties of the quantum state ψ^{AB} can be determined by either reduced density operator.

2.2.1.7 Quantum entanglement

The most intriguing phenomenon arising from quantum mechanics is quantum entanglement, which is the central theme of this thesis and will be described in detail later. In essence, entanglement is the quantum correlations between two or more quantum systems that can not be explained by classical physics, and is the fundamental resource that makes quantum computation and communication differ from their classical counterparts.

2.2.2 Quantum operations

The *quantum operation formalism* is the key tool for the description of the dynamics of *open* quantum systems [NC00]. A system, which interacts with some other system –its *environment* – whose dynamics we wish to average over, is an open system. Real systems are never perfectly closed, and the mathematical formalism of quantum operations can be used to describe a wide range of physical scenarios, namely closed systems that are opened suddenly and subject to

measurements, nearly closed systems that are weakly coupled to their environments, and systems that are strongly coupled to the environment. Its usefulness in quantum information theory draws from its suitability to describe the transformations between an initial state ρ and a final state ρ' without the complexity arising from explicit continuous-time consideration:

$$\rho' = \mathbb{E}(\rho), \tag{2.25}$$

the map $\mathbb{E}$ is a *quantum operation* that describes the dynamical change to a state after some physical process.

A map from an "input" set of density operators to an "output" set of density operators and satisfying the following three properties is defined to be a quantum operation $\mathbb{E}$:

1. $\mathbb{E}$ should preserve the normalisation of the initial state ρ:

$$\mathrm{Tr}[\mathbb{E}(\rho)] = 1 \quad \text{if} \quad \mathrm{Tr}[\rho] = 1. \tag{2.26}$$

2. $\mathbb{E}$ should be *linear*:

$$\mathbb{E}(\sum_i p_i \rho_i) = \sum_i p_i \mathbb{E}(\rho_i). \tag{2.27}$$

3. $\mathbb{E}$ is a *completely positive* map. If $\mathbb{E}$ only acts on the system **S** and we introduce an extra system (the environment) **E**, with ρ being any possible joint density matrix of **E** and **S**, then the result of the composite operation $(\mathcal{I} \otimes \mathbb{E})\rho$ is another positive operator, where $\mathcal{I}$ denotes the identity map on the environment **E**.

A quantum operation $\mathbb{E}$ is written as

$$\mathbb{E}(\rho) = \sum_i E_i \rho E_i^\dagger, \tag{2.28}$$

for some set of operators $\{E_i\}$ on Hilbert space, and $\sum_i E_i^\dagger E_i \leq \mathbb{1}$. This is known as the Kraus representation or operator-sum representation of the quantum operation, and the operators $\{E_i\}$ are known as the Kraus operators.

Unitary transformation, $\mathbb{E}(\rho) \equiv U\rho U^\dagger$, and measurements, $\mathbb{E}_i(\rho) \equiv M_i \rho M_i^\dagger$, are two examples of quantum operations. The state of the quantum system immediately after the measurement is

$$\frac{\mathbb{E}_i(\rho)}{\mathrm{Tr}[\mathbb{E}_i(\rho)]} \tag{2.29}$$

with the probability that the outcome i occurs being $p_i = \mathrm{Tr}[\mathbb{E}_i(\rho)]$. The dynamics of a closed quantum system are described by a unitary transformation. However, unlike unitary evolutions, which are reversible, quantum operations are, in general, irreversible.

2.2.3 Qubits

The basic unit of classical information is called a *bit*. In quantum information theory, the corresponding concept is termed a *qubit* (short for *quantum bit*). Whereas a classical bit only has either 0 or 1 as its state, a qubit is a two-dimensional quantum system, whose state $|\psi\rangle$ can be written as superpositions of *computational basis states*, $|0\rangle$ and $|1\rangle$ (arbitrary orthonormal states):

$$|\psi\rangle = \alpha|0\rangle + \beta|1\rangle, \tag{2.30}$$

where α and β are complex numbers such that $|\alpha|^2 + |\beta|^2 = 1$.

In classical information theory, bits can be perfectly copied. However, the *quantum no-cloning theorem* [WZ82] states that cloning of quantum bits is impossible and implies that the knowledge we can learn about an unknown quantum state is limited.

2.2.4 Von Neumann entropy

Just as classical information can be quantified by using the Shannon entropy, there is a unique measure of quantum information, the von Neumann entropy S_v. The von Neumann entropy of a density operator ρ written in diagonal form, equation 2.14, is defined as

$$S_v(\rho) \equiv -\mathrm{Tr}(\rho \log_2 \rho) \tag{2.31}$$

$$= -\sum_i p_i \log_2(p_i). \tag{2.32}$$

The von Neumann entropy is a continuous function of the probabilities p_i of outcomes of measurements made on a quantum system and is additive so that

$$S_v(\rho_1 \otimes \rho_2) = S_v(\rho_1) + S_v(\rho_2) \tag{2.33}$$

for two uncorrelated systems ρ_1 and ρ_2.

Chapter 3

Introduction to Quantum Entanglement

Quantum information theory opens up the possibility of utilising quantum entanglement as a physical resource for applications which are not possible classically. The study of quantum entanglement is therefore one of the most important and interesting topics in the field of quantum information processing.

3.1 What is an Entangled State

3.1.1 Local operations and classical communication

The ability to perform *local operations and classical communication* (LOCC) is essential for many quantum information processing protocols. LOCC means that if Alice and Bob share a quantum system, they can perform quantum operations only on their own subsystems and communicate only classically.

The concept of LOCC operations also plays an important part in the study of quantum entanglement. It can be used to distinguish *quantum correlations* that can occur in many-party quantum states from *classical correlations*. Classical correlations can be defined as those that can be generated by LOCC operations. LOCC operations alone, however, are not enough to simulate quantum effects in a quantum system. Therefore, these quantum correlations that can not be created by LOCC operations alone are what we call *quantum entanglement*. It follows from this definition of quantum entanglement that *LOCC operations cannot increase the degree of entanglement in quantum states.*

Any LOCC operation can be written in the form of a *separable operation*:

$$\sum_i \rho_i = \sum_i A_i \otimes B_i \rho A_i^\dagger \otimes B_i^\dagger \tag{3.1}$$

such that

$$\sum_i A_i^\dagger A_i \otimes B_i^\dagger B_i = \mathbb{1} \otimes \mathbb{1} \tag{3.2}$$

where A_i is an operator acting on Alice's subsystem, B_i is an operator acting on Bob's, $\mathbb{1}$ is the identity operator, ρ is the initial state and ρ_i's are possible operation outcomes that occur with probabilities $p_i = \mathrm{Tr}(A_i \otimes B_i \rho A_i^\dagger \otimes B_i^\dagger)$. The form $A \otimes B$ shows that Alice and Bob perform their operations locally so they can not interfere with each other's subsystem while the same index i means that their operations are classically correlated due to classical communications performed. Note, however, that not all separable operations can be implemented by using LOCC [BDF$^+$99].

The LOCC operation does not necessarily correspond to a measurement; this is only true if A_i and B_i are Hermitian and positive. For general measurements, where the post-measurement state is not necessarily known (unlike projective measurements), they are best described by the POVM (positive operator-valued measure) formalism. The POVM operators are always positive. However, if the measurement outcome i is found to occur with certainty, equation 3.1 becomes

$$\rho_i = \frac{A_i \otimes B_i \rho A_i^\dagger \otimes B_i^\dagger}{\mathrm{Tr}(A_i \otimes B_i \rho A_i^\dagger \otimes B_i^\dagger)}. \tag{3.3}$$

3.1.2 Separable states

A state ρ^{AB} shared by Alice and Bob is said to be *separable* [Wer89] if it can be written in the form

$$\rho^{AB} = \sum_i p_i \rho_i^A \otimes \rho_i^B, \tag{3.4}$$

where p_i is a probability distribution.

Separable states are the most general class of states that can be prepared perfectly from scratch by LOCC operations; Alice simply prepares a state ρ_i^A with some probability p_i and informs Bob (by telephone, for example) to prepare the state ρ_i^B. Therefore, *separable states contain no entanglement*.

Separability of a state is used to define quantum entanglement: *All non-separable states are entangled*. For example, if a bipartite pure quantum state ρ is entangled, doing a partial trace over any one of the subsystems leads to a mixed state, i.e. $\mathrm{Tr}(\mathrm{Tr}_B(\rho)^2) < 1$. In contrast, if the pure state is separable, $\rho = \rho^A \otimes \rho^B$, we will still be left with a pure state, either ρ^A or ρ^B, after tracing out Bob's or Alice's subsystem respectively.

3.1.3 Positive-partial-transpose-preserving operations

Even though the very notion of quantum entanglement is defined by LOCC operations, unfortunately it turns out that there is no unique entanglement measure under this set of operations [VC01, HSS03]. This leads to the consideration of a more general and closely related set of operations, the positive-partial-transpose-preserving operations (PPT operations). These

operations are defined as those that map any state which has positive partial transpose (for the definition of the partial transposition, see Section 3.2.3.5) into another state with positive partial transpose. Research in this direction so far has indicated the possibility of a unique entanglement measure under PPT operations [APE03], but further research is needed before it becomes clear whether this view is true.

3.1.4 Maximally entangled states

Entanglement does not change under local unitary operations, so two states related by local unitary operations have the same amount of entanglement. For a bipartite d-dimensional system (called a qudit), any pure state that is local unitarily equivalent to

$$|\psi_d^+\rangle = \frac{|0,0\rangle + |1,1\rangle + \ldots + |d-1,d-1\rangle}{\sqrt{d}} \tag{3.5}$$

is *maximally entangled* because any pure or mixed state of bipartite d-dimensional systems can be prepared from such states with certainty by using only LOCC operations [PV07].

For multi-partite systems, the situation is more complex, and there is no equivalent and unique concept of a multi-partite maximally entangled state.

3.1.5 Examples of entangled states

3.1.5.1 Bell states

An well-known example of entangled states is the *Bell states* (also called the EPR states or EPR pairs); the Bell states are four orthogonal two-qubit maximally entangled states:

$$|\Phi^{\pm}\rangle = \frac{|00\rangle \pm |11\rangle}{\sqrt{2}}; \tag{3.6}$$

$$|\Psi^{\pm}\rangle = \frac{|01\rangle \pm |10\rangle}{\sqrt{2}}. \tag{3.7}$$

3.1.5.2 Werner states

The Werner states are defined as a mixture of Bell states:

$$\rho_W = F|\Psi^-\rangle\langle\Psi^-| + \frac{1-F}{3}\left(|\Psi^+\rangle\langle\Psi^+| + |\Phi^+\rangle\langle\Phi^+| + |\Phi^-\rangle\langle\Phi^-|\right) \tag{3.8}$$

$$= \frac{4F-1}{3}|\Psi^-\rangle\langle\Psi^-| + \frac{1-F}{3}\mathbb{1}, \tag{3.9}$$

where the parameter F determines the degree of "mixedness" with $0 \leq F \leq 1$ and $\mathbb{1}$ is the identity operator. The Werner states are entangled for $F > 1/2$.

3.1.6 Pauli matrices

Three matrices are extremely useful in the study of quantum information; these are the *Pauli matrices* (also known as the Pauli operators):

$$\sigma_x \equiv \hat{X} \equiv \begin{pmatrix} 0 & 1 \\ 1 & 0 \end{pmatrix}; \tag{3.10}$$

$$\sigma_y \equiv \hat{Y} \equiv \begin{pmatrix} 0 & -i \\ i & 0 \end{pmatrix}; \tag{3.11}$$

$$\sigma_z \equiv \hat{Z} \equiv \begin{pmatrix} 1 & 0 \\ 0 & -1 \end{pmatrix}. \tag{3.12}$$

One or more of the Pauli matrices can be applied locally to change between any of the Bell states; for example, by applying the Pauli X-matrix to the first qubit while doing nothing to the second qubit, the state $|\Phi^+\rangle$ is converted into the state $|\Psi^+\rangle$:

$$(X \otimes \mathbb{1})|\Phi^+\rangle = \frac{1}{\sqrt{2}} \begin{pmatrix} 0 & 0 & 1 & 0 \\ 0 & 0 & 0 & 1 \\ 1 & 0 & 0 & 0 \\ 0 & 1 & 0 & 0 \end{pmatrix} \begin{pmatrix} 1 \\ 0 \\ 0 \\ 1 \end{pmatrix} \tag{3.13}$$

$$= \frac{1}{\sqrt{2}} \begin{pmatrix} 0 \\ 1 \\ 1 \\ 0 \end{pmatrix} \tag{3.14}$$

$$= |\Psi^+\rangle, \tag{3.15}$$

where $\mathbb{1}$ is the identity operator.

3.2 Quantification of Quantum Entanglement

3.2.1 Pure states

For pure states, the amount of entanglement $\mathcal{E}$ in a quantum state ρ can be completely and uniquely quantified by calculating the von Neumann entropy of the reduced density operator of ρ (for any of its subsystem). The entanglement quantified this way is sometimes known as the *entropy of entanglement*.

For example, the reduced density operator of the Bell state $|\Phi^+\rangle$ for the first qubit is

$$\rho_{Q1} = \mathrm{Tr}_{Q2}(|\Phi^+\rangle\langle\Phi^+|) \tag{3.16}$$

$$= \frac{|0\rangle\langle 0| + |1\rangle\langle 1|}{2}. \tag{3.17}$$

We can then calculate the von Neumann entropy (equation 2.31) to quantify entanglement:

$$\mathcal{E} = S_v(\rho_{Q1}) = 1. \tag{3.18}$$

This shows that the state $|\Phi^+\rangle$ is fully entangled. Note that $\mathcal{E}$ is completely determined by the Schmidt coefficients, which do not change irrespective of which subsystem the partial trace is over (see Section 2.2.1.6), i.e. $S_v(\rho_{Q1}) = S_v(\rho_{Q2})$. For a two-qubit system, the entropy of entanglement goes from 0 for an unentangled state to 1 for a maximally entangled state.

3.2.2 Mixed states

Quantification of entanglement in a mixed state, however, is not as straightforward as in the case of pure states because the Schmidt decomposition only works for pure states. Consider the following example:

$$\rho_E = \frac{1}{2}(|01\rangle\langle 01| + |01\rangle\langle 10| + |10\rangle\langle 01| + |10\rangle\langle 10|) = |\Psi^+\rangle\langle\Psi^+|; \tag{3.19}$$

$$\rho_S = \frac{1}{2}(|01\rangle\langle 01| + |10\rangle\langle 10|) = \frac{1}{2}|\Psi^+\rangle\langle\Psi^+| + \frac{1}{2}|\Psi^-\rangle\langle\Psi^-|. \tag{3.20}$$

Both states have the same entropy of entanglement according to the von Neumann entropy of the reduced density operator for each. This is clearly wrong. The state ρ_S is an equal mixture of two maximally entangled Bell states and is separable (equation 3.4). ρ_S therefore contains no entanglement whereas the state ρ_E is a maximally entangled Bell state. The von Neumann entropy therefore cannot be used to quantify the amount of entanglement in mixed states.

There is currently no definite and unique way to measure the entanglement of mixed states, and many entanglement measures have been proposed , each with some advantages and disadvantages [PV07, BBPS96, Rai99, HHT01, BDSW96, Woo98a, Woo01, VPRK97, VP98, VPJK97, CW04]. Here, only some of the entanglement measures relevant to our purpose will be introduced.

3.2.3 Entanglement measures

3.2.3.1 Properties of entanglement measures

There is no unique entanglement measure for mixed states and different measures do not all possess the same properties [VPRK97, DHR02]. A good entanglement measure $\mathcal{E}$ should satisfy the following desirable conditions:

1. For arbitrary bipartite systems, $\mathcal{E}(\rho)$ of a state ρ is a mapping from density operators into positive real numbers.

2. $\mathcal{E}(\rho) = 0$ if the state ρ is separable.

3. For any state ρ and any local unitary transformation U, the amount of entanglement remains unchanged, that is,

$$\mathcal{E}(\rho) = \mathcal{E}(U_A \otimes U_B \rho U_A^\dagger \otimes U_B^\dagger) \tag{3.21}$$

for local unitary transformation on both Alice's and Bob's parts.

4. The expected entanglement does not increase under LOCC operations:

$$\mathcal{E}(\rho) \geq \sum_i p_i \mathcal{E}(\frac{A_i \otimes B_i \rho A_i^\dagger \otimes B_i^\dagger}{p_i}), \tag{3.22}$$

where p_i, A_i and B_i are as defined in equation 3.1.

5. The entanglement measure reduces to the entropy of entanglement for a pure state $\rho = |\psi\rangle\langle\psi|$

$$\mathcal{E}(\rho) = S_v(\rho^A), \tag{3.23}$$

where ρ^A is the reduced density operator of ρ.

Different entanglement measures are the most appropriate under different contexts, and not all postulated measures possess all the above desired properties. Any function $\mathcal{E}$ that satisfy the first four conditions is called an *entanglement monotone*.

3.2.3.2 Entanglement of formation

The *entanglement of formation* of a mixed state ρ, shared by Alice and Bob, is defined by [BBPS96, Woo98a]

$$\mathcal{E}_F(\rho) \equiv \min \sum_i p_i S_v(\rho_i^A), \tag{3.24}$$

where S_v is the von Neumann entropy. The minimum is taken over all possible pure-state decompositions of the state $\rho = \sum_i p_i |\psi_i\rangle\langle\psi_i|$ and $\rho_i^A = \mathrm{Tr}_B(|\psi_i\rangle\langle\psi_i|)$ is the reduced density operator for Alice's subsystem. If we consider infinitely large number of copies of ρ, we can further define the *regularised* or *asymptotic* version of the entanglement of formation:

$$\mathcal{E}_F^\infty(\rho) \equiv \lim_{n\to\infty} \frac{\mathcal{E}_F(\rho^{\otimes n})}{n}. \tag{3.25}$$

There is a closely related measure of entanglement, namely the *entanglement cost* $\mathcal{E}_C$. The entanglement cost is defined as the asymptotic number of maximally entangled states that are required to create a given mixed state by LOCC operations, and equals the regularised entanglement of formation [HHT01]. However, it is currently unknown whether the entanglement cost is equal to the entanglement of formation generally, even though the yet proven additivity of the entanglement of formation would imply that $\mathcal{E}_F = \mathcal{E}_C$.

For a pure state $|\psi\rangle$, the limiting ratio $\lim_{n\to\infty} m/n$, which represents the minimum number m of maximally entangled states required in order to obtain a certain number of high-quality copies n of the (nonmaximally entangled) state ψ by LOCC actions only, is its (regularised) entanglement of formation $\mathcal{E}_F(|\psi\rangle\langle\psi|)$. This provides the operational interpretation of $\mathcal{E}_F$.

Apart from cases of low dimensionality and some cases with high symmetry [VW01, MV00, EFP$^+$00], it is usually extremely difficult to solve $\mathcal{E}_F$ analytically. In practice, one must apply numerical methods to evaluate $\mathcal{E}_F$ for general states [AVM01]. However, in the case of a two-qubit system, there is an exact formula for the entanglement of formation via the use of the *concurrence* [Woo98a, Woo01].

3.2.3.3 Concurrence

For a bipartite mixed state ρ, the two-qubit *concurrence* is defined as

$$\mathcal{C}(\rho) = \max\{0, \lambda_1 - \lambda_2 - \lambda_3 - \lambda_4\}, \tag{3.26}$$

where λ_n (n = 1, 2, 3, 4) are the square roots of the eigenvalues in decreasing order of the product matrix $\rho\tilde{\rho}$. Here $\tilde{\rho}$ is the "spin-flipped" state and is defined by

$$\tilde{\rho} = (\sigma_y \otimes \sigma_y)\rho^*(\sigma_y \otimes \sigma_y), \tag{3.27}$$

where the complex conjugate is taken in the standard basis, which for a pair of spin-1/2 particles is {$|11\rangle$=$|\uparrow\uparrow\rangle$, $|10\rangle$, $|01\rangle$, $|00\rangle$=$|\downarrow\downarrow\rangle$}, and σ_y expressed in the same standard basis is a Pauli matrix (equation 3.11). The eigenvalues λ_n are real and non-negative, and the value of the concurrence ranges from zero from an unentangled state to unity for a maximally entangled state.

The concurrence can then be used to calculate the entanglement of formation of a two-qubit mixed state ρ:

$$\mathcal{E}_F(\rho) = h\left(\frac{1+\sqrt{1-\mathcal{C}^2(\rho)}}{2}\right) \tag{3.28}$$

with

$$h(\epsilon) \equiv -\epsilon\log_2(\epsilon) - (1-\epsilon)\log_2(1-\epsilon). \tag{3.29}$$

There is one-to-one correspondence between the two-qubit concurrence and the two-qubit entanglement of formation. For higher dimensional systems, there is no unique definition of the concurrence.

3.2.3.4 Entanglement of distillation

The *entanglement of distillation* $\mathcal{E}_\mathcal{D}$ measures the rate at which a noisy mixed state can be converted into a maximally entangled state by LOCC actions alone [BBPS96, Rai99]. This has

the opposite operational interpretation to that of the entanglement of formation $\mathcal{E}_F$. Distilling a number m of maximally entangled states from an initial number n of copies of a nonmaximally entangled state ρ by using only LOCC, the limiting ratio $\lim_{n\to\infty} m/n$ is defined to be the entanglement of distillation of the state ρ, $\mathcal{E}_\mathcal{D}(\rho)$.

The ability to know how much entanglement in a given state is distillable is very important for quantum information processing but computation of $\mathcal{E}_\mathcal{D}$ in general is exceedingly difficult and little progress has been made. The entanglement of formation provides a upper bound on the entanglement of distillation [DHR02, PV07]

$$\mathcal{E}_F \geq \mathcal{E}_\mathcal{D}. \tag{3.30}$$

For pure states, the entanglement of distillation and the entanglement of formation are exactly the same, and both equal to the entropy of entanglement.

There are entangled states from which no entanglement can be distilled, these are the so-called *bound entangled* states. Consequently, $\mathcal{E}_\mathcal{D} = 0$ for all separable states but the converse is not true.

3.2.3.5 Negativity

If Alice and Bob share a bipartite mixed state ρ, described by the Hilbert space $\mathcal{H}_A \otimes \mathcal{H}_B$, its matrix elements are given by

$$\rho_{m\mu,n\nu} = \langle m| \otimes \langle \mu| \, \rho \, |n\rangle \otimes |\nu\rangle \tag{3.31}$$

in a local orthonormal basis (the Latin letters describe Alice's subsystem while the Greek letters describe Bob's). The *partial transposition* of the state ρ with respect to Bob is defined as

$$\rho^{T_B} \equiv \sum_{m,\mu,n,\nu} \rho_{m\mu,n\nu} |m\rangle\langle n| \otimes |\nu\rangle\langle\mu|, \tag{3.32}$$

such that

$$\rho^{T_B}_{m\mu,n\nu} \equiv \rho_{m\nu,n\mu}. \tag{3.33}$$

The form of the operator ρ^{T_B} depends on the choice of local basis, but its eigenvalues do not and are independent of whether the partial transposition is taken over Alice's subsystem or Bob's.

The Peres-Horodecki criterion is a well-known technique to detect entanglement: the positivity of the partially transposed density operator of a state is necessary for separability and is sufficient to prove that a given state ρ has no entanglement of distillation $\mathcal{E}_\mathcal{D}(\rho) = 0$ [Per96, HHH96, Hor97, HHH98].

The *negativity* $\mathcal{N}$ of a mixed state ρ is defined as [VW02, EP99, ZHSL98]

$$\mathcal{N}(\rho) \equiv \frac{\|\rho^{T_B}\| - 1}{2}, \tag{3.34}$$

where $\|X\| \equiv \mathrm{Tr}\sqrt{X^\dagger X}$ is the trace norm. This is an entanglement monotone [Ple05, JLL00, VW02] that attempts to quantify the "negativity" in the spectrum of the partially transposed density operator ρ^{T_B}, and therefore we can also define $\mathcal{N}$ as the sum of the absolute values of the negative eigenvalues λ_i of ρ^{T_B}:

$$\mathcal{N}(\rho) = \sum_{i \ \mathbf{s.t.}\ \lambda_i<0} |\lambda_i|. \tag{3.35}$$

The negativity $\mathcal{N}$ coincides with the entropy of entanglement for maximally entangled states but not for any other entangled pure states.

3.2.3.6 Logarithmic negativity

Another entanglement monotone [Ple05] can also be defined via the partially transposed density operator ρ^{T_B}: the *logarithmic negativity* which is defined as

$$\mathcal{E}_{\mathcal{N}}(\rho) \equiv \log_2\|\rho^{T_B}\|. \tag{3.36}$$

In contrast to the negativity $\mathcal{N}$, $\mathcal{E}_{\mathcal{N}}$ has a nice feature of being additive by construction and has an operational interpretation as the PPT-entanglement cost for exact preparation of a quantum state under the set of PPT operations [APE03].

$\mathcal{E}_{\mathcal{N}}$ is an upper bound to the entanglement of distillation $\mathcal{E}_{\mathcal{D}}$ [VW02]. However, unlike $\mathcal{E}_{\mathcal{D}}$ and $\mathcal{E}_F$, the logarithmic negativity does not reduce to the entropy of entanglement for all pure states.

3.3 Continuous-Variable Systems

So far the description of entanglement has mainly been formulated for bipartite systems with finite dimensional constituents. However, quantum information can be carried by either finite dimensional systems like electron spins, or by infinite dimensional systems such as harmonic oscillators. The finite dimensional setting is often also referred to as *discrete*, whereas the infinite dimensional setting is described as *continuous-variable* because in this case pure states are simply described by wavefunctions in continuous position or momentum variables. There are many reasons to focus on the entanglement of continuous-variable states [BvL05, BP03, EP03, CLP07], since the underlying degrees of freedom of physical systems carrying quantum information are frequently continuous, rather than discrete. Many experimental realisations of quantum information protocols are based on continuous-variable systems so it is not surprising that the study of entanglement of continuous-variable systems is a very active and important research area.

The quantification of entanglement of continuous-variable systems is as difficult, if not more, as the quantification of entanglement of discrete quantum states. Most attention has been

turned to a simple class of states, the *Gaussian states*, since these are common (especially in quantum optics) as the ground or thermal states of optical modes, and a significant amount of knowledge has been gained [WGC06, Sim00, DGCZ00, WW01, GKLC01, GDCZ01, EP02, ESP02a, GC02, GECP03, ESP02b, GWK$^+$03, WGK$^+$04, Shi04, APE03, AEPW02, PEDC05a, CEPD06].

3.3.1 Gaussian states

Any quantum state described by a density operator ρ can be equivalently represented by a *Wigner function* in phase space; the Wigner function is defined as [HOSW84]:

$$\mathcal{W}(\mathbf{x},\mathbf{p}) = \frac{1}{(\pi\hbar)^N}\int_{-\infty}^{\infty} \mathrm{d}^N\mathbf{y}\langle \mathbf{x}\text{-}\mathbf{y}|\rho|\mathbf{x}\text{+}\mathbf{y}\rangle e^{\frac{2i}{\hbar}\mathbf{p}\cdot\mathbf{y}}, \tag{3.37}$$

where N is the number of the variables of a mixed quantum state ρ and $\mathbf{x}$, $\mathbf{p}$ and $\mathbf{y}$ are N-dimensional vectors. The integration is over all components of $\mathbf{y}$. However, the Wigner function is generally not a probability distribution since it can be negative-valued. Quantum states of a system consisting of N degrees of freedom are called Gaussian if it has a Gaussian Wigner function (always positive definite in this case), or equivalently its *characteristic function* is Gaussian [Hol82, EP03, ADMS95, BP03].

The *displacement operator* (also called *Weyl operator*) is defined as

$$W = e^{i\xi^T\sigma R} \tag{3.38}$$

for the $2N$-dimensional vector $\xi \in \mathbb{R}^{2N}$, where the canonical coordinate operators $(R_1,\ldots,R_{2N}) = (X_1\ldots,,X_N,P_1\ldots,,P_N)$, and the *symplectic* $2N\times 2N$ matrix is given by

$$\sigma = \begin{pmatrix} 0 & \mathbb{1}_N \\ -\mathbb{1}_N & 0 \end{pmatrix}. \tag{3.39}$$

The characteristic function [Sch01, WM94] is defined as the expectation value of the displacement operator:

$$\chi(\xi) = \mathrm{Tr}(W\rho). \tag{3.40}$$

It is also the Fourier transform of the Wigner function with respect to both position and momentum variables:

$$\chi(\xi) = \int \mathrm{d}\mathbf{x}\int \mathrm{d}\mathbf{p}\, e^{\frac{i}{\hbar}(\xi_1 P_1\ldots+\xi_N P_N-\xi_{N+1}X_1\ldots-\xi_{2N}X_N)}\mathcal{W}(\mathbf{x},\mathbf{p}). \tag{3.41}$$

If χ takes the form,

$$\chi(\xi) = \chi(0)e^{i\xi^T\sigma d-\frac{1}{4}\xi^T\sigma^T\gamma\sigma\xi}, \tag{3.42}$$

the characteristic function is a Gaussian function in phase space. As a consequence, a Gaussian characteristic function (and hence a Gaussian state) is characterised by the displacement vector d and the *covariance matrix* γ.

d and γ are respectively the *first* and *second moments* of a quantum state. The first moments are the expectation values of the canonical coordinates, $d_j = \langle R_j \rangle_\rho = \mathrm{Tr}(R_j\,\rho)$, and they can be made to vanish by means of unitary translations so they do not affect the entanglement of the state in any way. The second moments are defined as the expectation values $\langle R_j R_k \rangle$ and can be embodied in the real symmetric $2n \times 2n$ covariance matrix γ, whose elements are given by

$$\begin{aligned} \gamma_{jk} &= 2\mathrm{Re}\,\mathrm{Tr}\Big[\rho(R_j - \langle R_j \rangle_\rho)(R_k - \langle R_k \rangle_\rho)\Big] \\ &= \mathrm{Tr}\Big[\rho\Big(\{R_j, R_k\} - 2\,\langle R_j \rangle_\rho \langle R_k \rangle_\rho\Big)\Big], \end{aligned} \tag{3.43}$$

where $\{\}$ denotes the anticommutator. Any real symmetric matrix γ satisfying the Heisenberg uncertainty principle [SSM87, SMD94, Ser06]

$$\gamma + i\sigma \geq 0, \tag{3.44}$$

where $i\sigma$ is the canonical commutation relation $[R_j, R_k] = i\sigma_{jk}$, represents a valid quantum state. Equation 3.44 is also a consequence of the positivity of the state ρ.

The covariance matrix and the uncertainty relation provide a necessary condition for the separability of Gaussian states. A bipartite Gaussian state of arbitrarily many modes is separable if the covariance matrix corresponding to its partially transposed state satisfies equation 3.44 [Sim00, DGCZ00, WW01, GKLC01, GDCZ01]. The use of the positivity of the convariance matrix of the partially transposed Gaussian state is similar to the use of the positivity of the partial transpose of a finite-dimensional state discussed earlier in Section 3.2.3.5.

3.3.1.1 Entanglement of formation

The entanglement of formation of Gaussian states can be defined either with respect to decompositions in pure Gaussian states (therefore called the Gaussian entanglement of formation) or with respect to decompositions in arbitrary pure states (see equation 3.24). The Gaussian entanglement of formation is an entanglement monotone under Gaussian operations. Gaussian operations are those quantum operations (completely positive maps) that map all Gaussian states onto other Gaussian states. For two-mode Gaussian states, the Gaussian entanglement of formation can be explicitly computed; furthermore, if the state is also symmetric, both definitions of the entanglement of formation coincide [GWK$^+$03, WGK$^+$04].

3.3.1.2 Entanglement of distillation

Unlike the entanglement of formation, the entanglement of distillation cannot be defined with respect to Gaussian operations only [ESP02a, GC02]; one must consider general quantum operations. Computations of the entanglement of distillation are extremely difficult. However, some other measures of entanglement (for example, the logarithmic negativity [VW02]) may be used to find its upper bounds.

3.3.1.3 Logarithmic negativity

In contrast to most other entanglement measures, for a bipartite Gaussian state, the logarithmic negativity is completely determined by the covariance matrix of its partially transposed state, and hence can be computed easily [AEPW02].

For a system of $n = n_A + n_B$ harmonic oscillators in a Gaussian state described by the covariance matrix γ (there must be no correlations between positions and momenta, such that the covariance matrix is a direct sum of a position part γ_x and a momentum part γ_p, $\gamma = (\gamma_x \oplus \gamma_p)/2$), the entanglement between the two groups of oscillators as quantified by the logarithmic negativity is

$$\mathcal{E}_{\mathcal{N}} = -\sum_{k=1}^{2n} \log_2 \left[\min\left(1, 2\left|\lambda_k(i\sigma^{-1}\gamma^{T_B})\right|\right)\right], \tag{3.45}$$

where $\{\lambda_k\}$, $1 \leq k \leq 2n$, are the eigenvalues of $i\sigma^{-1}\gamma^{T_B}$, σ is the symplectic matrix. The partial transpose of the covariance matrix γ is

$$\gamma^{T_B} = \Gamma\gamma\Gamma \tag{3.46}$$

with

$$\Gamma = \Gamma_x \oplus \Gamma_p \tag{3.47}$$

and

$$\Gamma_x = \mathbb{1}_n. \tag{3.48}$$

Γ_p is a $n \times n$ diagonal matrix. If the j-th diagonal element of Γ_p belongs to group A, $(\Gamma_p)_j = 1$. Otherwise, $(\Gamma_p)_j = -1$.

3.3.2 Non-Gaussian states

Even though there has been significant progress in the quantification of entanglement in Gaussian states, especially bipartite ones, we should remember that the *non-Gaussian states* are also extremely important; this is especially so in condensed-phase systems, where harmonic behaviour in any degree of freedom is likely to be only an approximation. Much less is known

about the entanglement of these non-Gaussian states. This motivates our research that we hope may shed some light into this direction.

For non-Gaussian states there is some progress in finding criteria for entanglement [KTSC06, AB05, NK06, HZ06a, SV05, MPHH, HZ06b, SV06, MBZ06], but much less in quantifying it. The common theme of these papers is the specification of sufficient conditions for entanglement; many of the papers use developments of the technique suggested by Shchukin and Vogel [SV05], allowing entanglement criteria to be specified in terms of the expectation values of products of annihilation and creation operators. They are therefore implicitly restricted to states (albeit non-Gaussian ones) of canonical systems, and by construction they detect the existence of entanglement but do not quantify it. We on the other hand are mainly concerned with the quantification of entanglement, and will therefore introduce a new approach to the analysis of entanglement and demonstrate in the rest of the thesis that it brings a new perspective on quantum entanglement of arbitrary continuous-variable states.

Chapter 4

A Local Approach to Quantum Entanglement

4.1 Introduction

We present a thought experiment, leading to a new approach to the analysis of quantum entanglement equally applicable to discrete or continuous-variable systems, based on a particular type of projective filtering operations, in which one or both parties makes a preliminary measurement of the state with only enough resolution to determine whether or not the particle resides in a chosen region, before attempting to make use of the entanglement. This approach will be particularly useful for the analysis of quantum entanglement in continuous-variable systems since it provides the systematic quantification of the entanglement in such states, especially where other means of quantification is lacking or extremely difficult. What we are concerned with is the entanglement remaining after preliminary measurements to localise particles in particular regions of finite-widths , instead of the *global* entanglement. Quantum entanglement is inherently non-local so this remaining entanglement is termed the *local entanglement*, without causing confusion, to emphasise the distinction between our new local approach and the usual way of analysing entanglement.

The theory is formulated here in terms of spatial entanglement, which plays a significant role in many physical realizations of quantum information processing. However our local approach to entanglement has a wide range of applicability to various types of quantum systems, and the results can be easily recast in terms of other types of entanglement. We first demonstrate how to apply our approach to discrete-variable systems by using a spin system as an example here, and show how the entanglement varies as a function of the parameters of the initial state. In this case, our results are examples of entanglement distillation and concentration [BBP$^+$96,BBPS96]. Then, in the next chapter and the rest of the thesis, we will concentrate solely on continuous-variable systems.

4.2 Theory

4.2.1 Restricting configuration space by von Neumann measurements

Consider Alice and Bob share a system, each subsystem is described by a single coordinate, and their parts are distinguishable: let the configuration space of the whole system of interacting particles be described by the coordinates q_A and q_B, where q_A describes Alice's particle and q_B describes Bob's. The particles are assumed to be distinguishable, and the effects of indistinguishability will be considered in detail in a later chapter. We will initially present the case in which only Alice makes a preparatory measurement on her system; suppose she has access to some restricted portion $\mathcal{A}$ of the configuration space of "her" particle, whose coordinate is q_A (alternatively, if only Bob makes a preparatory measurement, he will have access to some restricted portion $\mathcal{B}$ of the configuration space of his particle, whose coordinate is q_B). If she measures her system with just enough accuracy to determine whether it is in region $\mathcal{A}$ or not, but no more, the effect is to localise the wavefunction either inside, or outside, the chosen region. The restriction to lying inside the region corresponds to the projector

$$E_{\mathcal{A}} = \int_{\mathcal{A}} |q_A\rangle \langle q_A| \, \mathrm{d}q_A \otimes \mathbb{1}_{\mathrm{other}}, \tag{4.1}$$

where $\mathbb{1}_{\mathrm{other}}$ is the identity operation for all the other particles in the system.

4.2.2 The discarding ensemble

Suppose $\mathcal{A}$ is of finite extent, and Alice measures the position of her particle with just enough accuracy to determine whether it is in $\mathcal{A}$ or not. If so, she keeps the state for further use; if not, she discards it (and tells Bob she has done so). Then the density matrix appropriate to the ensemble of retained systems is

$$\begin{aligned} \rho_{D,\mathcal{A}} &= \frac{E_{\mathcal{A}}\,\rho\,E_{\mathcal{A}}}{\mathrm{Tr}(E_{\mathcal{A}}\,\rho)} \\ &= \frac{\theta_{\mathcal{A}}(q_A)\,\rho(q_A, q_{\mathrm{other}}; q'_A, q'_{\mathrm{other}})\,\theta_{\mathcal{A}}(q'_A)}{\int\int_{\mathcal{A}} \rho(q_A, q_{\mathrm{other}}; q_A, q_{\mathrm{other}}) \mathrm{d}q_A \mathrm{d}q_{\mathrm{other}}}, \end{aligned} \tag{4.2}$$

where $\theta_{\mathcal{A}}$ is a generalised Heavyside function defined so that

$$\theta_{\mathcal{A}}(q) = \begin{cases} 1 & \text{if } q \in \mathcal{A} \\ 0 & \text{otherwise} \end{cases}. \tag{4.3}$$

The subscript D refers to the discarding of the unwanted states; we refer to this density matrix as describing the *discarding ensemble*. Note that, if the original ρ was a pure state $|\psi\rangle\langle\psi|$, then the post-selected density matrix is also pure:

$$\rho_{D,\mathcal{A}} = \frac{E_{\mathcal{A}}|\psi\rangle\langle\psi|E_{\mathcal{A}}}{\langle\psi|E_{\mathcal{A}}|\psi\rangle}. \tag{4.4}$$

In particular this means that even though the system has continuous variables and is therefore infinite-dimensional, its entanglement $\mathcal{E}_{D,\mathcal{A}}$ (in the discarding ensemble) is in principle determined by the von Neumann entropy S_v of the reduced density matrix $\rho^A_{D,\mathcal{A}} = \mathrm{Tr}_B(\rho_{D,\mathcal{A}})$:

$$\mathcal{E}_{D,\mathcal{A}} = S_v(\rho^A_{D,\mathcal{A}}) = -\mathrm{Tr}\left(\rho^A_{D,\mathcal{A}} \log_2 \rho^A_{D,\mathcal{A}}\right). \tag{4.5}$$

If, however, the state ρ is mixed, the entanglement of the post-selected state $\rho_{D,\mathcal{A}}$ can still be quantified by simply choosing other entanglement measures instead, such as the entanglement of formation $\mathcal{E}_F$ or the negativity $\mathcal{N}$.

4.2.3 The nondiscarding ensemble

On the other hand if Alice chooses *not* to discard the system when she fails to detect a particle in region $\mathcal{A}$, the appropriate density matrix is

$$\rho_{ND,\mathcal{A}} = E_{\mathcal{A}}\, \rho\, E_{\mathcal{A}} + E_{\mathcal{A}'}\, \rho\, E_{\mathcal{A}'}, \tag{4.6}$$

where the subscript ND refers to "nondiscarding" and the complementary projector $E_{\mathcal{A}'}$ is defined as

$$E_{\mathcal{A}'} \equiv \mathbb{1} - E_{\mathcal{A}} = \int_{q_A \notin \mathcal{A}} |q_A\rangle\langle q_A| \mathrm{d}q_A \otimes \mathbb{1}_{\mathrm{other}}. \tag{4.7}$$

Equation (4.6) describes a mixed state in which Alice can (by hypothesis) perform no further operation or measurements on the component projected by $E_{\mathcal{A}'}$. It differs from the original density matrix ρ in that off-diagonal elements of ρ connecting $q_A \in \mathcal{A}$ and $q_A \notin \mathcal{A}$ have been set to zero.

Let $p_{\mathcal{A}} = \mathrm{Tr}(E_{\mathcal{A}}\, \rho\, E_{\mathcal{A}})$ be the probability of finding Alice's particle in $\mathcal{A}$. Since the first and second components of $\rho_{ND,\mathcal{A}}$ can be distinguished by Alice and Bob using LOCC, they can teleport $p_{\mathcal{A}}\mathcal{E}_{D,\mathcal{A}} + (1-p_{\mathcal{A}})\mathcal{E}_{D,\mathcal{A}'}$ qubits on average between them. Hence the entanglement in the nondiscarding ensemble $\mathcal{E}_{ND,\mathcal{A}}$ (as quantified by the entanglement of distillation $\mathcal{E}_{\mathcal{D}}$) is not less than $p_{\mathcal{A}}\mathcal{E}_{D,\mathcal{A}} + (1-p_{\mathcal{A}})\mathcal{E}_{D,\mathcal{A}'}$. That is, for any entanglement measure that has an operational interpretation in terms of resources available for exploitation (for example, $\mathcal{E}_{\mathcal{D}}$, the entanglement of formation $\mathcal{E}_F$ and the logarithmic negativity $\mathcal{E}_{\mathcal{N}}$),

$$\mathcal{E}_{ND,\mathcal{A}} \geq p_{\mathcal{A}}\mathcal{E}_{D,\mathcal{A}} + (1-p_{\mathcal{A}})\mathcal{E}_{D,\mathcal{A}'}. \tag{4.8}$$

On the other hand, equation 4.6 also constitutes a valid decomposition of the nondiscarding density matrix $\rho_{ND,\mathcal{A}}$ into orthogonal states distinguishable by local measurements; it follows that the entanglement in the discarding ensemble $\mathcal{E}_{ND,\mathcal{A}}$ (as quantified by the entanglement of formation) is not greater than the average entanglement of this decomposition: $\mathcal{E}_{ND,\mathcal{A}} \leq p_{\mathcal{A}}\mathcal{E}_{D,\mathcal{A}} + (1-p_{\mathcal{A}})\mathcal{E}_{D,\mathcal{A}'}$. Actually, the prior statement is true for a larger class of entanglement

measures; provided the entanglement measure is convex (such as $\mathcal{E}_F$ and the negativity $\mathcal{N}$, but not $\mathcal{E}_\mathcal{N}$), we have:

$$\mathcal{E}_{ND,\mathcal{A}} \leq p_\mathcal{A}\mathcal{E}_{D,\mathcal{A}} + (1-p_\mathcal{A})\mathcal{E}_{D,\mathcal{A}'}. \tag{4.9}$$

The only way these two observations can be consistent is if the entanglement in the nondiscarding ensemble (measured by the entanglement of formation) is equal to

$$\mathcal{E}_{ND,\mathcal{A}} = p_\mathcal{A}\mathcal{E}_{D,\mathcal{A}} + (1-p_\mathcal{A})\mathcal{E}_{D,\mathcal{A}'}. \tag{4.10}$$

If all the operators available to Alice have support only in region $\mathcal{A}$ (i.e. if she can neither measure her particle's properties, nor manipulate it in any way, except when it is in $\mathcal{A}$) then the component projected by $E_{\mathcal{A}'}$ is "out of reach", and the second component $E_{\mathcal{A}'}\,\rho\,E_{\mathcal{A}'}$ of the state $\rho_{ND,\mathcal{A}}$ is functionally equivalent to the separable state $(E_{\mathcal{A}'}\,\mathbb{1}^A\,E_{\mathcal{A}'})\otimes\rho'^B$, where

$$\rho'^B \equiv \mathrm{Tr}_A(E_{\mathcal{A}'}\,\rho\,E_{\mathcal{A}'}), \tag{4.11}$$

as far as any operation that Alice and Bob can perform is concerned. It does not possess any entanglement properties that are useful to Alice and Bob. In that case, equation (4.10) reduces to

$$\mathcal{E}_{ND,\mathcal{A}} = p_\mathcal{A}\,\mathcal{E}_{D,\mathcal{A}}. \tag{4.12}$$

This is the *useful* entanglement in the nondiscarding ensemble. Since only the usable entanglement is of any interest, we shall from now on define the entanglement in the nondiscarding ensemble in terms of the useful part, i.e. equation 4.12, instead of equation 4.10, and focus on $\mathcal{E}_{D,\mathcal{A}}$, noting that $\mathcal{E}_{ND,\mathcal{A}}$ can be simply obtained from it.

Both the entanglement in the discarding ensemble $\mathcal{E}_{D,\mathcal{A}}$ and the entanglement in the nondiscarding ensemble $\mathcal{E}_{ND,\mathcal{A}}$ will be referred as the *local entanglements* because in contrast to the *global* entanglement initially present within the whole quantum system, they represent the entanglement remaining after one or more subsystems have been *localised*. The term local entanglement will make it clear that we take a local view in our analysis, complementary to the more usual global picture of entanglement, without implying that the entanglement is "local" (which is impossible).

4.2.4 Precise measurements of position

If, on the other hand, Alice measures the position accurately, but again keeps only those occasions when the results lie within $\mathcal{A}$ (of width a), the discarding ensemble's density matrix is

$$\rho_\mathcal{P} = \frac{\int E_{Q_A}\,\rho\,E_{Q_A}\mathrm{d}Q_A}{\int \mathrm{Tr}(E_{Q_A}\,\rho)\,\mathrm{d}Q_A} \quad \text{as} \quad a\to 0, \quad Q_A\in\mathbb{A} \tag{4.13}$$

where the integration is over the set $\mathbb{A}$ of values of q_A located *precisely at* $q_A = Q_A$, the subscript $\mathcal{P}$ refers to measuring precisely and E_{Q_A} is the projector corresponding to measuring Alice's particle A precisely at position Q_A:

$$E_{Q_A} = \delta(q_A - Q_A) \otimes \mathbb{1}^B. \tag{4.14}$$

Equation (4.13) describes a density matrix that is diagonal in Q_A; it is a mixed state even if all the measurements where the particle is not found in $\mathcal{A}$ are discarded. Furthermore, unless there are some additional degrees of freedom of particle A which are not measured, the overall density matrix can be written as an incoherent sum of product states:

$$\rho_{\mathcal{P}} \quad \Longrightarrow \quad \rho(Q_A, q_B; Q_A, q_B) = \sum_n p_n(Q_A)\psi_n(Q_A, q_B)\psi_n^*(Q_A, q'_B) \tag{4.15}$$

where $\psi_n(Q_A, q_B)$ is a state in which particle A is located exactly at Q_A without any information about where particle B is and $p_n(Q_A)$ is the probability of Q_A being the n-th element of the set $\mathbb{A}$. $\rho_{\mathcal{P}}$ therefore contains no remaining entanglement with Bob's particle B.

Note that in the limit of very small measurement regions, the distinction between precise and imprecise measurements blurs. The case of vanishingly small regions will be investigated further and surprising results presented in the later chapters.

4.2.5 Measurements by both parties

Exactly analogous formulae can be written down for the cases where Bob makes a preliminary measurement on his particle, or both partners make a measurement. The density matrix in the discarding ensemble, after both parties make preliminary measurements to localise their particles, is

$$\begin{aligned} \rho_{D,\mathcal{AB}} &= \frac{E_{\mathcal{A}} E_{\mathcal{B}}\, \rho\, E_{\mathcal{B}} E_{\mathcal{A}}}{\mathrm{Tr}(E_{\mathcal{A}} E_{\mathcal{B}}\, \rho)} \\ &= \frac{\theta_{\mathcal{A}}(q_A)\theta_{\mathcal{B}}(q_B)\, \rho(q_A, q_B; q'_A, q'_B)\, \theta_{\mathcal{B}}(q'_B)\theta_{\mathcal{A}}(q'_A)}{\int_{\mathcal{B}}\int_{\mathcal{A}} \rho(q_A, q_B; q_A, q_B) \mathrm{d}q_A \mathrm{d}q_B}, \end{aligned} \tag{4.16}$$

where $E_{\mathcal{B}}$ is the projector corresponding to Bob localising his particle to region $\mathcal{B}$ of its configuration space

$$E_{\mathcal{B}} = \int_{\mathcal{B}} \mathrm{d}q_B \mathbb{1}_{\mathrm{other}} \otimes |q_B\rangle \langle q_B| \,, \tag{4.17}$$

with $\mathbb{1}_{\mathrm{other}}$ being the identity operation for all the other particles in the system, and $\theta_{\mathcal{B}}$ is another generalised Heavyside function defined so that

$$\theta_{\mathcal{B}}(q) = \begin{cases} 1 & \text{if } q \in \mathcal{B} \\ 0 & \text{otherwise} \end{cases} . \tag{4.18}$$

It follows from equation 4.12 that *for any convex entanglement measure $\mathcal{E}$ with an operational definition*, the (useful) entanglement in the nondiscarding ensemble is simply related to the entanglement in the discarding ensemble by

$$\mathcal{E}_{ND,\mathcal{AB}} = p_{\mathcal{AB}}\, \mathcal{E}_{D,\mathcal{AB}}, \tag{4.19}$$

where p_{AB} is the probability of finding Alice's particle within the region $\mathcal{A}$ and Bob's particle in the region $\mathcal{B}$.

4.2.6 An inequality for the discarding entanglement

Suppose Alice and Bob divide their configuration spaces into a set of segments $\mathcal{A}$ and $\mathcal{B}$ respectively, and each make a measurement determining in which segment the system is located. In the nondiscarding ensemble, equation 4.6 generalises to

$$\rho_{ND,\mathcal{AB}} = \sum_{\mathcal{AB}} E_{\mathcal{B}}\, E_{\mathcal{A}}\, \rho\, E_{\mathcal{A}}\, E_{\mathcal{B}}, \tag{4.20}$$

where

$$\begin{aligned} \sum_{\mathcal{A}} {E_{\mathcal{A}}}^2 &= \mathbb{1}^A, \\ \sum_{\mathcal{B}} {E_{\mathcal{B}}}^2 &= \mathbb{1}^B. \end{aligned} \tag{4.21}$$

However, this corresponds to a local operation performed by Alice and Bob. Their shared entanglement is non-increasing under this operation; therefore,

$$\mathcal{E}(\rho) \geq \mathcal{E}(\rho_{ND,\mathcal{AB}}). \tag{4.22}$$

But, by a straightforward extension of the argument given previously (Section 4.2.3), the entanglement in the nondiscarding ensemble is

$$\mathcal{E}(\rho_{ND,\mathcal{AB}}) = \sum_{\mathcal{AB}} p_{\mathcal{AB}}\, \mathcal{E}(\rho_{D,\mathcal{AB}}), \tag{4.23}$$

where

$$p_{\mathcal{AB}} = \mathrm{Tr}(E_{\mathcal{B}}\, E_{\mathcal{A}}\, \rho) \tag{4.24}$$

is the probability of finding Alice's part of the system in $\mathcal{A}$ and Bob's part in $\mathcal{B}$, and $\rho_{D,\mathcal{AB}}$ is the density matrix in the discarding ensemble after this measurement result has been obtained, given in equation 4.16. Combining equation 4.22 and equation 4.23 we obtain the following inequality for the average of the entanglements in the discarding ensemble over all the partitions $\bar{\mathcal{E}}_D$:

$$\begin{aligned} \bar{\mathcal{E}}_D &= \sum_{\mathcal{AB}} p_{\mathcal{AB}}\, \mathcal{E}(\rho_{D,\mathcal{AB}}) \\ &\leq \mathcal{E}(\rho). \end{aligned} \tag{4.25}$$

4.3 Spin Systems

We can make an exactly analogous theory for the case where Alice and Bob share a system defined on some other state space, for example a spin system—perhaps more familiar in quantum information theory. We simply replace the projection operator $E_{\mathcal{A}}$ by one defined in spin space; for example, $E_{\mathcal{A}}$ might project onto states with a specified spin component in a given direction. The rest of the theory is then as outlined previously. We now give an example to demonstrate how this works.

4.3.1 An example of pure spin states

Suppose that both Alice and Bob each possess two spins; the first spins belonging to each of them are entangled, as are the second spins, and the overall state $|\psi\rangle$ of the system is a product of the state of the two pairs. For example, we could write

$$|\psi\rangle = \Big(\cos\theta_1|\uparrow_{A1}\uparrow_{B1}\rangle + \sin\theta_1|\downarrow_{A1}\downarrow_{B1}\rangle\Big) \otimes \Big(\cos\theta_2|\uparrow_{A2}\uparrow_{B2}\rangle + \sin\theta_2|\downarrow_{A2}\downarrow_{B2}\rangle\Big); \quad (4.26)$$

the state is pure so entanglement between Alice's and Bob's subsystems is well quantified by the von Neumann entropy of the reduced density matrix. Suppose also that Alice and Bob can only handle systems if the total spins M_s available to each party are such that $M_s = 0$; perhaps the parts of the state with non-zero moment are lost because of the presence of large fluctuating fields in the environment. In the discarding ensemble defined by this restriction, the state becomes

$$\begin{aligned} |\psi\rangle_R &= \frac{\sqrt{2}}{\sqrt{1-\cos 2\theta_1 \cos 2\theta_2}} \\ &\Big(\cos\theta_1|\uparrow_{A1}\uparrow_{B1}\rangle \sin\theta_2|\downarrow_{A2}\downarrow_{B2}\rangle + \sin\theta_1|\downarrow_{A1}\downarrow_{B1}\rangle \cos\theta_2|\uparrow_{A2}\uparrow_{B2}\rangle\Big), \end{aligned} \quad (4.27)$$

again this restricted state is pure but entanglement should become quite different.

This type of measurement is familiar in other contexts—for example entanglement distillation and concentration [BBP$^+$96, BBPS96].

4.3.1.1 Results

We present results in Figure 4.1. For the spin system we consider, the full entanglement present in the state equation 4.26 depends on θ_1 and θ_2 with periods of $\pi/2$, as shown in Figure 4.1(**a**). The maximum entanglement is 2 ebits and occurs ($\theta_1 = \theta_2 = (2n+1)\pi/4$) when both pairs of spins are in the Bell state $|\Phi^+\rangle$ (equation 3.6). When $\theta_1 = \theta_2 = n\pi/2$, the state reduces to all spins either all up or down so completely loses any entanglement.

Now if the restricted region for both Alice and Bob is chosen to be the subspace in which the total z-component of spin takes the value zero, and we work in the discarding ensemble so

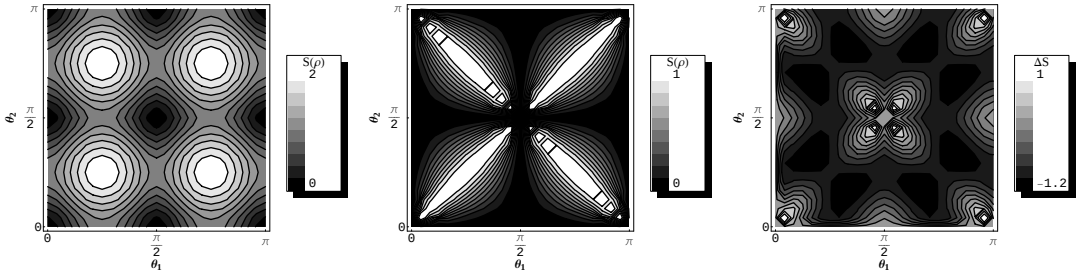

(a) Unrestricted (b) Restricted (discarding ensemble) (c) Differences

Figure 4.1: Entanglement (von Neumann entropy $S_v(\rho^A)$) present in the chosen spin system (a) when the total spins M_s are unrestricted, (b) in the discarding ensemble when M_s for each party must be 0. (c) Entanglement differences between the two cases; $\Delta S_v = S_v(\rho_D^A) - S_v(\rho^A)$.

all other states are eliminated, the entanglement properties of the system become very different. Figure 4.1(**b**) shows that the entanglement distribution of the restricted state has periods of π instead of $\pi/2$, and the maximum possible entanglement (now 1 ebit since the restricted subspaces for both Alice and Bob are two-dimensional) is achieved whenever $\theta_1 = \theta_2$ or $\theta_1 + \theta_2$ are integer multiples of π so that the restricted state is in the Bell state. Note that there is a singularity whenever $\cos 2\theta_1 \cos 2\theta_2 = 1$, corresponding to nodes in the restricted wavefunction (equation 4.27). Further treatment of nodes will be fully discussed later in Section 7.3.4.

If we compare Figure 4.1(**a**) and Figure 4.1(**b**), we see that in some instances the restricted state has higher entanglement. This is indeed the case as shown in Figure 4.1(**c**), where $\Delta S_v = S_v(\rho_D^A) - S_v(\rho^A)$ is plotted against both θ_1 and θ_2. This is an example of the familiar process of entanglement concentration [BBP$^+$96, BBPS96], in which some partial entanglement is concentrated after chosen local measurements. Entanglement is not created on average in our example because the probability of finding $M_s = 0$ is not 100%. Therefore the inequality equation 4.25 is not violated.

Entanglement of a bipartite mixed spin state can also be easily quantified by using negativity $\mathcal{N}(\rho)$ instead as the entanglement measure.

4.3.2 An example of mixed spin states

Consider the mixed state defined by

$$\rho = \frac{16F - 1}{15}|\psi\rangle\langle\psi| + \frac{1 - F}{15}\mathbb{1}, \tag{4.28}$$

where $|\psi\rangle$ is as defined in equation 4.26 (in contrast to the definition of Werner states, this is not in general a maximally entangled state) and $F \in [1/16, 1]$. Note that when $F = 1$, the state becomes pure. Again an example of discarding ensembles can be obtained by projecting the

state (4.28) onto $M_s = 0$ subspace and renormalising accordingly.

4.3.2.1 Results

Now we perform a similar calculation for the mixed state (equation 4.28), comparing the entanglement (as measured by the negativity) present when the total spins M_s are unrestricted and the entanglement in the discarding ensemble when M_s for each party must be 0. The results are presented in Figure 4.2. We choose three values of F for comparison; $F = 0.3$, $F = 0.65$ and $F = 1$.

In Figure 4.3, we plot the variation of the entanglement, quantified by $\mathcal{N}$, with F by choosing (a) both θ_1 and θ_2 to be $\pi/4$ and (b) both θ_1 and θ_2 to be $2\pi/5$. The original entanglement $\mathcal{E}_o$ when the total spins M_s are unrestricted is plotted as a red line, the entanglement in the discarding ensemble $\mathcal{E}_D$ when the total M_s for each party must be 0 is plotted as a green line, and the average of $\mathcal{E}_D$ over all possible values of the total M_s ($= 0, \pm 2, \pm 4$)

$$\bar{\mathcal{E}}_D = \sum_{M_s} p_{M_s} \mathcal{E}_D(M_s) \tag{4.29}$$

is plotted as a blue line. For both cases, $\mathcal{E}_o = \bar{\mathcal{E}}_D$. The entanglements in case (a) vanish at the same point, $F = 0.25$. This is similar to what we will observe in a later chapter (Section 6.4): in that occasion, we showed that the entanglement (as measured by the negativity) of a two-mode Gaussian thermal state vanishes at the same temperature regardless of whether the initial state, or the post-selected state in the discarding ensemble, is studied. However, this is not a general phenomenon as it is clear that $\mathcal{E}_D$ vanishes much earlier than the other entanglements.

We also plot the variation of the entanglement, but this time quantified by the logarithmic negativity $\mathcal{E}_{\mathcal{N}}$, under the same circumstances in Figure 4.4. Again, we see that the entanglements vanish at the same place in (a) $\theta_1 = \theta_2 = \pi/4$ but not in (b) $\theta_1 = \theta_2 = 2\pi/5$. In both Figure 4.3 and Figure 4.4, the entanglement in the discarding ensemble can sometimes be larger than the original entanglement, but the average entanglement in the discarding ensemble over all possible partitions is always less or equal to the original entanglement as expected from equation 4.25. It is important to remember that since both the negativity and the logarithmic negativity do not fully satisfy the criteria for being convex and having an operational interpretation, $\bar{\mathcal{E}}_D$ does not give us the entanglement in the nondiscarding ensemble.

4.4 Summary

We have presented a thought experiment that gives an approach to the analysis of quantum entanglement, equally applicable to discrete or continuous-variable systems. It involves choosing a region of the two-party configuration space and making a projective measurement with only

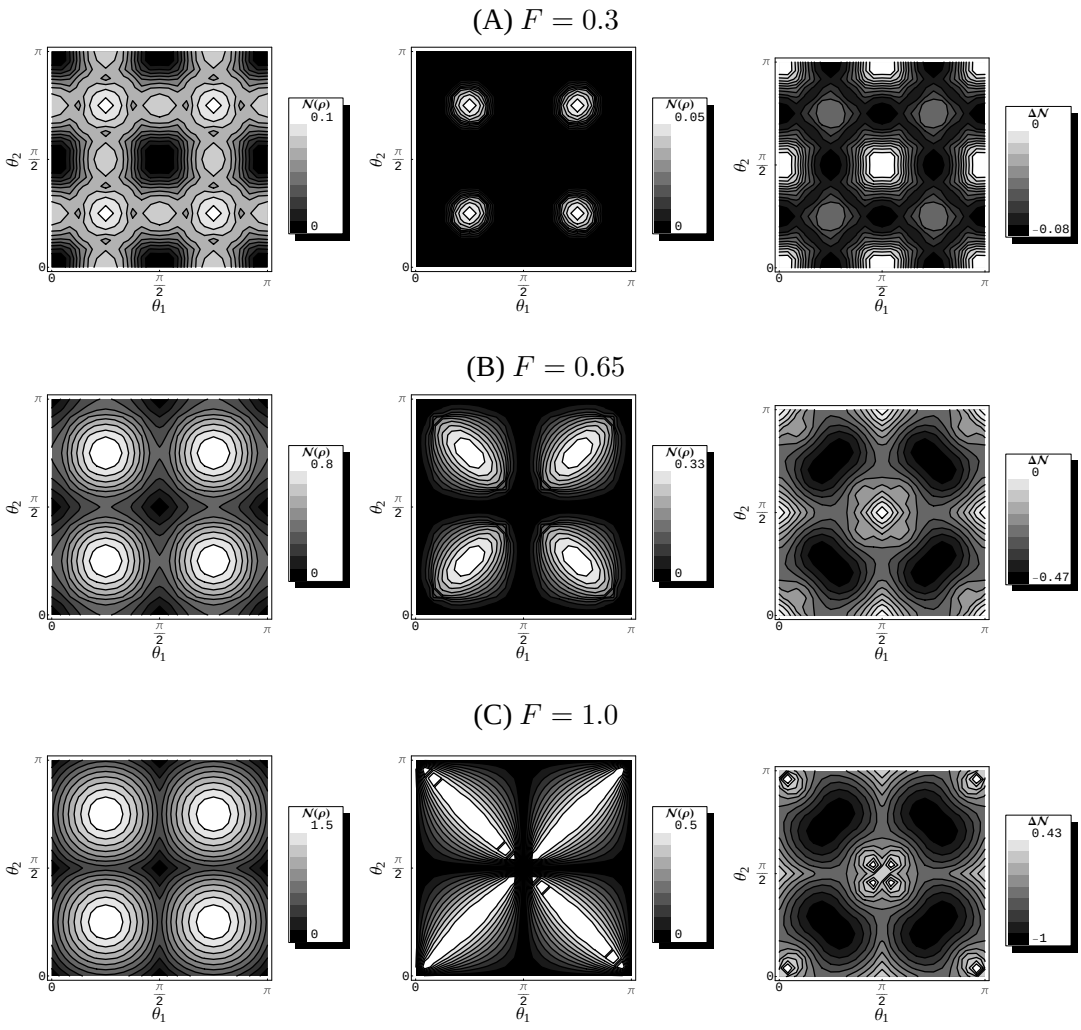

(a) Unrestricted (b) Restricted (discarding ensemble) (c) Differences

Figure 4.2: Entanglement (negativity $\mathcal{N}$) present in the mixed state (equation 4.28) (a) when the total spins M_s are unrestricted, (b) in the discarding ensemble when M_s for each party must be 0. (c) Entanglement differences between the two cases; $\Delta\mathcal{N} = \mathcal{N}(\rho_D) - \mathcal{N}(\rho_o)$. F determines the "mixedness" of the state; when $F = 1$, the state is pure.

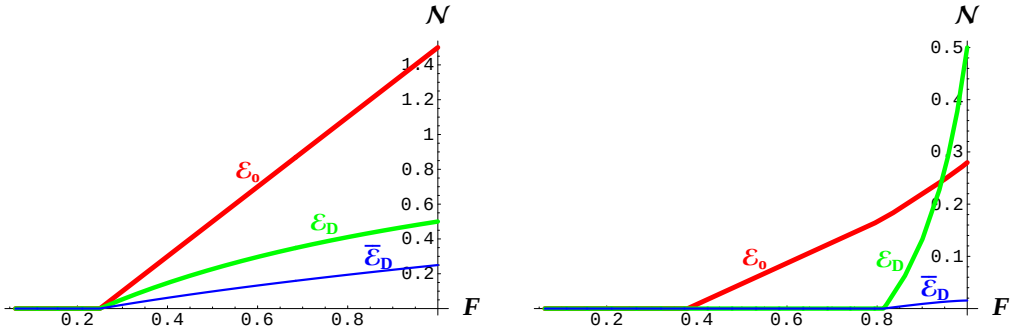

(a) $\theta_1 = \theta_2 = \frac{\pi}{4}$ (b) $\theta_1 = \theta_2 = \frac{24\pi}{25}$

Figure 4.3: Variation of the entanglement (negativity $\mathcal{N}$) with $F \in [1/16, 1]$. F is a quantity that determines the mixedness of the state as defined by equation 4.28. The red line is for the original entanglement $\mathcal{E}_o$ when the total spins M_s are unrestricted, whereas the green line is for the entanglement in the discarding ensemble $\mathcal{E}_D$ when M_s for each party must be 0, and the blue line is for the average of $\mathcal{E}_D$, $\bar{\mathcal{E}}_D$, over all possible combinations of M_s ($= 0, \pm 2$). Note that $\mathcal{E}_o \geq \bar{\mathcal{E}}_D$ always, even though sometimes $\mathcal{E}_D > \mathcal{E}_o$. (a) Both θ_1 and θ_2 have been set to $\pi/4$ to produce the plots. (b) Both θ_1 and θ_2 have been set to $24\pi/25$.

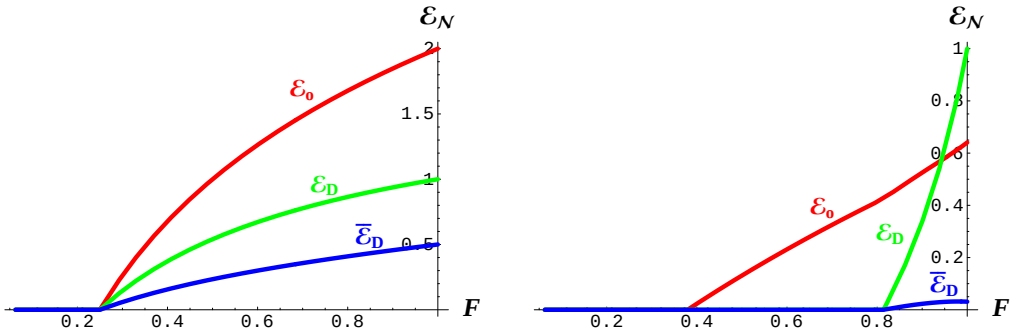

(a) $\theta_1 = \theta_2 = \frac{\pi}{4}$ (b) $\theta_1 = \theta_2 = \frac{24\pi}{25}$

Figure 4.4: Variation of the entanglement (the logarithmic negativity $\mathcal{E}_\mathcal{N}$) with $F \in [1/16, 1]$. F is a quantity that determines the mixedness of the state as defined by equation 4.28. The red line is for the original entanglement $\mathcal{E}_o$ when the total spins M_s are unrestricted, whereas the green line is for the entanglement in the discarding ensemble $\mathcal{E}_D$ when M_s for each party must be 0, and the blue line is for the average of $\mathcal{E}_D$, $\bar{\mathcal{E}}_D$, over all possible combinations of M_s ($= 0, \pm 2$). Note that $\mathcal{E}_o \geq \bar{\mathcal{E}}_D$ always, even though sometimes $\mathcal{E}_D > \mathcal{E}_o$. (a) Both θ_1 and θ_2 have been set to $\pi/4$ to produce the plots. (b) Both θ_1 and θ_2 have been set to $24\pi/25$.

enough resolution to determine whether or not the system resides in this region, then characterising the entanglement remaining in the corresponding sub-ensemble (the local entanglement). Our approach is particularly simple to implement for pure states, since in this case the sub-ensemble in which the system is definitely located in the required region after the measurement is also a pure state, and hence its entanglement can be simply characterised by the entropy of the reduced density matrices.

Even though the thought experiment described is based on position coordinates, our local approach to entanglement is not limited to only the analysis of spatial entanglement. To clearly illustrate this point, an example of the application of our method to states of a simple spin system, where Alice and Bob share two pairs of spin-1/2 particles is given here (whereas the application to the analysis of spatial entanglement is discussed in detail in the next chapter). It is shown how the amount of entanglement located in the chosen region (in this case the $M_s = 0$ manifold) varies as the characteristics of the states shared by Alice and Bob are altered. We presented results for both pure and mixed states, and show how entanglement is affected by parameters of the states, in this case the "mixedness" F, both qualitatively and quantitatively. The entanglement in the discarding ensemble $\mathcal{E}_D$ in some situations can be "concentrated" to be higher than the original entanglement $\mathcal{E}(\rho)$ of the state ρ but the *average* entanglement in the discarding ensemble $\bar{\mathcal{E}}_D$ is always less or equal to the original entanglement (equation 4.25). We have only discussed systems with *discrete* variables here but our local approach can also be used to analyse entanglement arising from *continuous* degrees of freedom (not only spatial coordinates), which actually is one of the major strengths of our approach. From this point onwards, we will concentrate exclusively on continuous-variable quantum entanglement.

Our approach suffers from the disadvantage that there is no sum rule on the entanglements in the discarding ensemble: the sum of the entanglements from all the sub-regions defined by a given decomposition of configuration space does not yield the full entanglement of the system. Instead, the entanglements from the sub-regions satisfy the inequality in equation 4.25. Further studies will therefore be needed in order to understand in more detail the relationship between the local entanglement and the global entanglement.

Chapter 5

Entanglement Distributions: Mapping the Entanglement in Coupled Harmonic Oscillators

5.1 Introduction

Studying the entanglement properties of a number of spatially extended many-body systems including spin chains, coupled fermions, and harmonic oscillators [ON02, OAFF02, VLRK03, LRV04, JK04, ZW02, MD, AEPW02, PHE04, Ved03] has both given information on the potential uses of these systems in quantum information processing, and yielded insight into their fundamental properties. The ground states of these interacting systems are generally entangled due to interactions.

In this chapter we address the question: *where in configuration space is the entanglement between two particles located?* Specifically, we investigate the location dependence of the ground-state entanglement between two interacting subsystems by applying our local approach, described fully in Chapter 4. We choose a pair of coupled harmonic oscillators as an example, since this is a system for which many exact results are available [AEPW02, GWK$^+$03]. We assign one oscillator to each of the two communicating parties Alice and Bob, but perform a thought experiment in which one or both of them first measure the system in configuration space, with just enough precision to localise it in some chosen region, and thereafter are restricted to operations only within that region. We ask how this restriction affects the spatial entanglement available to them for other purposes—for example, for teleporting additional qubits between them. Our research is concerned with the entanglement between *localised* particles, and hence contrasts with previous studies [BR04, PEDC05b, HAV06] of the entanglement of a finite region of space with the rest of the system.

We shall focus on studying the variations of the entanglement properties with the size of

the region. For the present the two particles are assumed to be distinguishable. We argue that the shared entanglement remaining to Alice and Bob provides a natural measure of where in configuration space the entanglement was originally located. First, we introduce the system of interest, the ground state of coupled harmonic oscillators, in Section 5.2. Then, two different ways to numerically compute the local entanglements, allowing mapping of the entanglement distributions with variable resolution, are described in Section 5.3. Results are presented in Section 5.4. Particularly, it is shown that the entanglement distributions are very different from that of the classical correlations. Last, we summarise briefly in Section 5.6.

5.2 Quantum Harmonic Oscillators

Consider a harmonic system with a Hamiltonian (taking $\hbar = 1$)

$$\hat{H} = R^T \begin{pmatrix} \mathbf{V} m\omega^2/2 & 0 \\ 0 & \mathbb{1}_N/(2m) \end{pmatrix} R, \tag{5.1}$$

where the vector R of quadrature operators is given by the positions $R_j = X_j$ and conjugate momenta $R_{N+j} = P_j$, for $1 \leq j \leq N$, the positive-definite $N \times N$ matrix $\mathbf{V}$ contains the coupling coefficients among the positions, and ω is the natural frequency of uncoupled oscillators of mass m. For a translationally invariant system the potential matrix elements depend only on the difference between the indices: $\mathbf{V}_{j,k} = v_{(j-k) \bmod N}$ for $1 \leq j, k \leq N$. The covariance matrix γ (equation 3.43) of the ground state is then [AEPW02]

$$\begin{aligned} \gamma &= \frac{1}{2}\Big(\frac{\gamma_x}{m\omega} \oplus m\omega\gamma_p\Big) \\ &= \frac{1}{2}\Big(\frac{\mathbf{V}^{-1/2}}{m\omega} \oplus m\omega\mathbf{V}^{1/2}\Big). \end{aligned} \tag{5.2}$$

The ground state we seek is an example of a Gaussian state. The density matrix of a Gaussian state for N degrees of freedom can be written in the coordinate representation [SSM87] as[1]

$$\begin{aligned} \langle \mathbf{q}|\rho|\mathbf{q}'\rangle &\equiv \rho(\mathbf{q};\mathbf{q}') \\ &= \Big(\frac{2}{\pi}\Big)^{N/2} (\det \mathbf{L})^{1/2} \\ &\quad \exp\Big[-\mathbf{q}^T\mathbf{L}\,\mathbf{q} - \mathbf{q}'^T\mathbf{L}\,\mathbf{q}' - \frac{1}{2}(\mathbf{q}-\mathbf{q}')^T\mathbf{M}(\mathbf{q}-\mathbf{q}') + \frac{\mathrm{i}}{2}(\mathbf{q}-\mathbf{q}')^T\mathbf{K}(\mathbf{q}+\mathbf{q}')\Big], \end{aligned} \tag{5.3}$$

where $\mathbf{L}$, $\mathbf{M}$ and $\mathbf{K}$ are real N-dimensional matrices with $\mathbf{L}$ and $\mathbf{M}$ symmetric, while $\mathbf{K}$ is

[1] The density matrix of equation 5.3 describes a *centred* Gaussian state, i.e. one with $\langle X\rangle = \langle P\rangle = 0$. The results in this thesis are also valid for displaced Gaussian states since displacements can be implemented by local unitaries.

arbitrary. These matrices are related to the covariance matrix γ by

$$\frac{1}{2}\gamma^{-1} = \begin{pmatrix} \mathbb{1} & 0 \\ -\mathbf{K} & \mathbb{1} \end{pmatrix}^T \begin{pmatrix} 2\mathbf{L} & 0 \\ 0 & \frac{1}{2}(\mathbf{L}+\mathbf{M})^{-1} \end{pmatrix} \begin{pmatrix} \mathbb{1} & 0 \\ -\mathbf{K} & \mathbb{1} \end{pmatrix}. \tag{5.4}$$

We note that for a pure Gaussian state, $\mathbf{M} = 0$ and $\mathbf{K}$ is symmetric. Since the Hamiltonian given in equation 5.1 has no coupling between position and momentum variables, γ is block diagonal and hence $\mathbf{K} = 0$. Furthermore if there are only nearest-neighbour interactions, with a Hooke's-law spring constant K, the interaction strength is characterised by the single dimensionless parameter

$$\alpha = \frac{2K}{m\omega^2}. \tag{5.5}$$

For the two-oscillator ground state we therefore have only one non-zero matrix (see Appendix A for details):

$$\mathbf{L} = \frac{m\omega}{4} \begin{pmatrix} 1+\sqrt{1+4\alpha} & 1-\sqrt{1+4\alpha} \\ 1-\sqrt{1+4\alpha} & 1+\sqrt{1+4\alpha} \end{pmatrix}. \tag{5.6}$$

The one-particle reduced density matrices can then be easily obtained by quadrature; for Particle 1,

$$\begin{aligned} \rho^A(q_A; q'_A) &= \int_{-\infty}^{\infty} \mathrm{d}q_B \rho(q_A, q_B; q'_A, q_B) \\ &= \sqrt{\frac{2\upsilon_1 - 2\upsilon_2}{\pi}} \exp[-\upsilon_1(q_A^2 + q_A'^2) + 2\upsilon_2 q_A q'_A], \end{aligned} \tag{5.7}$$

where the state is normalised to unity and the constants υ_1 and υ_2 are

$$\begin{aligned} \upsilon_1 &= L_{11} - \frac{(L_{12}+L_{21})^2}{8L_{22}} \\ &= \frac{1+2\alpha+3\sqrt{1+4\alpha}}{4+4\sqrt{1+4\alpha}} m\omega \end{aligned} \tag{5.8}$$

and

$$\begin{aligned} \upsilon_2 &= \frac{(L_{12}+L_{21})^2}{8L_{22}} \\ &= \frac{1+2\alpha-\sqrt{1+4\alpha}}{4+4\sqrt{1+4\alpha}} m\omega \end{aligned} \tag{5.9}$$

where $\{L_{ij}\}$, $1 \leq i,j \leq 2$, are the elements of the $\mathbf{L}$ matrix. From equation 5.7, we can also define the Gaussian characteristic length σ which characterises the probability distribution of a single particle:

$$\begin{aligned} \sigma &= \frac{1}{2}(\upsilon_1+\upsilon_2)^{-\frac{1}{2}} \\ &= \frac{1}{2}\left[m\omega\left(\frac{\sqrt{1+4\alpha}}{1+1\sqrt{1+4\alpha}}\right)\right]^{-\frac{1}{2}}. \end{aligned} \tag{5.10}$$

In the case of the ground state of our system, the entanglement is determined by[2]

$$S_v(\rho^A) = -\log_2(1-w) - \frac{w\log_2 w}{(1-w)}, \tag{5.11}$$

where

$$w = \frac{1+3\sqrt{1+4\,\alpha}+2\,[\alpha-\,(1+4\,\alpha)^{\frac{1}{4}}-\,(1+4\,\alpha)^{\frac{3}{4}}]}{1+2\,\alpha-\sqrt{1+4\,\alpha}}. \tag{5.12}$$

5.3 Method

Because only the ground state is considered here, we can calculate the von Neumann entropy $S_v(\rho_D^A)$, and hence the local entanglement, numerically by using two different approaches.

5.3.1 Expansion in a complete set

We define an orthonormal set of functions, $\{\phi_i(q)\}$, with support in a region $\mathcal{A}$ of configuration space of width $2a$ centred at coordinate $\bar{q}$:

$$\int_{\bar{q}-a}^{\bar{q}+a} \phi_i(q)\phi_j^*(q) = \delta_{ij}. \tag{5.13}$$

A suitable choice is

$$\begin{aligned} \phi_i(q) &= \sqrt{\frac{1}{a}}\cos(\frac{(q-\bar{q})i\pi}{2a}) \quad i \text{ is odd} \\ \phi_i(q) &= \sqrt{\frac{1}{a}}\sin(\frac{(q-\bar{q})i\pi}{2a}) \quad i \text{ is even,} \\ &= 0 \quad \text{if} \quad |q-\bar{q}| > a \end{aligned} \tag{5.14}$$

We then approximate the appropriate post-selected density matrix by an expansion in a finite set of the functions defined in equation 5.14; as an example, if only Alice makes a preliminary measurement to localise her particle in the region $\mathcal{A}$, we have the density matrix in the discarding ensemble as (see Section 4.2.2. For simplicity, we will drop regions "$\mathcal{A}$" and "$\mathcal{B}$" from the previously used notation $\rho^A_{D,\mathcal{AB}}$ from here onwards.)

$$\rho_D^A(q_A;q'_A) = \sum_{ij}^{N} \rho_{ij}\phi_i(q_A)\phi_j^*(q'_A), \tag{5.15}$$

with ρ_{ij} given by

$$\begin{aligned} \rho_{ij} &= \int_{\bar{q}_A-a}^{\bar{q}_A+a} \mathrm{d}q_A \int_{\bar{q}_A-a}^{\bar{q}_A+a} \mathrm{d}q'_A \\ &\qquad \phi_i^*(q_A)\rho^A(q_A;q'_A)\phi_j(q'_A), \end{aligned} \tag{5.16}$$

where $\rho^A(q_A;q'_A)$ is given by equation 5.7. We normalise $\rho_D^A(q_A;q'_A)$ by its trace and can then quantify entanglement by calculating the von Neumann entropy from this normalised

[2]Our derivation is in Appendix A. A similar but much more complete treatment is published earlier elsewhere so that the entanglement of general pure Gaussian two-mode states is known exactly [RR05].

$\rho_D^A(q_A; q'_A)$. Unfortunately the quadratures in equation 5.16 must be performed numerically, making this approach quite time-consuming.

5.3.2 Configuration-space grid

We therefore explored also a direct real-space approach, in which we first *discretise* the configuration space into a finite number of measurement "bins", then select only those bins that correspond to the regions within which Alice's and Bob's respective particles localise. For example, consider again the case in which only Alice makes a preliminary measurement, if the region is $\bar{q}_A - a \leq q_A \leq \bar{q}_A + a$, we divide this space into N_B regions with $N_B + 1$ equally spaced points (q_A's) covering the intervals from $q_A = \bar{q}_A - a$ to $\bar{q}_A + a$. We then build the $(N_B + 1) \times (N_B + 1)$ post-selected one-particle reduced density matrix $\rho_D^A(q_A; q'_A)$ by calculating its elements ρ_{ij}'s from the one-particle reduced density matrix, equation 5.7:

$$\rho_{ij} = \rho^A(q_A^i; q_A^j) \quad \text{for} \quad 1 \leq i, j \leq N_B + 1. \tag{5.17}$$

As in the other approach, we calculate the von Neumann entropy of the normalised $\rho_D^A(q_A; q'_A)$ in order to quantify the entanglement.

Note that if on the other hand both parties make a preliminary measurement, we start from the full 2-particle density matrix and apply Bob's restrictions with respect to his oscillator before we reduce it into the one-particle density matrix for Alice's oscillator.

We compare both approaches in Figure 5.1 by computing the local entanglement (the von Neumann entropy S_v) in the case described later in Section 5.4.2.1 with varying N, which is the number of expansion functions in equation 5.15 for the expansion-in-a-complete-set approach (the blue line) but is the number of bins N_B for the configuration-space-grid approach (the red line). $2a = 4$, $\bar{q} = 0$ and $\alpha = 6$ for all the calculations. We find that results from the two approaches converge to the same value as the number of grid points, or the number of expansion functions, tend to infinity but the expansion-in-a-complete-set approach is prone to numerical errors and takes much longer to compute. Therefore, we conclude that the grid-based approach is superior, and it has been used for all the results presented in this chapter.

5.4 Results

5.4.1 The limit of very small region sizes

For the Gaussian system described in Section 5.2, the entanglement can be evaluated analytically in the limit of very small region sizes by following the method described in Chapter 6. Here we briefly describe the relevant results for completeness.

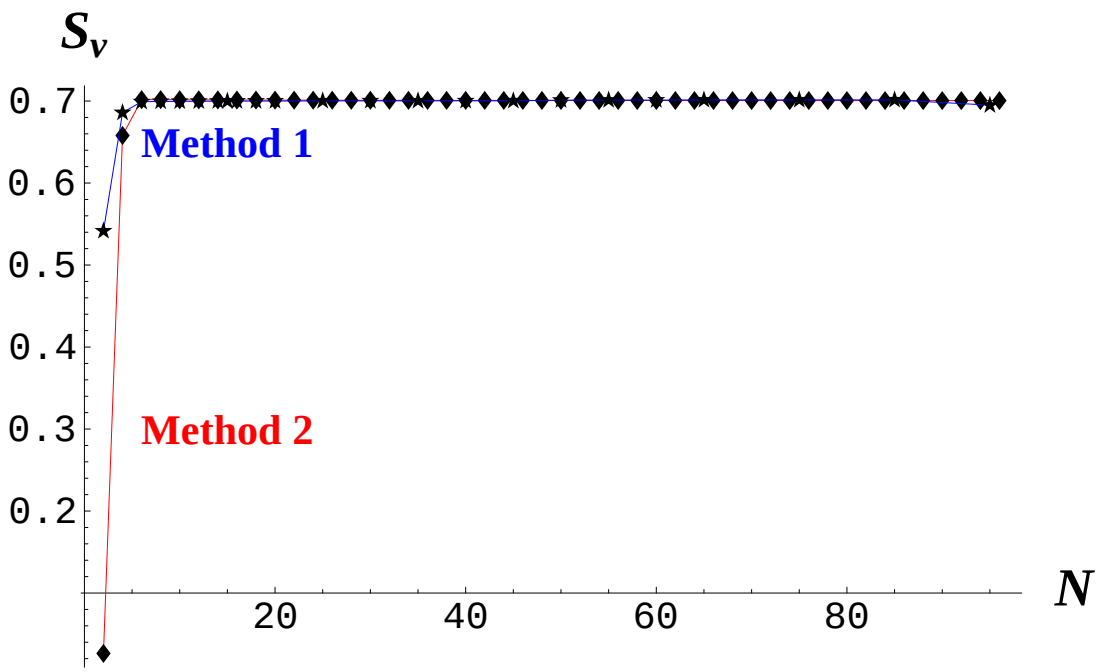

Figure 5.1: Comparison of the two methods for quantifying the local entanglement (measured by the von Neumann entropy S_v) numberically. Method 1 (the blue line) is the expansion-in-a-complete-set approach (described in Section 5.3.1) while Method 2 (the red line) is the configuration-space-grid approach (Section 5.3.2). N is the number of expansion functions in equation 5.15 for Method 1, and is the number of bins N_B for Method 2. $2a = 4$, $\bar{q} = 0$ and $\alpha = 6$ for all the calculations.

5.4.1.1 Only Alice's particle restricted

Suppose only Alice makes a preliminary measurement, and determines that her particle is located in a region of length $2a$ centred at coordinate $\bar{q}_A$, as in Section 5.3: $\bar{q}_A - a \leq q_A \leq \bar{q}_A + a$. In the discarding ensemble, the entanglement is $\mathcal{E}_D = h(\epsilon)$ in equation 3.29 with

$$\begin{aligned} \epsilon &= \frac{a^2(L_{12}+L_{21})^2}{12L_{22}} \\ &= a^2 m\omega \frac{\alpha(\sqrt{1+4\alpha}-1)}{6(1+2\alpha+\sqrt{1+4\alpha})}. \end{aligned} \tag{5.18}$$

Note that this depends only on a and on the parameters of the underlying oscillator system; it is independent of $\bar{q}$. Note also that the entanglement is non-zero for any non-zero α, and can be made arbitrarily large (for a given very small a) by increasing α.

5.4.1.2 Both particles restricted

On the other hand, if both parties make measurements, thereby also restricting Bob's particle to a region of length $2b$ around $\bar{q}_B$, the entanglement is once again given by $h(\epsilon)$ but now ϵ

becomes

$$\begin{aligned} \epsilon &= \frac{a^2b^2(L_{12}+L_{21})^2}{9} \\ &= \frac{a^2b^2m^2\omega^2}{18}(1+2\alpha-\sqrt{1+4\alpha}). \end{aligned} \tag{5.19}$$

Once again, this result depends only on the dimensionless coupling strength α and the fundamental length unit $(m\omega)^{-1/2}$ of the oscillators; it is again *independent* of the location of the centres of the measurement regions (this is the consequence of equation 7.27). Later we will see that as a and b increase, the entanglement distribution gradually changes so that more entanglement is located at some parts of configuration space than the others.

5.4.2 Finite region sizes

5.4.2.1 Only Alice's particle restricted

We will set $m = 1/2$, $\omega = 1$ and choose the Gaussian characteristic length (equation 5.10) for an uncoupled harmonic system, $\sigma = 1$, as our unit of length.

In this section, we consider the case in which only Alice makes a preliminary measurement to determine that her particle lies within a finite-size region. Suppose that the size of this region is $2a$ and the location of the centre of the region is $\bar{q}$, the von Neumann entropy $S_v(\rho_D^A)$ depends on both $2a$ and $\bar{q}$. This is shown in Figure 5.2. We look at the variation with $\bar{q}$ first; Figure 5.2 along the $\bar{q}$-axis shows some of the examples. For finite a, the entanglement is higher if we measure around the centre of the wavefunction, where the probability of finding a particle is highest, than if we take our measurements further away from the centre of the wavefunction where the chance of finding a particle is very low.

We can understand this variation by examining Alice's post-selected reduced density matrix in the centre of Figure 5.2 ($\bar{q} = 0$) and at the edge ($\bar{q} = \pm 4$). At the edge, the diagonal elements increase rapidly towards one end; the eigenvalues of this density matrix are dominated by these terms, resulting in one eigenvalue being close to 1 and the other eigenvalues being very small. The von Neumann entropy will therefore also be small. In contrast, the diagonal elements in the centre case, instead of being dominated by a single element at one end, are approximately constant. The resulting spread of eigenvalues leads to a higher von Neumann entropy.

We would also expect that as the region size approaches the total configuration space, the entanglement in the discarding ensemble should tend to the entanglement originally present in the whole system; this is shown in the upper part of Figure 5.2, where the entanglement rises with a until it saturates to the peak value of magnitude $S_v(\rho_D^A) = 0.702$ given by equation 5.11.

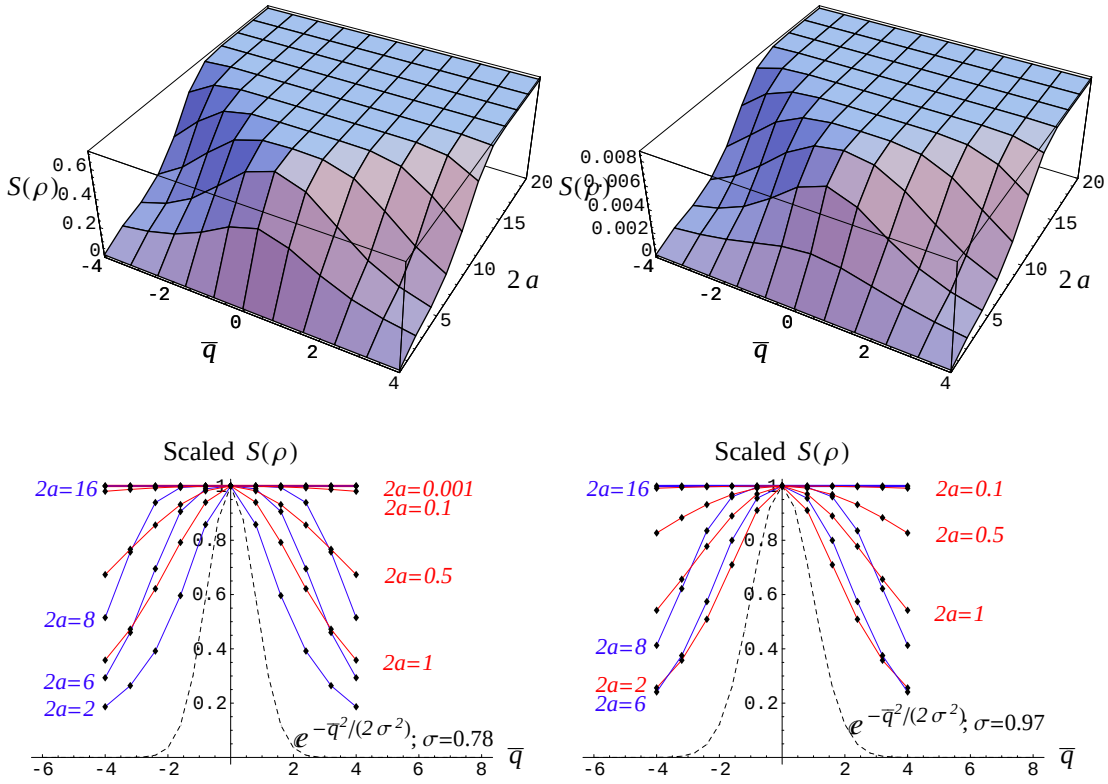

(a) $\alpha = 6$ (b) $\alpha = 0.06$

Figure 5.2: Top: Variation of the entanglement $S_v(\rho_D^A)$ with both the width $2a$ and the centre $\bar{q}$ of the preliminary-measurement region. Bottom: $S_v(\rho_D^A)$ plotted against $\bar{q}$ for different widths, re-scaled such that $S_v(\rho_D^A)$ has the same peak value at $\bar{q} = 0$. A plot (the black dashed line) of the corresponding Gaussian probability distribution for Alice's particle, with a standard deviation σ determined by the coupling strength α, is shown for comparison. The different plots correspond to two different coupling strengths, (a) $\alpha = 6$ v.s. (b) $\alpha = 0.06$. The number of bins N_B used in the calculation was 200 in both cases.

Roughly speaking, this saturation occurs once the region has expanded to include a significant portion of the central part of the harmonic oscillator wavefunction.

We have already seen that in the limit of small a the entanglement becomes independent of position. In fact, even for finite a the entanglement is distributed very differently from the probability distribution of Alice's particle. This is shown in the lower part of Figure 5.2, where the coloured curves show the entanglement (scaled to a common maximum value) as a function of $\bar{q}$ for different widths $2a$; for comparison, the black dashed plot shows the Gaussian one-particle probability distribution with standard deviation σ given by equation 5.10. Note that the width of the entanglement plot varies non-monotonically with a: the entanglement is constant in the limits of small and large a, and has a minimum width around $2a = 2$ (for $\alpha = 6$). Note also that $S_v(\rho_D^A)$ is very small but is non-zero even for small α, as expected from equation 5.18.

For comparison, we also present in Figure 5.2(b) results for a much weaker coupling, $\alpha = 0.06$ compared with $\alpha = 6$: for weak coupling, the entanglement has smaller peak values ($= 0.00859$ in this case) and its spread is narrower, but the qualitative features are similar in both cases.

5.4.2.2 Both particles restricted: entanglement distributions

Next we consider the case where both Alice and Bob make preliminary measurements, but not necessarily in the same way.

We start by considering two different cases; the first (Case 1) is that both parties' preliminary measurements restrict their particles to regions with identical widths and centres ($a = b$ and $\bar{q}_A = \bar{q}_B$), whereas in the second case (Case 2) the region widths are the same but the centre of Bob's region is always fixed around the centre of the wavefunction ($a = b$, $\bar{q}_B = 0$). The results, for $\alpha = 6$, are shown together with the previous result (Case 3; only Alice makes a preliminary measurement, as shown in Figure 5.2(a)) for comparison in Figure 5.3. The entanglement in the discarding ensemble of Case 3 is the highest out of the three cases; this is as expected, since the entanglement can only decrease under the additional (local) measurements made by Bob. When the width $2a$ is small, the entanglement of Case 1 is higher than of Case 2. However, as $2a$ increases, Case 2 converges more rapidly to Case 3 so that its entanglement is now higher than that of Case 1, until $2a$ becomes so large that the differences between all three cases disappear.

5.4.2.3 Both particles restricted: classical correlations

We now compare the entanglement distributions to the classical correlations between the particles. Suppose that Alice and Bob localise their respective particles to regions with the same widths but different centres; the entanglement in the discarding ensemble will depend on both

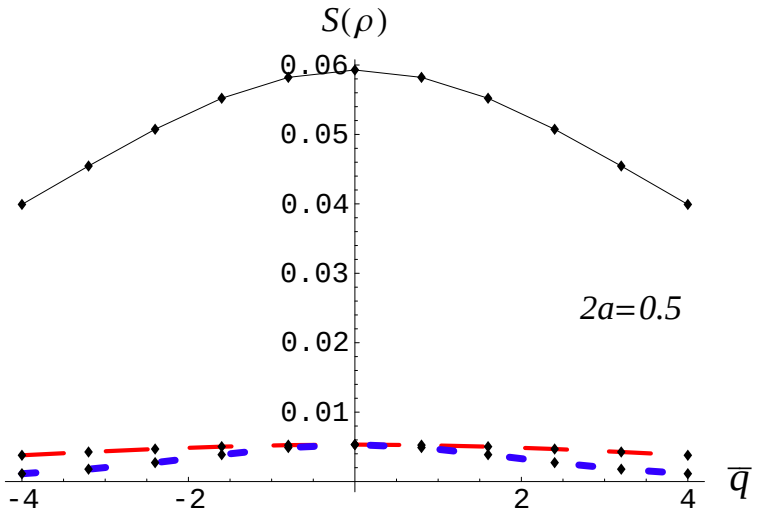

(a) $2a = 0.5$

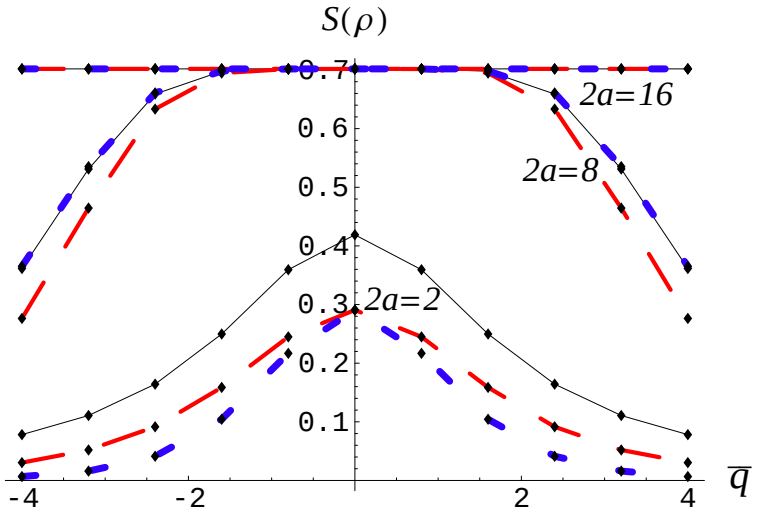

(b) Larger $2a$'s

Figure 5.3: Comparison of the two different cases of preliminary measurements done by both parties together with the case that only one party makes a preliminary measurement. The entanglement $S_v(\rho_D^A)$ is plotted against the centre $\bar{q}$ of the preliminary-measurement region with width $2a$. (a) For $2a = 0.5$. (b) For other larger values of $2a$. Red long-dashed line (Case 1): Both parties' preliminary measurements localise their particles in regions with identical widths and centres ($a = b$ and $\bar{q}_A = \bar{q}_B$). Blue thick short-dashed line (Case 2): The widths of the regions are the same but one centre is always fixed around the centre of the wavefunction while there is no restriction on the other centre ($a = b$, $\bar{q}_B = 0$). Black thin solid line (Case 3): Only one party makes a preliminary measurement. In all three cases, the number of bins used in the calculation is $N_B = 100$ and $\alpha = 6$.

$\bar{q}_A$ and $\bar{q}_B$. We shall compare the entanglement distribution with the 2-particle probability distribution $P(q_A \in \mathcal{A} \cap q_B \in \mathcal{B})$, and the conditional probability distribution for Bob's particle given the position of Alice's particle, $P(q_B \in \mathcal{B} \mid q_A \in \mathcal{A})$.

The two-particle probability is

$$P(q_A \in \mathcal{A} \cap q_B \in \mathcal{B}) = \int_{\bar{q}_A-a}^{\bar{q}_A+a} \mathrm{d}q_A \int_{\bar{q}_B-b}^{\bar{q}_B+b} \mathrm{d}q_B \, \rho(q_A, q_B; q_A, q_B), \tag{5.20}$$

and in the limit of small a, b we have

$$P(q_A \in \mathcal{A} \cap q_B \in \mathcal{B}) = 4ab\,\rho(\bar{q}_A, \bar{q}_B; \bar{q}_A, \bar{q}_B). \tag{5.21}$$

The conditional probability is

$$P(q_B \in \mathcal{B} \mid q_A \in \mathcal{A}) = \frac{P(q_A \in \mathcal{A} \cap q_B \in \mathcal{B})}{P(q_A \in \mathcal{A})}, \tag{5.22}$$

where $P(q_A \in \mathcal{A})$ is the one-particle probability. In the limit of small a, b this becomes

$$P(q_B \in \mathcal{B} \mid q_A \in \mathcal{A}) = 2b\frac{\rho(\bar{q}_A, \bar{q}_B; \bar{q}_A, \bar{q}_B)}{\rho^A(\bar{q}_A, \bar{q}_A)}. \tag{5.23}$$

In each case the small-a, b limit can be easily evaluated: we find

$$\rho(\bar{q}_A, \bar{q}_B; \bar{q}_A, \bar{q}_B) = \zeta_2 \exp(-\frac{(\bar{q}_A + \bar{q}_B)^2}{2\sigma_+^2} - \frac{(\bar{q}_A - \bar{q}_B)^2}{2\sigma_-^2}) \tag{5.24}$$

with 'classical' standard deviations

$$\begin{aligned} \sigma_+^C &= \frac{1}{2(L_{11} + L_{12})} \\ &= \sqrt{2}, \end{aligned} \tag{5.25}$$

$$\begin{aligned} \sigma_-^C &= \frac{1}{2(L_{11} - L_{12})} \\ &= (\frac{2}{\sqrt{1+4\alpha}})^{\frac{1}{2}}, \end{aligned} \tag{5.26}$$

and

$$\frac{\rho(\bar{q}_A, \bar{q}_B; \bar{q}_A, \bar{q}_B)}{\rho^A(\bar{q}_A, \bar{q}_A)} = \zeta_3 \exp(-\frac{\bar{q}_A^2}{2\sigma_1^2} + \frac{\bar{q}_A\bar{q}_B}{2\sigma_{12}^2} - \frac{\bar{q}_B^2}{2\sigma_2^2}) \tag{5.27}$$

with

$$\begin{aligned} \sigma_1 &= \frac{4}{(L_{11} + \upsilon_2 - \upsilon_1)} \\ &= (\frac{(1+\sqrt{1+4\alpha})(1+2\alpha+\sqrt{1+4\alpha})}{4\alpha^2})^{\frac{1}{2}}; \\ \sigma_2 &= \frac{1}{4L_{11}} \end{aligned} \tag{5.28}$$

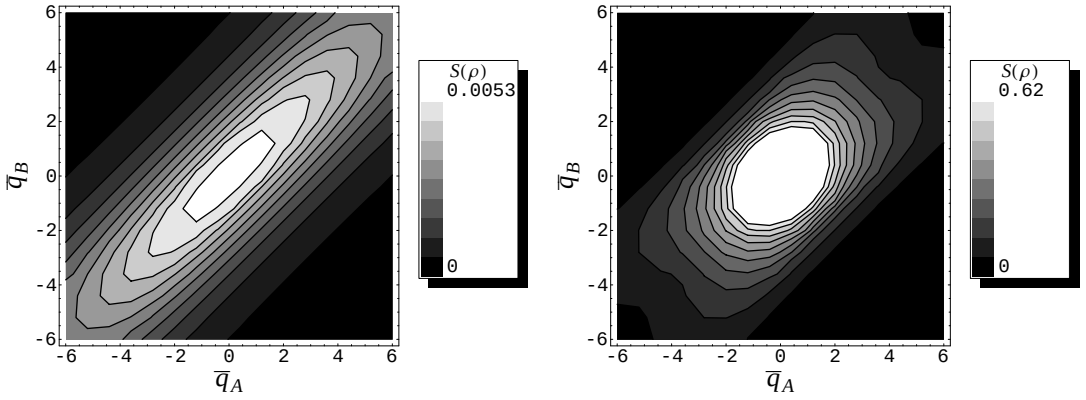

(a) $2a = 0.5$ (b) $2a = 4$

Figure 5.4: Dependence of the entanglement $S_v(\rho_D^A)$ on the locations of the centres of the preliminary-measurement regions $\bar{q}_A$ and $\bar{q}_B$. (a) the width $2a$ of the regions is 0.5. (b) $2a = 4$. In both cases, $N_B = 100$ and $\alpha = 6$.

$$= \left(\frac{2}{1+\sqrt{1+4\alpha}}\right)^{\frac{1}{2}}; \tag{5.29}$$

$$\sigma_{12} = \frac{-1}{8L_{12}}$$

$$= \left(\frac{1}{\sqrt{1+4\alpha}-1}\right)^{\frac{1}{2}}, \tag{5.30}$$

where ζ_2 and ζ_3 are normalisation constants.

For finite a and b we capture the shape of the distributions by fitting the numerically calculated values of $P(q_A \in \mathcal{A} \cap q_B \in \mathcal{B})$, and $P(q_B \in \mathcal{B} \mid q_A \in \mathcal{A})$ using the same expressions, equation 5.24 and equation 5.27, thereby extracting numerical values for $\sigma_{\pm}^C$, $\sigma_{1,2}$ and σ_{12}. We also use the function, equation 5.24, to fit the entanglement distribution, thereby obtaining two further parameters $\sigma_{\pm}^Q$ which quantify the extent of the entanglement distribution along its principal axes.

As before, we take $\alpha = 6$. In Figure 5.4, we show two cases of entanglement distributions for different widths ($2a = 0.5$ and $2a = 4$) of the preliminary-measurement regions. We see that the entanglement distribution with larger $2a$ is more symmetric. The corresponding joint probability distributions and conditional probability distributions are shown respectively in Figure 5.5 and Figure 5.6. (Note that the figures show different range of $\bar{q}_A$ and $\bar{q}_B$.) The classical probability distributions $P(\bar{q}_A \cap \bar{q}_B)$ are more localised and symmetric in space than the entanglement distributions.

In the limit of very small a, $S_v(\rho_D^A)$ is constant everywhere (equation 5.19) so σ_+^Q and σ_-^Q must diverge; the results in Table 5.1 show that σ_+^Q diverges more quickly as a reduces, while

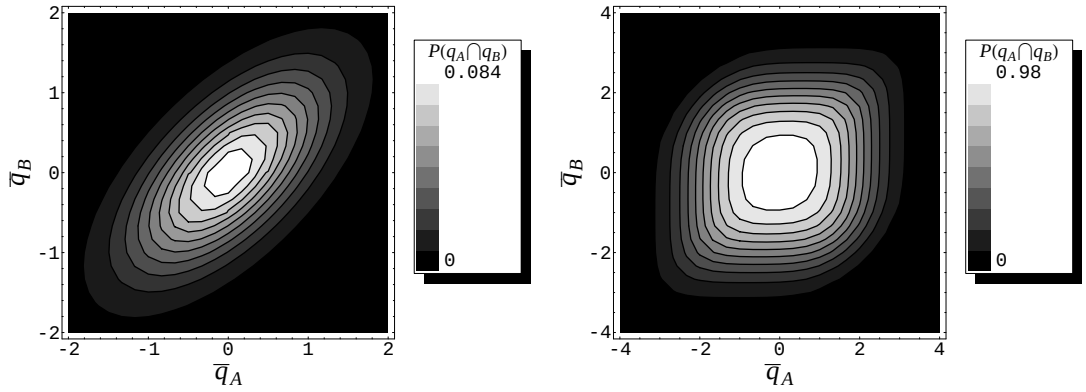

(a) $2a = 0.5$ (b) $2a = 4$

Figure 5.5: The dependence of the classical joint probability $P(q_A \in \mathcal{A} \cap q_B \in \mathcal{B})$ on $\bar{q}_A$ and $\bar{q}_B$. (a) $2a = 0.5$. (b) $2a = 4$. In both cases, $\alpha = 6$.

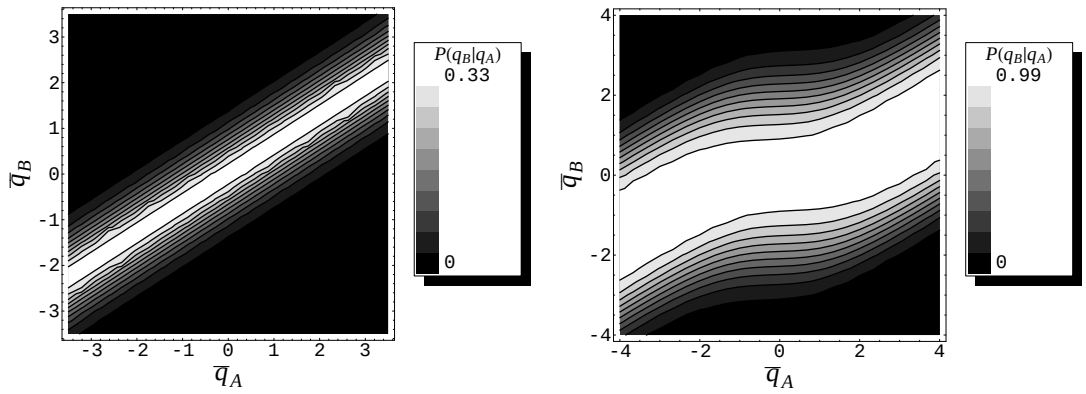

(a) $2a = 0.5$ (b) $2a = 4$

Figure 5.6: Dependence of the conditional probability $P(q_B \in \mathcal{B} \mid q_A \in \mathcal{A})$ on $\bar{q}_A$ and $\bar{q}_B$. (a) $2a = 0.5$. (b) $2a = 4$. In both cases, $\alpha = 6$.

$\alpha = 6$	σ_+^Q	σ_-^Q	σ_+^C	σ_-^C	σ_1	σ_2	σ_{12}
$2a \to 0$	∞	∞	1.41	0.632	0.866	0.577	0.500
$2a = 0.5$	10.4	2.29	1.43	0.665	0.937	0.603	0.531
$2a = 4$	3.44	2.10	2.37	2.00	11.0	1.53	2.64

Table 5.1: Table of σ values for $\alpha = 6$.

the two parameters become comparable for large a as the entanglement distribution becomes more symmetric. Indeed, the distributions of the entanglement and the classical correlations become more alike as $2a$ increases, because both distributions are flat out to a distance a either side of the wavefunction's central peak.

We can also study the effect of varying the coupling strength α for a fixed (small) $2a$. We plot σ_+^Q and σ_-^Q against α with $2a = 0.5$ in Figure 5.7a whereas σ_+^C, σ_-^C, σ_1, σ_2 and σ_{12} in Figure 5.7b. The entanglement distribution is the most asymmetrical and as α increases, the difference between σ_+^Q and σ_-^Q widens. Of the quantities determining the classical probability distribution, σ_+^C remains constant with increasing α, but σ_-^C gradually decreases. These trends arise because the two particles tend to move together when the spring joining them becomes strong. Therefore, as α increases, the white rod in Figure 5.6 rotates about the centre of the square from the line $\bar{q}_B = 0$ towards the diagonal $\bar{q}_A = \bar{q}_B$. σ_1 is always the largest out of the three parameters for the conditional probability distribution. For weak α, σ_{12} is larger than σ_2 but as α becomes larger, at some point the two plots intercept and σ_{12} is no longer larger than σ_2.

How in the limit of very small a these quantities (equations 5.25, 5.26, 5.28, 5.29, 5.30) vary with α is shown in Figure 5.7c. We see that the behaviour of these quantities does not change much, compared with the previous results when $2a = 0.5$, apart from that the interception points happen at smaller α. Note that $\sigma_\pm^Q$ diverge as $a \to 0$, so these parameters are not shown.

5.5 Non-Gaussian Mixed States

5.5.0.4 The state

Even though we have so far only considered Gaussian pure states, it is also straightforward to apply our local approach to map the entanglement distributions of non-Gaussian mixed states, provided we use suitable quantities as the entanglement measure (for example, the negativity $\mathcal{N}$). Here we will provide an example to demonstrate this.

Consider a mixed state that is a mixture of Bell states:

$$\rho_e = p|\Phi^+\rangle\langle\Phi^+| + (1-p)|\Psi^+\rangle\langle\Psi^+| \tag{5.31}$$

$$= \frac{p}{2}\Big(|00\rangle + |11\rangle\Big)\Big(\langle 00| + \langle 11|\Big) + \frac{(1-p)}{2}\Big(|01\rangle + |10\rangle\Big)\Big(\langle 01| + \langle 10|\Big), \tag{5.32}$$

with a probability p. Note that when $p = 1/2$, the state ρ_e is separable. By choosing $|0\rangle$ and $|1\rangle$ as the ground state and the first excited state of a system with a infinite symmetric square-well

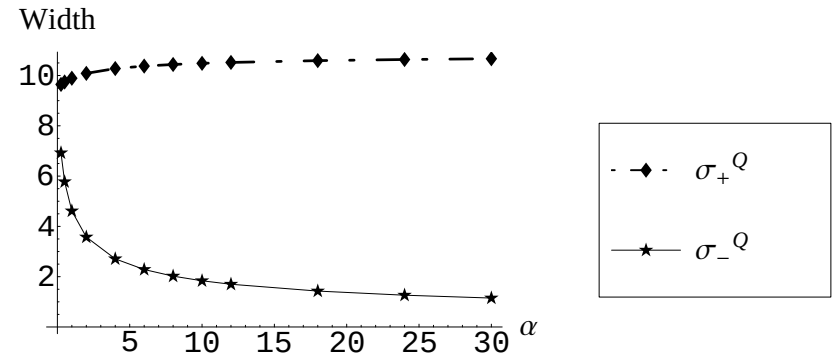

(a) $\sigma_{\pm}^{Q}$; $2a = 0.5$

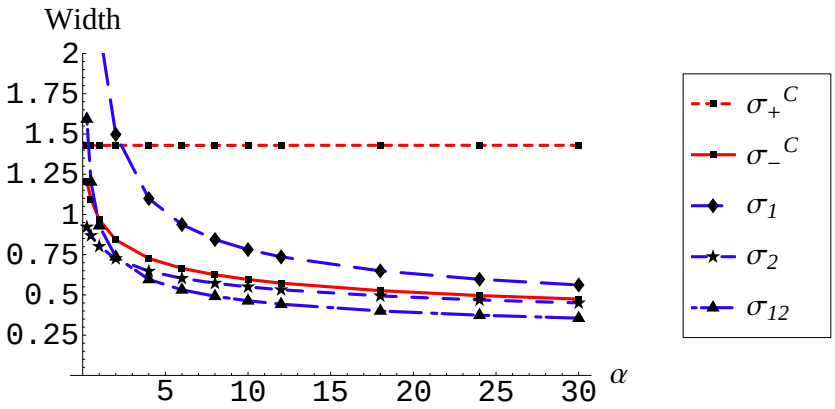

(b) $2a = 0.5$

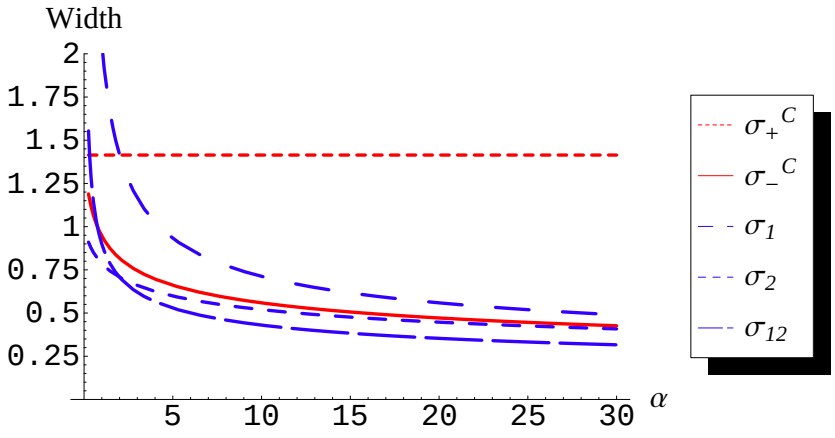

(c) Small-a limit

Figure 5.7: Plots of σ_+, σ_-, σ_1, σ_{12} and σ_2 against α. In the plot legend, Q stands for the 'quantum' entanglement distribution and C for the 'classical' probability distribution. (a) and (b): Numerical results: $2a$ is chosen to be 0.5 for all the cases. (c) Analytical results: in the limit of very small a.

potential (from $q = -0.5$ to $q = +0.5$) [Zet01]:

$$|0\rangle = \sqrt{2}\cos(\pi q) \tag{5.33}$$

$$|1\rangle = \sqrt{2}\sin(2\pi q), \tag{5.34}$$

ρ_e describes a non-Gaussian continuous-variable system.

5.5.0.5 Results

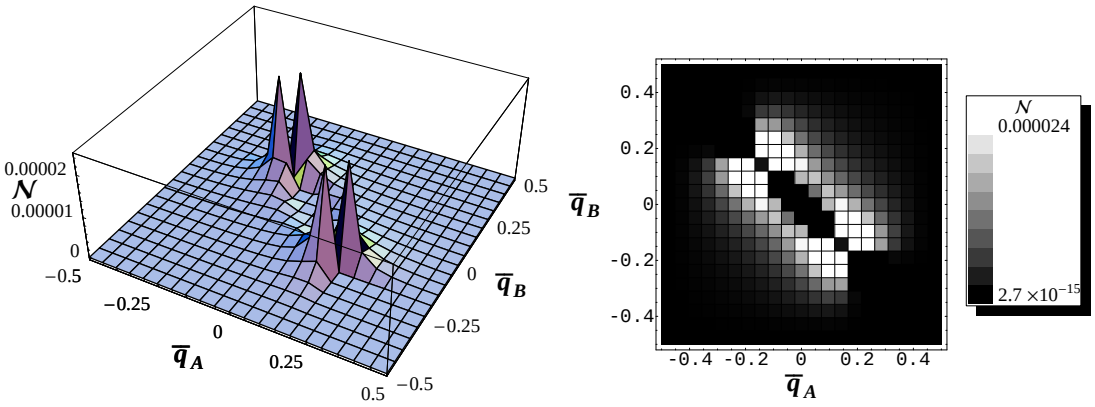

(a) $2a = 0.001$

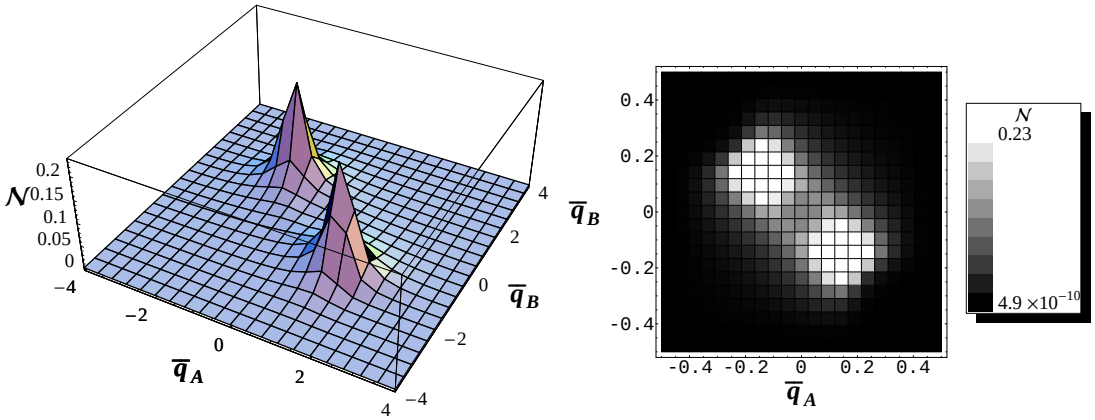

(b) $2a = 0.1$

Figure 5.8: Dependence of the entanglement $\mathcal{N}(\rho_D)$ on the locations of the centres of the preliminary-measurement regions $\bar{q}_A$ and $\bar{q}_B$ for a non-Gaussian mixed state ρ_e, described in Section 5.5. (a) the width $2a$ of the regions is 0.001. (b) $2a = 0.1$. In both cases, $N_B = 20$.

The state ρ_e with $p = 0.2$ is chosen as an example. We consider the case where both parties make preliminary measurements and the rest of the analysis follows from Section 5.3.2. Note that here the entanglements are quantified by the negativity; the original density matrix ρ_e will be discretised instead of the reduced density matrix ρ^A. The widths of the measured

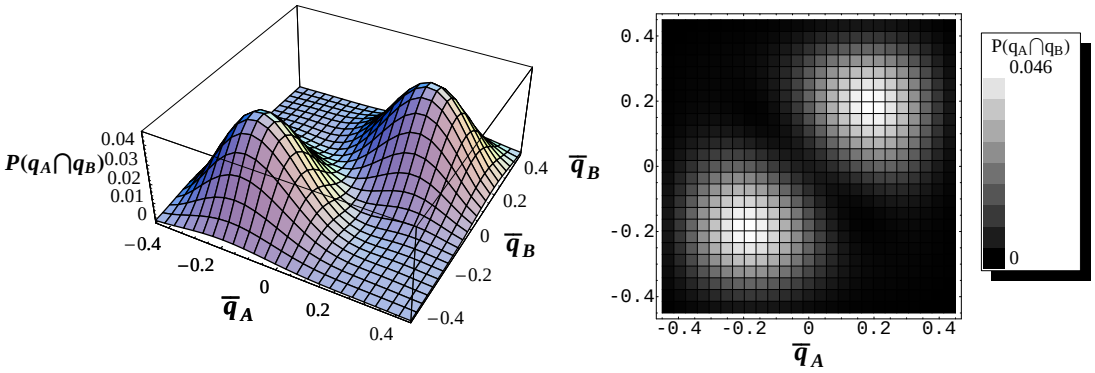

Figure 5.9: Dependence of the joint probability $P(q_A \in \mathcal{A} \cap q_B \in \mathcal{B})$ on the locations of the centres of the preliminary-measurement regions $\bar{q}_A$ and $\bar{q}_B$ for a non-Gaussian mixed state ρ_e, described in Section 5.5. (a) the width $2a$ of the regions is 0.001. (b) $2a = 0.1$.

regions are the same for both parties $a = b$. In Figure 5.8, we show two cases of entanglement distributions, by moving the centres of the measured regions $\bar{q}_A$ and $\bar{q}_B$ within the potential well, for different widths: (a) $2a = 0.001$ and (b) $2a = 0.11$. The corresponding distribution of the two-particle probability $P(q_A \in \mathcal{A} \cap q_B \in \mathcal{B})$ (as defined by equation 5.20) is also shown in Figure 5.9 for comparison; the widths are set to $2a = 2b = 0.1$ and the region centres, $\bar{q}_A$ and $\bar{q}_B$, vary from -0.45 to $+0.45$. Interestingly, the entanglements are not the highest at places where the particles are most likely to be found in contrast to the earlier Gaussian examples. We can also see that the entanglements are "concentrated" in particular places, and the entanglement distribution is broadened out for the larger region.

5.6 Summary

Our local approach to entanglement (Section 4.2) is applied to determine the location in configuration space of the entanglement between two interacting subsystems. Specifically, we consider states of a continuous-variable system in which Alice and Bob share a pair of coupled harmonic oscillators is given. The results are presented as a function of the strength of the coupling between the oscillators, as well as of the size and location of the preliminary measurement regions. In all cases the remaining entanglement saturates to the total entanglement of the system as the measured regions become large. For small measured regions the entanglement tends to zero, but for a fixed region size, the configuration-space location can be varied in order to give a variable-resolution map of the entanglement distribution. We find that the distribution of the entanglement is qualitatively different from the classical correlations between the particles,

being considerably more extended in configuration space than the joint probability density and becoming more and more diffuse as the size of the regions decreases.

An example is also given to demonstrate that it is straightforward to apply the local approach to make a variable-resolution map of entanglement distributions of mixed non-Gaussian states by using suitable quantities (for example, the negativity $\mathcal{N}$) as the entanglement measure instead of the von Neumann entropy S_v that is applicable only to pure states. The entanglement maps show that the entanglements are concentrated at some portions of configuration space and by increasing the size of the measured region, the entanglement distribution is smoothed out. The previous Gaussian example shows that the entanglement distribution and the joint probability distribution peak around the same region of space, but this is not true in this non-Gaussian example.

We conclude that this approach therefore provides an operational answer to the question of how much entanglement was originally located within the chosen region. We shall thus focus on the limiting cases where the sizes of the chosen regions are extremely small in the rest of the thesis, surprisingly many interesting results can then be derived.

Chapter 6

Entanglement in General Two-Mode Continuous-Variable States: Local Approach and Mapping to Two-Qubit Systems

6.1 Introduction

In this chapter we demonstrate how to apply our local approach to the analysis of continuous-variable entanglement, allowing entanglement to be quantified locally in general (including non-Gaussian) smooth two-mode continuous-variable states. We follow the approach, laid out in Section 4.2 and applied to some harmonic system in Chapter 5, but this time we consider the limit where the sizes of the preliminary regions are supposed to be extremely small. Interestingly in this limit, the description of each mode in the continuous-variable quantum state becomes isomorphic to a single qubit. This enable us to derive simple closed-form formulae for local entanglements (concurrence and negativity), yielding natural definitions for corresponding densities in configuration space.

First, we treat the pure states in Section 6.2 by making the low-order Taylor series approximation; the use of the approximation is justified in the small-region limit. Next, the analysis is extended to mixed states in Section 6.3, where we give the recipe to compute the local concurrence numerically and derive an analytical formula for the local negativity. We apply our formula to two-mode Gaussian states in Section 6.4 and show how the two local entanglements are simply related (differing only by a factor of 2). Some examples of non-Gaussian states are then analysed in Section 6.5. Finally, we summarise in Section 6.7.

6.2 Pure States

6.2.1 Preliminary measurement on Alice's particle only

The localising process is as described in Section 4.2. Suppose the state ρ is pure; so is ρ_D. It is therefore straightforward to calculate its local entanglement from the von Neumann entropy of the corresponding reduced density matrix $\rho_D^A = \mathrm{Tr}_B[\rho_D]$. Suppose further that the initial preliminary measurement is performed by Alice only, by determining whether q_A lies in the region $\mathcal{A} := \{\overline{q}_A - a \leq q_A \leq \overline{q}_A + a\}$, and all instances in which this is not the case are discarded. Now, since a is to be very small, Alice's original reduced density matrix ρ^A (before the measurement) in the neighbourhood of $\overline{q}_A$ can be expanded (provided it is smooth in configuration space) as [1]

$$\begin{aligned}\rho^A(q_A, q'_A) &= \rho^A(\overline{q}_A + x, \overline{q}_A + y) \\ &= \rho^A_{00} + \rho^A_{10}x + \rho^A_{01}y + \rho^A_{11}xy + \mathcal{O}(x^2, y^2),\end{aligned} \tag{6.1}$$

where

$$\rho^A_{nm} \equiv \frac{\partial^n}{\partial {q_A}^n}\frac{\partial^m}{\partial {q'_A}^m}\rho^A(q_A, q'_A)\Big|_{q_A = q'_A = \overline{q}_A}. \tag{6.2}$$

Within region $\mathcal{A}$, ρ_D^A is obtained by rescaling ρ^A according to equation 4.2, where $\mathrm{Tr}[E_{\mathcal{A}}\,\rho] = 2a[\rho^A_{00} + \mathcal{O}(a^2)]$.

Now seek right eigenfunctions ϕ_n of ρ_D^A within the region $\mathcal{A}$:

$$\int_{-a}^{a} \mathrm{d}y\, \rho_D^A(x, y)\phi_n(y) = \lambda_n \phi_n(x). \tag{6.3}$$

Expanding ϕ_n as a power series

$$\phi_n(x) = a_n + b_n x + \mathcal{O}(x^2), \tag{6.4}$$

the eigenfunction condition becomes a matrix-vector equation operating on the expansion coefficients $\{a, b, \ldots\}$:

$$\begin{aligned}&\frac{1}{2a[\rho^A_{00} + \mathcal{O}(a^2)]}\left[a\begin{pmatrix} 2\rho^A_{00} & 0 & \ldots \\ 2\rho^A_{10} & 0 & \ldots \\ \vdots & \vdots & \ddots \end{pmatrix} + a^3\begin{pmatrix} \frac{\rho^A_{20}}{3} & \frac{2\rho^A_{01}}{3} & \ldots \\ 0 & \frac{2\rho^A_{11}}{3} & \ldots \\ \vdots & \vdots & \ddots \end{pmatrix}\right]\begin{pmatrix} a_n \\ b_n \\ \vdots \end{pmatrix} \\ \equiv\ &\mathbf{M}\begin{pmatrix} a_n \\ b_n \\ \vdots \end{pmatrix} = \lambda_n \begin{pmatrix} a_n \\ b_n \\ \vdots \end{pmatrix}.\end{aligned} \tag{6.5}$$

[1] The low-order Taylor series approximation is well justified. In practice any state that could be prepared would be smooth and differentiable; in such cases Taylor's theorem ensures that the expansion we use becomes rapidly better for small region sizes. Later in this chapter, Figure 6.1 shows explicitly how the local entanglement converges to our predicted small-region limit as the region size is varied.

Expanding $\det(\mathbf{M}-\lambda\mathbb{1})$ to order a^4 and equating to zero, to order a^2, the non-zero eigenvalues are:

$$\begin{aligned}\lambda_1 &= \frac{a^2}{3(\rho^A_{00})^2}(\rho^A_{11}\rho^A_{00}-\rho^A_{01}\rho^A_{10}) \\ \lambda_2 &= 1-\lambda_1. \end{aligned} \tag{6.6}$$

So to the lowest non-trivial[2] order (a^2), the eigenvalues, and hence the von Neumann entropy of ρ^A_D, are entirely determined by the quantity

$$\epsilon \equiv \lambda_1. \tag{6.7}$$

Specifically, the von Neumann entropy in this case is $S_v(\rho^A_D) = h(\epsilon)$ in equation 3.29. Note that if Alice's state is pure,

$$\begin{aligned}\rho^A(q_A,q'_A) &= \psi(q_A)\psi^*(q'_A) \\ \Rightarrow \quad \rho^A_{00} &= \psi(\overline{q}_A)\psi^*(\overline{q}_A) \\ \rho^A_{10} &= \frac{\partial\psi(q_A)}{\partial q_A}\Big|_{q_A=\overline{q}_A}\psi^*(\overline{q}_A) \\ \rho^A_{01} &= \psi(\overline{q}_A)\frac{\partial\psi^*(q'_A)}{\partial q'_A}\Big|_{q'_A=\overline{q}_A} \\ \rho^A_{11} &= \frac{\partial\psi(q_A)}{\partial q_A}\Big|_{q_A=\overline{q}_A}\frac{\partial\psi^*(q'_A)}{\partial q'_A}\Big|_{q'_A=\overline{q}_A}\end{aligned} \tag{6.8}$$

and therefore

$$\rho^A_{11}\rho^A_{00} = \rho^A_{01}\rho^A_{10}, \tag{6.9}$$

so $S_v(\rho^A_D)$ is zero as we would expect.

To find the leading corrections to this result (equation 6.6), we include all terms proportional to x^2 or x'^2 in the expansion 6.1 for ρ^A:

$$\begin{aligned}\rho^A(x;x') &= \rho^A_{00}+\rho^A_{10}x+\rho^A_{01}x' \\ &\quad +\frac{1}{2}(\rho^A_{20}x^2+\rho^A_{02}x'^2+2\rho^A_{11}xx') \\ &\quad +\frac{1}{2}(\rho^A_{21}x^2x'+\rho^A_{12}xx'^2) \\ &\quad +\frac{1}{4}\rho^A_{22}x^2x'^2+\mathcal{O}(x^3,x'^3).\end{aligned} \tag{6.10}$$

[2]If the amplitude of the wavefunction (or density matrix) is perfectly constant over the measurement region, there is no entanglement. Indeed, this is why we find no term in the local entanglement zeroth-order in the region size. Our point is that by capturing the extent to which the state is *not* constant (through including the lowest-order non-constant terms in its Taylor expansion), we extract the most important contributions to the local entanglement for small region sizes.

and then carry equation 6.4 to third order:

$$\phi_n(x) = a_n + b_n x + \frac{1}{2}c_n x^2 + \frac{1}{6}d_n x^3 + \mathcal{O}(x^4). \tag{6.11}$$

From the eigenfunction condition 6.3, we find the third non-zero eigenvalue to be

$$\begin{aligned}\lambda_3 \;=\; & \frac{a^4}{90{\rho_{00}^A}^2(\rho_{01}^A\rho_{10}^A - \rho_{11}^A\rho_{00}^A)}\big(\rho_{02}^A\rho_{11}^A\rho_{20}^A \\ & +\rho_{01}^A\rho_{22}^A\rho_{10}^A + \rho_{12}^A\rho_{00}^A\rho_{21}^A - \rho_{01}^A\rho_{12}^A\rho_{20}^A \\ & -\rho_{10}^A\rho_{02}^A\rho_{21}^A - \rho_{00}^A\rho_{11}^A\rho_{22}^A\big) + \mathcal{O}(a^6).\end{aligned} \tag{6.12}$$

Therefore, the corrections due to higher eigenvalues, arising from the higher-order terms in equation 6.1, affect ϵ (and hence the local entanglement) only to order a^4. This provides a measure of the extent of the breakdown of the approximation.

6.2.2 Preliminary measurement on both particles

It is possible to generalise this analysis to the case where both Alice and Bob make a preliminary measurement to localise their particles, within regions $\mathcal{A} := \{\overline{q}_A - a \leq q_A \leq \overline{q}_A + a\}$ and $\mathcal{B} := \{\overline{q}_B - b \leq q_B \leq \overline{q}_B + b\}$ respectively. In that case one can expand ρ as a joint power series in $\{q_A, q'_A, q_B, q'_B\}$, calculate the reduced density matrix ρ^A (also as a power-series expansion) and proceed as above. However, further insight can be obtained by an alternative approach. Define for both Alice and Bob two-dimensional state spaces consisting of

$$\begin{aligned}\phi_{A0}(x_1) &= \sqrt{\frac{1}{2a}}; \qquad \phi_{A1}(x_1) = \sqrt{\frac{3}{2a^3}}x_1; \\ \phi_{B0}(x_2) &= \sqrt{\frac{1}{2b}}; \qquad \phi_{B1}(x_2) = \sqrt{\frac{3}{2b^3}}x_2,\end{aligned} \tag{6.13}$$

which are orthonormal on the intervals $-a < x_1 < a$ and $-b < x_2 < b$ respectively; ϕ_0 represents the constant component of the wave function, and ϕ_1 the spatially varying part. So long as terms varying as x^2 or higher can be neglected, a Taylor expansion of the joint state to linear order (equation 6.1) is equivalent to expanding ψ in the basis (equation 6.13), thereby reducing the joint system to a two-qubit one. It can be shown (Appendix E) that the third largest eigenvalue of ρ^A (corresponding to the extent to which the two-qubit approximation fails) is now of order $(ab)^4$.

We can now use any of the standard measures of the entanglement of the two-qubit system. For pure states, the tangle [Woo98c] is

$$\tau = \frac{1}{4}\left(\frac{1}{ab|\psi_{00}|^2}\right)^2 \left|\frac{4a^2b^2}{3}(\psi_{00}\psi_{11} - \psi_{01}\psi_{10})\right|^2, \tag{6.14}$$

where

$$\psi_{nm} \equiv \frac{\partial^n}{\partial {q_A}^n}\frac{\partial^m}{\partial {q_B}^m}\psi(q_A, q_B)|_{q_A=\overline{q}_A, q_B=\overline{q}_B}. \tag{6.15}$$

The prefactor in equation 6.14 comes from the normalisation condition

$$\int_{-a}^{a} \mathrm{d}x_1 \int_{-b}^{b} \mathrm{d}x_2 |\psi(x_1, x_2)|^2 = 1. \tag{6.16}$$

The entanglement is therefore

$$h\left((1-\sqrt{1-\tau})/2\right) = h\left(\tau/4 + \mathcal{O}(\tau^2)\right). \tag{6.17}$$

By analogy with the definition of concurrence $\mathcal{C} = \sqrt{\tau}$ for two-qubit states [Woo98b], we define the *concurrence density* $c \equiv \mathcal{C}/(ab)$ such that $\tau = (cab)^2$; then

$$\begin{aligned} c &= \frac{2}{3\rho_{0000}}[\rho_{1100}\rho_{0011} + \rho_{0000}\rho_{1111} \\ &\quad -\rho_{1000}\rho_{0111} - \rho_{0100}\rho_{1011}]^{1/2}, \end{aligned} \tag{6.18}$$

where

$$\rho_{ijkl} \equiv \frac{\partial^i}{\partial {q_A}^i} \frac{\partial^j}{\partial {q'_A}^j} \frac{\partial^k}{\partial {q_B}^k} \frac{\partial^l}{\partial {q'_B}^l} \rho(q_A, q_B; q'_A, q'_B)\Big|_{q_A = q'_A = \overline{q}_A, q_B = q'_B = \overline{q}_B}. \tag{6.19}$$

For pure states, $\rho_{ijkl} = \psi_{ik}\psi^*_{jl}$.

The negativity $\mathcal{N}$, defined by equation 3.34 can also be computed. For pure states, negativity and concurrence are simply related [EP99, CAF05]: $\mathcal{N} = \mathcal{C}/2$.

The accuracy of the two-qubit approximation is guaranteed (for sufficiently small a and b) by the fact that each party's reduced density matrix has only two non-zero eigenvalues of the density matrix to order $(ab)^2$.

6.3 Mixed States

The mapping to a two-qubit system applies also to mixed states, where exact recipes for the entanglement of formation [Woo98b] and other measures are known. We find that for mixed states ρ with the *rank* greater or equal to 4, all eigenvalues μ_i of $\rho\tilde{\rho}$ (as defined in [Woo98b], where $\tilde{\rho}$ is the "spin-flipped" matrix) are at leading order proportional to $(ab)^2$. However, the rank determines the number of eigenvalues μ_i that are non-zero to order $(ab)^2$ so the rank-1 states have only one non-zero eigenvalue (μ_4) to order $(ab)^2$, the rank-2 states have only two (μ_3, μ_4) and the rank-3 states have only three (μ_2, μ_3, μ_4).

The local concurrence is determined by $\mathcal{C} = \max\{0, \sqrt{\mu_4} - \sqrt{\mu_3} - \sqrt{\mu_2} - \sqrt{\mu_1}\}$ so again there is a well-defined concurrence density c (since the local concurrence $\mathcal{C} \propto (ab)$). These leading terms (and hence the concurrence $\mathcal{C}$) can be found by solving a quartic, although its roots are not simple in general. The solutions for rank-2 states are nevertheless given in Appendix B.

6.3.1 Negativity

Particularly simple expressions can be found for the local negativity of a mixed state. The eigenvalues of the partially transposed density matrix $\hat{\rho}^{T_A}$ are found to be

$$\begin{aligned}
\lambda_1 &= 1 - A_1 a^2 - A_2 b^2 - B_1 a^2 b^2 + \mathcal{O}(a^4, b^4) \\
\lambda_2 &= C_2 a^2 b^2 + \mathcal{O}(a^4, b^4) \\
\lambda_3 &= \frac{1}{2}\left(D_1 a^2 + D_2 b^2 + \sqrt{4C_1 a^2 b^2 + (D_1 a^2 + D_2 b^2)^2}\right) + \mathcal{O}(a^4, b^4) \\
\lambda_4 &= \frac{1}{2}\left(D_1 a^2 + D_2 b^2 - \sqrt{4C_1 a^2 b^2 + (D_1 a^2 + D_2 b^2)^2}\right) + \mathcal{O}(a^4, b^4)
\end{aligned} \tag{6.20}$$

where A_1, A_2, B_1, C_1, C_2, D_1 and D_2 are all real numbers. D_1 and D_2 are always positive (Appendix C). Only C_1, C_2, D_1 and D_2 are important for quantifying the local entanglement[3], and their exact expressions are.

$$D_1 = \frac{1}{3{\rho_{0000}}^2}(\rho_{1100}\rho_{0000} - \rho_{0100}\rho_{1000}); \tag{6.21}$$

$$D_2 = \frac{1}{3{\rho_{0000}}^2}(\rho_{0011}\rho_{0000} - \rho_{0001}\rho_{0010}); \tag{6.22}$$

$$\begin{aligned}
C_1 = \frac{1}{9{\rho_{0000}}^3}(&\rho_{0000}\rho_{0101}\rho_{1010} + \rho_{0011}\rho_{0100}\rho_{1000} + \rho_{0010}\rho_{0001}\rho_{1100} \\
&-\rho_{0001}\rho_{0100}\rho_{1010} - \rho_{0000}\rho_{0011}\rho_{1100} - \rho_{0010}\rho_{1000}\rho_{0101});
\end{aligned} \tag{6.23}$$

$$\begin{aligned}
C_2 = \frac{-1}{81\, C_1\, {\rho_{0000}}^4}(&\rho_{0101}\rho_{0110}\rho_{1001}\rho_{1010} - \rho_{0100}\rho_{0111}\rho_{1001}\rho_{1010} - \rho_{0101}\rho_{0110}\rho_{1000}\rho_{1011} \\
&+\rho_{0100}\rho_{0111}\rho_{1000}\rho_{1011} - \rho_{0011}\rho_{0110}\rho_{1001}\rho_{1100} + \rho_{0010}\rho_{0111}\rho_{1001}\rho_{1100} \\
&+\rho_{0001}\rho_{0110}\rho_{1011}\rho_{1100} - \rho_{0000}\rho_{0111}\rho_{1011}\rho_{1100} + \rho_{0011}\rho_{0110}\rho_{1000}\rho_{1101} \\
&-\rho_{0010}\rho_{0111}\rho_{1000}\rho_{1101} - \rho_{0001}\rho_{0110}\rho_{1010}\rho_{1101} + \rho_{0000}\rho_{0111}\rho_{1010}\rho_{1101} \\
&+\rho_{0011}\rho_{0100}\rho_{1001}\rho_{1110} - \rho_{0010}\rho_{0101}\rho_{1001}\rho_{1110} - \rho_{0001}\rho_{0100}\rho_{1011}\rho_{1110} \\
&+\rho_{0000}\rho_{0101}\rho_{1011}\rho_{1110} + \rho_{0001}\rho_{0010}\rho_{1101}\rho_{1110} - \rho_{0011}\rho_{1101}\rho_{1110}\rho_{0000} \\
&-\rho_{0011}\rho_{0100}\rho_{1000}\rho_{1111} + \rho_{0010}\rho_{0101}\rho_{1000}\rho_{1111} + \rho_{0001}\rho_{0100}\rho_{1010}\rho_{1111} \\
&-\rho_{0000}\rho_{0101}\rho_{1010}\rho_{1111} - \rho_{0001}\rho_{0010}\rho_{1100}\rho_{1111} + \rho_{0000}\rho_{0011}\rho_{1100}\rho_{1111}).
\end{aligned} \tag{6.24}$$

The entanglement can be quantified by the negative eigenvalue, and in the effective two-qubit approximation, there is only one negative eigenvalue [VADM01]. We will now discuss which λ is negative under all the possible circumstances.

[3]Local entanglement should vanish when either a or b become zero. If λ_1 is negative, the local negativity will depend on it. In this case, we can always find some sufficiently small values of a and b such that λ_1 becomes positive, whatever the values of the coefficients A_1, A_2 and B_1, to make the local entanglement vanish at some very small but non- zero values of a and b. Combined with the fact that the partial transpose of a two-qubit density matrix has only one negative eigenvalue, this implies that λ_1 must always be positive.

We note λ_2 and λ_4 are invariant under the change of sign of either a or b; provided that $C_1 > 0$, λ_4 is always negative, and it becomes zero when either a or b vanishes so there is no entanglement ($\mathcal{N} = 0$) as expected. The negativity in this case is second order in a and b. However, if $C_1 < 0$ and $C_2 \geq 0$, the state is unentangled whereas if $C_1 < 0$ but $C_2 < 0$, λ_2 becomes the only negative eigenvalue, and hence the negativity in this case is proportional to $(ab)^2$.

It is worth noting that there is also no entanglement whenever $C_1 = 0$. Since the positivity of the partial transpose of a state is a sufficient condition to prove that the *distillable entanglement* is zero, there is no entanglement if either $C_1 = 0$ or $C_1 < 0$ and $C_2 \geq 0$ is true.

When the initial joint quantum state is pure, C_2 reduces to C_1, i.e. $C_2 = C_1$ for pure states, while D_1 and D_2 vanish, and C_1 reduces to the same expression for the pure-state concurrence divided by 2, i.e.[4]

$$\mathcal{N}(\psi) = \frac{\mathcal{C}(\psi)}{2} \tag{6.25}$$

as what we would expect (with our definition of negativity) for a two-qubit pure state.

We could not analytically obtain the eigenvalues of $\rho\tilde{\rho}$ in the most general case but we found from our calculations that the concurrence is always proportional to (ab) in the leading order for any smooth two-mode state in contrast to negativity. Therefore, equation (6.25) does not generally hold for mixed states. This observation is consistent with the prior study [MG04] on the ordering of two-qubit states with respect to concurrence and negativity: the concurrence and the negativity are the same for two-qubit pure states[5] but for those states with the same concurrence, their negativity can vary between the maximum and the minimum. In general, the maximal negativity of two-qubit mixed states with a fixed concurrence can never exceed that concurrence [VADM01] while the minimum negativity is proportional to the concurrence squared (for small concurrence) [MG04]. It is not surprising then that the maximal local negativity is proportional to (ab), like the local concurrence, but the minimal local negativity is proportional to $(ab)^2$ instead.

Also, the local concurrence depends only on the "area" ab, whereas the local negativity depends on the "shape" (i.e. on a, b separately) as well. However, if we seek the maximum negativity while keeping (ab) fixed, we find this occurs when $a^2 D_1 = b^2 D_2$, to define the *maximised negativity* given by (only valid for $C_1 \geq 0$)

$$\mathcal{N}_{\max} = (\sqrt{C_1 + D_1 D_2} - \sqrt{D_1 D_2})ab, \tag{6.26}$$

[4]For pure states, as we will see later, we can apply equation 7.6 to obtain these results.

[5]They define the negativity in a way that makes it exactly two times larger than our version.

and subsequently obtain the corresponding *negativity density* $n = \mathcal{N}_{\max}/(ab)$ given by

$$n = \sqrt{C_1 + D_1 D_2} - \sqrt{D_1 D_2}. \tag{6.27}$$

Here we maximise the negativity by varying the shape (a/b) *for a fixed state*. Note the contrast with the approach of Miranowicz *et. al.* [MG04], where the states are varied so as to change the negativity while keeping the concurrence constant *for a given* a *and* b.

Since the local negativity of two-mode mixed states can be readily determined by our very simple closed-form formulae, this may lead one to wonder whether this result is straightforward to be extended to multi-mode mixed states. Unfortunately, this is not the case.[6] However, local entanglement of mixed states of higher-dimensional systems can still be easily computed numerically, provided the state is exactly known and the negativity (or the logarithmic negativity) is the chosen entanglement measure.

6.3.2 Bound states.

It is known that there is no bound entanglement for a two-qubit system. For (global) bound states, our local measures will give no local entanglement because there is no distillable entanglement $\mathcal{N} = 0$ and it follows that concurrence is also zero in the effective two-qubit approximation.

6.4 Gaussian States

The *characteristic function* χ is defined in terms of the Weyl operator W (taking $\hbar = 1$) through

$$\chi(X, P) = \mathrm{Tr}(\rho W(X, P)); \quad W(X, P) = e^{\mathrm{i}(X\hat{p} - P\hat{q})}, \tag{6.28}$$

where the position operator is denoted by $\hat{q}$ and the momentum operator by $\hat{p}$. A state ρ is said to be Gaussian when its characteristic function is a Gaussian in phase space. This important set of states includes both thermal and 'squeezed' states of harmonic systems and plays a key role in several fields of theoretical and experimental physics; we use them as an example because their entanglement properties are better understood than those of other continuous-variable systems, while recognising that our approach is general. The corresponding configuration-space density matrix $\rho(\mathbf{q}; \mathbf{q}')$ can be written as in equation 5.3. In order for $\rho(\mathbf{q}; \mathbf{q}')$ to be a valid quantum

[6] Later, we will show that the local concurrence and the local negativity differs only by a factor of 2 in the limit of very small measurement regions for any multi-mode bipartite pure states (equation 7.24) and the *squared* concurrence has a simple summation structure with linear contributions from each mode (equation 7.25). Consequently, each mode contributes *non-linearly* to the (non-squared) concurrence, and hence the negativity as well. This non-linear structure of the local negativity for pure multi-mode states therefore makes the derivation of the corresponding mixed-state results a non-trivial task.

state, the parameter matrices must have the following properties: $\mathbf{L} > 0$, $\mathbf{L} + \mathbf{M} > 0$ and $\mathbf{M} \geq 0$, such that the diagonal elements of the matrices satisfy $L_{ii} > 0$, $(L_{ii} + M_{ii}) > 0$ and $M_{ii} \geq 0$ for all i. In contrast to Section 5.2, here we are interested in the Gaussian state in its most general form so all matrices ($\mathbf{L}$, $\mathbf{M}$ and $\mathbf{K}$) are assumed to be non-zero.

6.4.1 $N = 2$: General states

The density matrix of a general two-mode Gaussian state is written as

$$\begin{aligned}\rho(q_1, q_2; q_1', q_2') &= \frac{2}{\pi}(L_{11}L_{22} - L_{12}^2)^{1/2} \exp\Big[-(q_1 L_{11} q_1 + q_1 L_{12} q_2 + q_2 L_{21} q_1 + q_2 L_{22} q_2) \\ &\quad -(q_1' L_{11} q_1' + q_1' L_{11} q_2' + q_2' L_{11} q_1' + q_2' L_{11} q_2') \\ &\quad -\frac{1}{2}(q_1 - q_1')M_{11}(q_1 - q_1') - \frac{1}{2}(q_1 - q_1')M_{12}(q_2 - q_2') \\ &\quad -\frac{1}{2}(q_2 - q_2')M_{21}(q_1 - q_1') - \frac{1}{2}(q_2 - q_2')M_{22}(q_2 - q_2') \\ &\quad +\frac{\mathrm{i}}{2}(q_1 - q_1')K_{11}(q_1 + q_1') + \frac{\mathrm{i}}{2}(q_1 - q_1')K_{12}(q_2 + q_2') \\ &\quad +\frac{\mathrm{i}}{2}(q_2 - q_2')K_{21}(q_1 + q_1') + \frac{\mathrm{i}}{2}(q_2 - q_2')K_{22}(q_2 + q_2')\Big]. \end{aligned} \tag{6.29}$$

In this case, the matrix conditions imply that $L_{12} = L_{21}$, $M_{12} = M_{21}$. By substituting equation 5.3 into equation 6.21, equation 6.22, equation 6.23 and equation 6.24, we obtain

$$D_1 = \frac{M_{11}}{3}; \tag{6.30}$$

$$D_2 = \frac{M_{22}}{3}; \tag{6.31}$$

$$C_1 = \frac{1}{36}\Big((K_{12} + K_{21})^2 + 4(2L_{12} + M_{12})^2 - 4M_{11}M_{22}\Big); \tag{6.32}$$

$$C_2 = \frac{1}{36}\Big((K_{12} + K_{21})^2 + 4(2L_{12} + M_{12})^2 + M_{11}M_{22}\Big). \tag{6.33}$$

D_1 and D_2 are always positive, as expected but note that C_2 is also always positive so the local negativity for two-mode Gaussian states is always proportional to (ab). Therefore, it is possible for the maximised negativity of a Gaussian state to be simply related to the local concurrence. We will prove now that this is indeed true.

From equation 6.26, the maximised negativity is equal to

$$\mathcal{N}_{\max} = \frac{ab}{6}\left(\sqrt{(K_{12} + K_{21})^2 + 4(2L_{12} + M_{12})^2} - 2\sqrt{M_{11}M_{22}}\right). \tag{6.34}$$

However, in this case, we can also find concurrence exactly; we find all eigenvalues μ_i of $\rho\tilde{\rho}$:

$$\mu_1 = \frac{a^2b^2}{36}\left(\sqrt{(K_{12} + K_{21})^2 + 4M_{12}^2} - 2\sqrt{M_{11}M_{22}}\right)^2; \tag{6.35}$$

$$\mu_2 = \frac{a^2b^2}{36}\left(\sqrt{(K_{12} + K_{21})^2 + 4M_{12}^2} + 2\sqrt{M_{11}M_{22}}\right)^2; \tag{6.36}$$

$$\mu_3 = \frac{a^2b^2}{36}\Bigg(\sqrt{(K_{12}+K_{21})^2+4(2L_{12}+M_{12})^2} - \sqrt{2K_{12}^2+2K_{21}^2+4(2L_{12}+M_{12})^2+4M_{12}^2+4M_{11}M_{22}}\Bigg)^2; \quad (6.37)$$

$$\mu_4 = \frac{a^2b^2}{36}\Bigg(\sqrt{(K_{12}+K_{21})^2+4(2L_{12}+M_{12})^2} + \sqrt{2K_{12}^2+2K_{21}^2+4(2L_{12}+M_{12})^2+4M_{12}^2+4M_{11}M_{22}}\Bigg)^2. \quad (6.38)$$

The matrix conditions ensure that μ_4 is the largest eigenvalue so the local concurrence $\mathcal{C}$ can be obtained from

$$\sqrt{\mu_4}-\sqrt{\mu_3}-\sqrt{\mu_2}-\sqrt{\mu_1} = \frac{ab}{3}\Bigg(\sqrt{(K_{12}+K_{21})^2+4(2L_{12}+M_{12})^2}-2\sqrt{M_{11}M_{22}}\Bigg). \quad (6.39)$$

Compared with equation 6.34, we note that the local concurrence $\mathcal{C}$ of any two-mode Gaussian states is always equal to two times the corresponding maximised negativity $\mathcal{N}_{\max}$. Unfortunately, this is not necessarily true for non-Gaussian states so for these non-Gaussian states, we have to either resort to numerical analysis or use the negativity as our choice of entanglement measure.

In addition, by comparing equation 6.32 with equation 6.39, we find that if $C_1 \leq 0$, equation 6.39 is zero or negative, and hence there is no local entanglement. It follows, for two-mode Gaussian state, the local concurrence and negativity both are *always* proportional to (ab).

6.4.2 Thermal states of two harmonic oscillators

For thermal states of two similar but distinguishable oscillators each having mass m, angular frequency ω and coupling spring constant K with corresponding dimensionless coupling $\alpha = 2K/m\omega^2$, $\mathbf{K} = 0$ and the values of $\mathbf{L}$ and $\mathbf{M}$ are given by equation A.7 and in equation A.8 respectively in Appendix A. We adopt $(m\omega)^{-1/2}$ as our length unit here.

First we consider the ground state. Equation 6.18 becomes

$$c = \frac{\sqrt{2}m\omega}{3}\sqrt{1+2\alpha-\sqrt{1+4\alpha}}. \quad (6.40)$$

So, for a given small a and b, the entanglement depends only on α and the fundamental length unit; it is *independent* of the location of the centres $(\overline{q}_A, \overline{q}_B)$ of the measurement regions. The lack of dependence on $(\overline{q}_A, \overline{q}_B)$ is a special feature of Gaussian states (see equation 7.27), and this result does not hold in general[7]; note also that the concurrence density can be made arbitrarily large by increasing α.

[7]The result that the concurrence density is independent of the region centres may seem obvious to some; they

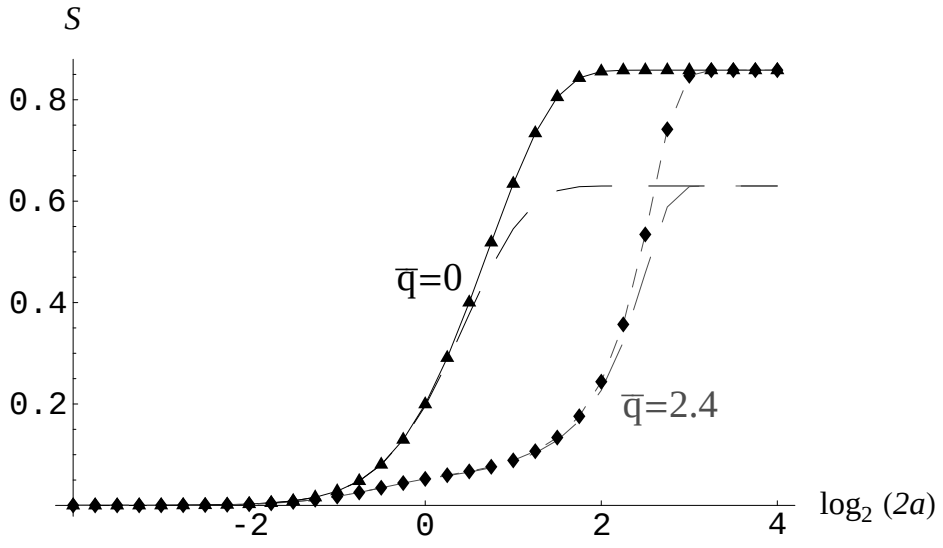

(a) Entropy of entanglement S_v

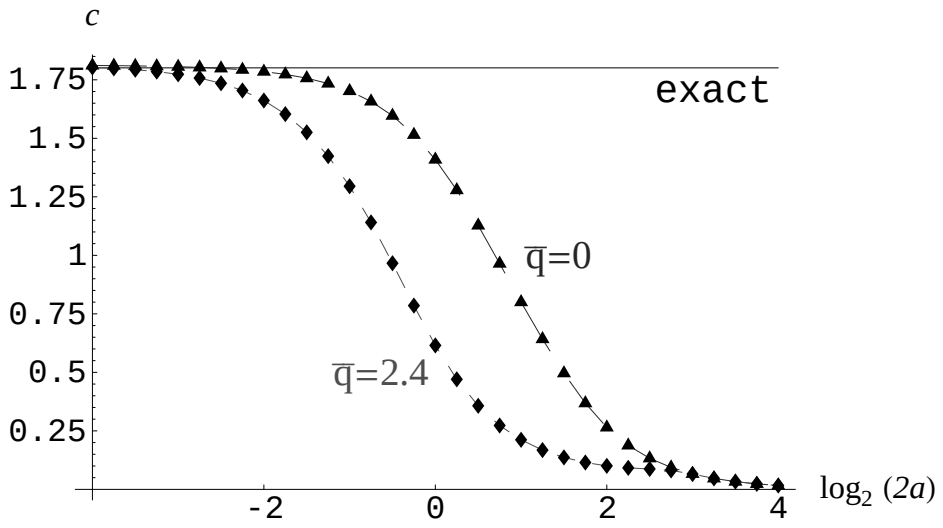

(b) Concurrence density c

Figure 6.1: Entanglement properties as a function of region size for a Gaussian ground state with $\alpha = 10$ and $m = \omega = 1$, in the case where both Alice and Bob make preliminary measurements and the region sizes are chosen to be the same. (a) Entanglement S_v (dimensionless) as a function of region size $2a$ (in units of $(m\omega)^{-1/2}$; log scale) for two different positions (data points); the entanglements contained in the effective two-level systems constructed from the two largest eigenvalues of ρ^A are also shown (dashed lines). (b) The concurrence density c (in units of $m\omega$), computed from the entanglement of formation by inverting the relation $S_v = h((cab)^2/4)$; note how it saturates to the exact result predicted by equation 6.40 (horizontal line) for small regions.

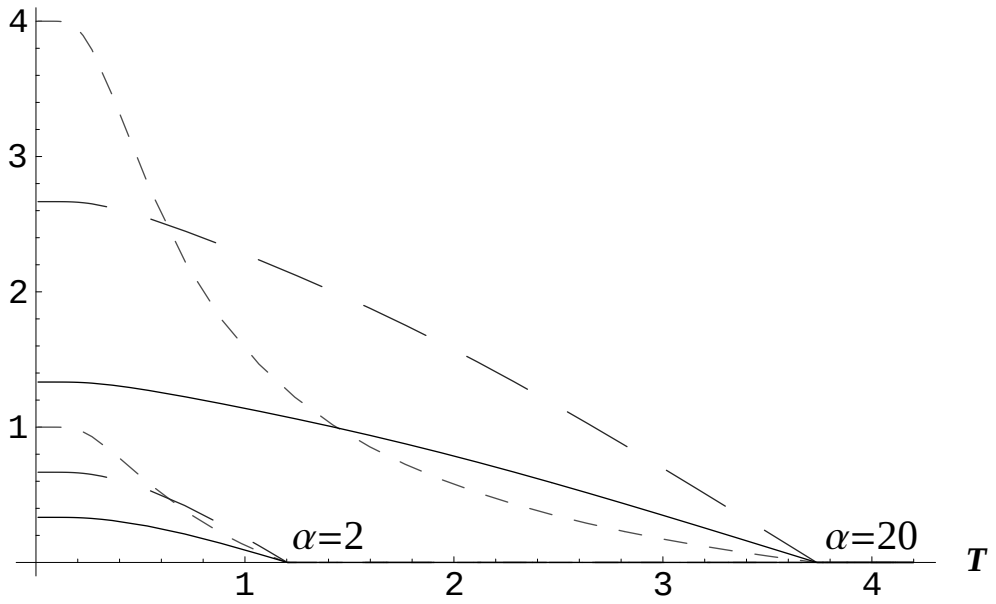

Figure 6.2: Negativity density n (full lines; in units of $m\omega$) and concurrence density c (long dashes; in units of $m\omega$) as a function of temperature T (in units of ω) for a thermal state of the two-oscillator system discussed in the text having $k_B = m = \omega = 1$, and for two different values of the coupling α. The global negativity $\mathcal{N}_g$ [AEPW02] is shown for comparison (short dashed lines; dimensionless).

Figure 6.1 shows the variation of the local entanglement, measured by the von Neumann entropy S_v (computed numerically), with the region size. Note how the local entanglement saturates to the full entanglement given in equation 5.11 for large regions, while for small regions it reduces to the value predicted by equation 6.40. To obtain entanglements of a substantial fraction of one ebit, it is necessary to choose a region size comparable to the fundamental length unit of the oscillator; around this point the two-qubit approximation is just starting to break down. Calculation details and full results are presented in Chapter 5.

For mixed Gaussian states, we find that the concurrence density and negativity density are again independent of position. In Figure 6.2 we plot both quantities as a function of temperature for thermal states of the two-oscillator system with different coupling strengths ($\alpha = 2$ and $\alpha = 20$). The concurrence density is exactly twice the negativity density as we would expect

may argue that since moving those centres corresponds to acting with local displacements in phase space, which amount to local unitary operations on the Hilbert space, entanglement is preserved by definition. This is not, in fact, correct for general states. The argument would hold only if the translation operation were applied to the projected state - i.e. if both the initial state and the measurement region were displaced by the same amount. In general a displacement of the measurement region alone will alter the entanglement. That it does not is a special feature of Gaussian states.

from Section 6.4.1. We also show the conventional (global) negativity for these states (given in equation 3.45 and [AEPW02]). Interestingly, both local entanglement densities vanish at the same temperature as the global negativity, showing that for this set of states, those which are entangled from the global point of view are also entangled by our local measures[8]. Unfortunately, this property is not universal as can be seen from a counter-example in Section 4.3.2.1.

Other counter-examples are also easy to set up. Consider an entangled composite quantum state shared by Alice and Bob

$$|\Psi\rangle_{AB} = \alpha|00\rangle_A|00\rangle_B + \frac{\beta}{\sqrt{2}}\Big(|01\rangle_A|01\rangle_B + |10\rangle_A|10\rangle_B\Big), \tag{6.41}$$

the α-part of the wavefunction is separable whereas the β-part is entangled. If after the preliminary measurements, the state $|\Psi\rangle_{AB}$ is projected onto the state $|00\rangle_A|00\rangle_B$, the entanglement in the discarding ensemble is zero whereas the entanglement of the original state is not. Take another example, the composite state $|\Phi\rangle_{AB}$ is entangled but the component states $\{|\phi_j\rangle\}$ are non-overlapping:

$$|\Phi\rangle_{AB} = \sum_i \sqrt{\lambda_i}|\phi_i\rangle_A|\phi_i\rangle_B, \tag{6.42}$$

where

$$\langle\phi_i|\phi_j\rangle = \delta_{ij}. \tag{6.43}$$

After measurements, the state $|\Phi\rangle_{AB}$ could be localised to a product state, for example, $|\phi_1\rangle_A|\phi_1\rangle_B$. Once localised, the entanglement in the discarding ensemble is again zero despite the original state being entangled . Therefore, no entanglement in the discarding ensemble does not necessarily imply that the original state is definitely unentangled.

6.5 Non-Gaussian States

Although the quantification of quantum entanglement of non-Gaussian states is in general extremely difficult, our local approach provides a systematic way to analyse aspects of entanglement in such systems since the local entanglement is easily quantifiable, once the exact state is known. We show an example here to demonstrate the applicability of our local approach to the analysis of entanglement of non-Gaussian states.

This example is also based on the density matrix ρ_e, defined in equation 5.31, that is a mixture of Bell states characterised by a probability p. By choosing $|0\rangle$ and $|1\rangle$ as the ground

[8] Some may find it strange to see in Figure 6.2 that the negativity density sometimes exceeds the global negativity. The suspicion is correct: the entanglement cannot increase under the local projective measurements (a point made explicitly in Section 4.2.6). The confusion arises because we plot in Figure 6.2 quantities with different dimensions on the same scale: the negativity density and concurrence density have dimensions, (length)$^{-2}$, and therefore depend on the choice of length units, while the global negativity is dimensionless.

state and the first excited state of a simple harmonic oscillator [Zet01],

$$|0\rangle = \frac{1}{\sqrt{\sqrt{\pi}q_0}} e^{\frac{-q^2}{2q_0^2}} \tag{6.44}$$

$$|1\rangle = \frac{1}{\sqrt{\sqrt{\pi}q_0}} \sqrt{2}q\, e^{\frac{-q^2}{2q_0^2}}, \tag{6.45}$$

where $q_0 = \sqrt{\hbar/(m\omega)}$ is a constant that sets the length scale of the oscillator and is set to $q_0 = 1$ here, ρ_e will describe non-Gaussian continuous-variable states. The $|0\rangle$ and $|1\rangle$ basis states used here should not be confused with the ones used in Section 5.5; those are eigenstates of a symmetric potential well instead of a harmonic oscillator.

6.5.1 Results

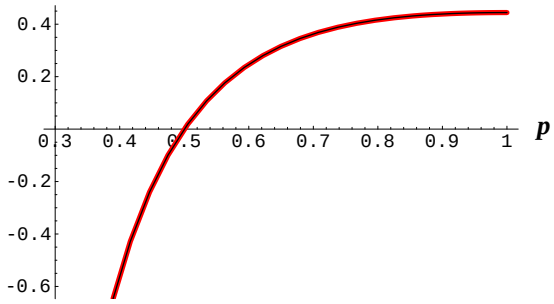

(a) $\bar{q}_A = 0, \bar{q}_B = 0$

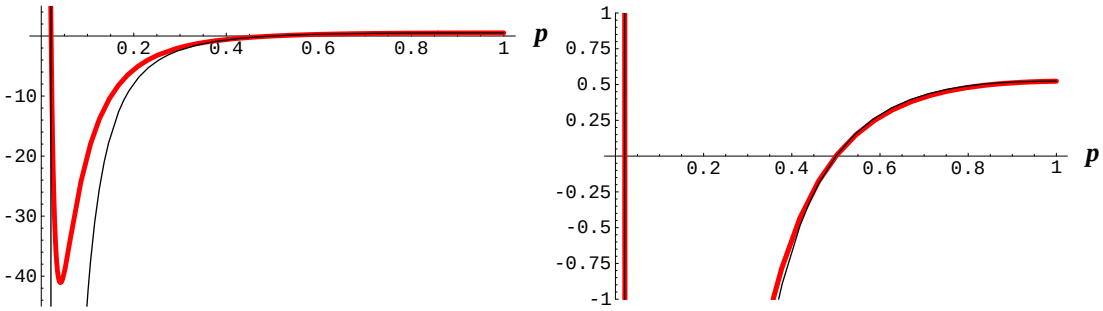

(b) $\bar{q}_A = -0.2, \bar{q}_B = 0.1$

Figure 6.3: The variations of C_1 (the red line) and C_2 (the black line) with the probability p in equation 5.31. (a) The centres of the measured regions are both taken to be at the origin $\bar{q}_A = 0$ and $\bar{q}_B = 0$. (b) The centres are not at the origin $\bar{q}_A = -0.2$ and $\bar{q}_B = 0.1$. The two graphs of (b) are the same plots, but plotted with different ranges for more details.

Fist we plot in Figure 6.3 the variations of C_1 (the red line) and C_2 (the black line) with the probability p for two cases: (a) the centres of the measured regions are both taken to be at the origin $\bar{q}_A = 0$ and $\bar{q}_B = 0$; (b) the centres are not at the origin $\bar{q}_A = -0.2$ and $\bar{q}_B = 0.1$.

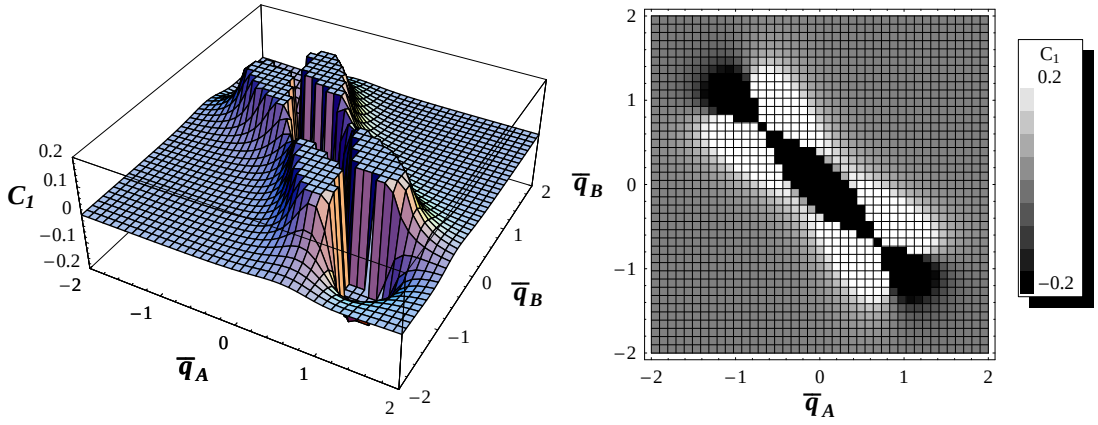

(a) C_1

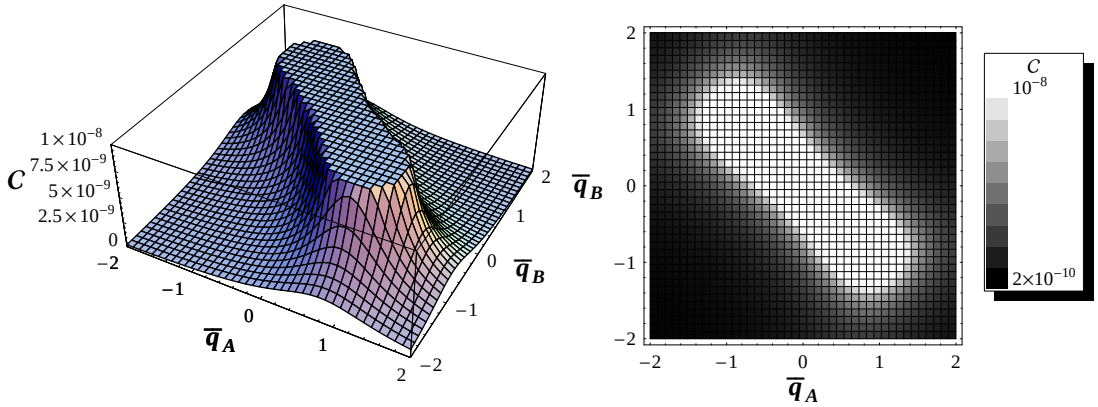

(b) Concurrence $\mathcal{C}$

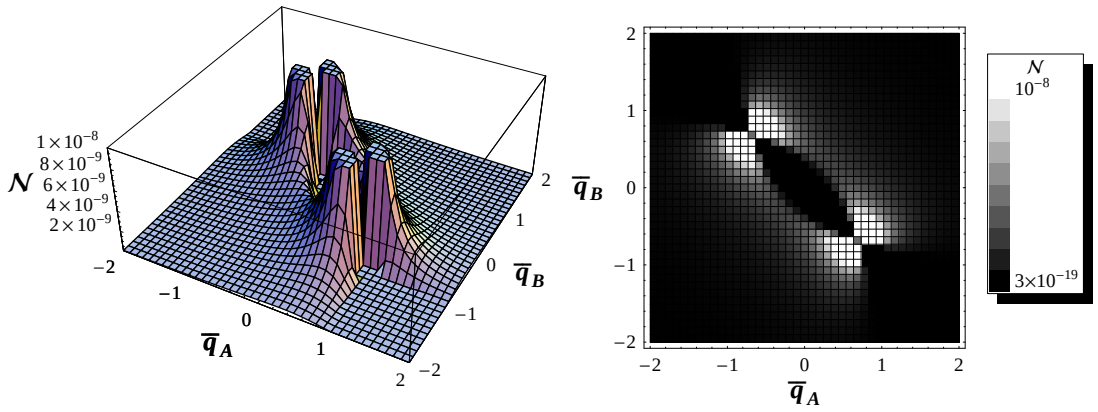

(c) Negativity $\mathcal{N}$

Figure 6.4: The distributions of various quantities: (a) C_1; (b) $\mathcal{C}$; (c) $\mathcal{N}$ of the state ρ_e described in Section 6.5 are plotted by varying the centres of the measured regions $\bar{q}_A = 0$ and $\bar{q}_B = 0$. The widths of the measured regions are taken to be $a = b = 0.0001$.

We find that when both centres are at the origin, $C_1 = C_2$ and C_1 only crosses the horizontal axis ($C_1 = 0$) at the point $p = 0.5$, exactly where the state ρ_e becomes separable. However, when the centres are away from the origin, C_1 and C_2 are no longer equal to each other, and C_1 becomes zero at the point $p = 0.021$ as well as the point $p = 0.5$. The two graphs in Figure 6.3 (b) are the same plots, but with different plotting ranges. We also see in both Figure 6.3 (a) and (b) that C_1 and C_2 are of the same sign so that at these two positions we consider, the local entanglement is only zero when $C_1 = 0$; that is, we can not make $C_1 < 0$ and $C_2 > 0$ by varying p. There is another interesting feature of Figure 6.3; namely, for the same state (i.e. p is fixed), it is possible to change the leading order of the local negativity in the quantity (ab) simply by moving from $(\bar{q}_A, \bar{q}_B) = (0, 0)$ to $(\bar{q}_A, \bar{q}_B) = (-0.2, 0.1)$. For the position chosen, this happens between $p = 0$ and $p = 0.021$. Within this range, C_1 and C_2 are both negative when the measurement centres are at the origin so the local negativity is proportional to $(ab)^2$. In contrast, C_1 and C_2 become positive when the centres are not at the origin, and hence the local negativity in this case is in the second order of a and b.

Next, we fix the probability $p = 0.2$ to find the entanglement distributions. The widths of the measured regions are taken to be $a = b = 0.0001$. We plot the distributions of various quantities: (a) C_1; (b) $\mathcal{C}$; (c) $\mathcal{N}$ by varying the centres of the measured regions $\bar{q}_A$ and $\bar{q}_B$. All the graphs do not show the whole range of values to make it easier to see the features. Both $\mathcal{C}$ and $\mathcal{N}$ are computed numerically from the effective two-qubit density matrix directly (after substituting appropriate values into it) for comparison with our analytical formulae in Section 6.3.1. We find that for regions where C_1 is negative (black areas in the right graph of Figure 6.4 (a)), the local concurrences $\mathcal{C}$ (plotted in Figure 6.4 (b)) are not zero and are of the order 10^{-8} over the whole region (where $C_1 \neq 0$). In comparison, the values of the local negativity $\mathcal{N}$ (plotted in Figure 6.4 (c)) in the regions, where $C_1 < 0$, are roughly 10^{-8} times smaller than in the regions, where $C_1 > 0$. But note that $a(b) = 10^{-8}$ in this example so that the local negativities vary greatly by up to a factor of (ab) from place to place, depending on the sign of C_1. The region sizes are very small and the numerically obtained values of the local negativity agree with the values given by the closed-form expression (equation 6.20). These findings are consistent with the earlier analytical analysis.

The corresponding probability-density distribution $p(\bar{q}_A, \bar{q}_B)$ of the state ρ_e with $p = 0.2$ is also shown in Figure 6.5 for comparison. The distribution of probability densities is obtained from

$$p(\bar{q}_A, \bar{q}_B) = \langle \bar{q}_A, \bar{q}_B | \rho_e | \bar{q}_A, \bar{q}_B \rangle. \tag{6.46}$$

We see that the entanglement distributions are very different from the probability-density dis-

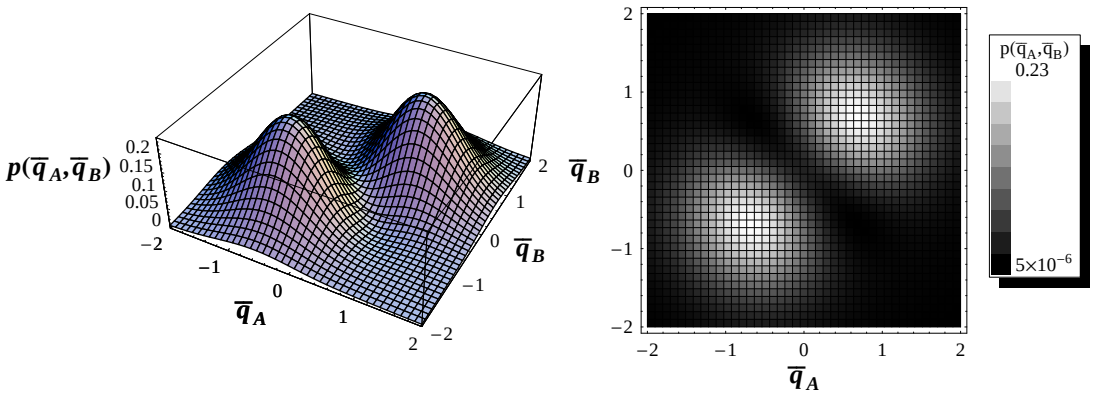

Figure 6.5: The distribution of probability densities $p(\bar{q}_A, \bar{q}_B)$ of the state ρ_e described in Section 6.5.

tribution. Notably, the local entanglements are concentrated along the diagonal $\bar{q}_A = -\bar{q}_B$ whereas the probability densities are higher along the other diagonal $\bar{q}_A = \bar{q}_B$.

6.6 Extraction of the Local Entanglement.

Methods of extracting the entanglement from a squeezed continuous-variable state into a pair of two-level system were previously studied in [SKLA02, PSK$^+$04, KC04] Using our mapping to an effective two-qubit system, we can swap the entanglement in a small region of the continuous wavefunction to local qubits (i.e. true two-level systems). Remembering that the states ϕ_0 and ϕ_1 drop to zero outside the region $[-a, a]$ we find that the Pauli operators $\hat{X}$ and $\hat{Y}$ of the effective qubit can be represented in terms of the canonical position and momentum operators $\hat{q}$ and $\hat{p}$ by (Appendix D)

$$\hat{X} = \frac{\sqrt{3}}{a}\hat{q}; \qquad \hat{Y} = -\frac{2a}{\sqrt{3}\hbar}\hat{p}. \tag{6.47}$$

The experiment could be performed as follows: first, localise the continuous degree of freedom (for example, through a homodyne measurement in the case of an electromagnetic field mode), then perform a SWAP operation by composing three controlled-X gates [NC00]:

$$\begin{aligned} \hat{U}_{SWAP} &= \exp\left[\frac{\mathrm{i}\pi}{4}(\sigma_y - 1)(\frac{\sqrt{3}}{a}\hat{q} - 1)\right] \\ &\quad \times \exp\left[\frac{\mathrm{i}\pi}{4}(\sigma_x - 1)(-\frac{2a}{\sqrt{3}\hbar}\hat{p} - 1)\right] \\ &\quad \times \exp\left[\frac{\mathrm{i}\pi}{4}(\sigma_y - 1)(\frac{\sqrt{3}}{a}\hat{q} - 1)\right], \end{aligned} \tag{6.48}$$

where (σ_x, σ_y) are Pauli operators for a local qubit. Using this procedure one could therefore extract the full two-level entanglement shown in the dashed curves of Figure 6.1(a) provided

the swap operation is successful.

6.7 Summary

The literature on entanglement in continuous-variable systems has so far concentrated almost exclusively on Gaussian states. Such states can be prepared easily in quantum optics, but are exceptional in other systems (such as solids and molecules). As far as we know this work provides the first systematic approach to characterising aspects of the entanglement in such arbitrary non-Gaussian states.

After preliminary measurements to localise the subsystems inside certain portions of configuration space, it is simple to characterise the entanglement in a continuous-variable system. In the case where the subsystem is localised to very small regions, each mode of the system is isomorphic to a single qubit. We derive simple expressions for the local concurrence in pure states and for the negativity in mixed states. Even though, we do not offer analytical expressions for the local concurrence (except for rank-2 mixed states), a recipe to numerically compute it for arbitrary two-mode states with ease is provided, and it is found that the local concurrence is always proportional to the product of region sizes (ab). The local negativity in contrast depends not only on the "area" (ab) but also on the "shape" (b/a), and can sometimes be proportional to $(ab)^2$ subject to the parameter C_1 in equation 6.23. Provided $C_1 \geq 0$, we can define the maximised negativity, which is always proportional to (ab), and then go on to define the negativity density, together with the concurrence density. However, the concurrence and negativity are not extensive, in the sense that the sum of these quantities over all the sub-regions of configuration space does not yield the full entanglement of the original system.

For Gaussian states, we find a closed-form formula for the local concurrence in terms of elements of the density matrix of the state and show that in this case it is always equal to two times the maximised negativity. However, this is not necessarily true for non-Gaussian states. We show that as region sizes become larger, the local entanglement as quantified by the von Neumann entropy saturates to the full global entanglement of the Gaussian ground state, and also shows that by making the region sizes very small, the concurrence density converges to the value given by equation 6.18. Thermal states are then considered, and this example shows that the states which are entangled from the global point of view are also entangled by our local measures, i.e. global entanglement of the initial state vanishes at the same point as the entanglement remaining in the discarding ensemble after the preliminary measurements to locate the system in a chosen subspace. However, this interesting behaviour is not a universal phenomenon. Consequently, the absence of any local entanglement does not guarantee that the

original state is unentangled.

The strength of our local approach lies on its application to non-Gaussian state, we demonstrate this by analysing the entanglement of a non-Gaussian state. We map its local-negativity distribution and show how it varies with the coordinates of the system, in comparison to the local-entanglement distribution of Gaussian states, which is independent of position coordinates.

One could generalise our results to multimode pure states by making multivariate Taylor expansions of ρ so our focus in the next chapter will be turned to the local entanglement in pure states of multidimensional continuous-variable systems. Our experience tells that it is not straightforward to extend our results to multi-mode mixed states. However, local entanglements of mixed states of higher-dimensional systems can still be easily computed numerically, provided the state is exactly known and the negativity (or logarithmic negativity) is the chosen entanglement measure. It will be interesting to characterise further the relationship between the local and global views of continuous-variable entanglement; in any case our results open a wide range of non-Gaussian states to further study.

Chapter 7

Local Entanglement of Multimode Continuous-Variable Systems

7.1 Introduction

In Chapter 6, we demonstrated that, by using our local approach (see Section 4.2) to quantify quantum entanglement, simple formulae exist for the local entanglement of any (mixed) two-mode continuous-variable states in the limit where the region to which the system is confined after the preliminary measurement becomes very small (i.e. where the measurement becomes more and more accurate). Here we will generalise these results to general smooth bipartite pure states[1], and in particular show that correspondingly simple closed-form formulae exist for the entanglement in the multimode case. Our results therefore enable the local entanglement to be computed directly and explicitly, without the time-consuming numerical evaluation of the global entanglement in a high-dimensional system, once the state of the system is known.

We first re-derive the results for two-mode states in Section 7.2 in a way that makes it easier to generalise to multi-mode states in Section 7.3. Finally in Section 7.4 we show examples of our approach applied to some systems (semiclassical WKB systems, multi-dimensional harmonic oscillators, and a hydrogen atom as three examples) in which analytical expressions for the energy eigenfunctions are easily obtained, before summarising in Section 7.5.

[1]Our choice of concentrating here only on pure states to demonstrate the power of our local approach for quantifying general (non-Gaussian) multimode continuous variable states may be questionable since entanglement of a pure state can be fully characterised by the von Neumann entropy no matter whether the given state is Gaussian or not. This fact is indeed at the heart of our approach. However, the calculation of this entropy for a high-dimensional system is in general an extremely difficult problem, since it involves computing the logarithm of the reduced density operator and tracing over all the degrees of freedom. The calculation will almost always have to be performed numerically, and it is generally intractable.

7.2 Two-Mode States

The case where only Alice makes a preliminary measurement is fully treated in Section 6.2.1. Now suppose both parties restrict their measurements: Alice's particle must lie in region $\mathcal{A} := \{\overline{q}_A - a \leq q_A \leq \overline{q}_A + a\}$, and Bob's in region $\mathcal{B} := \{\overline{q}_B - b \leq q_B \leq \overline{q}_B + b\}$. In Section 6.2.2 we attacked this problem by reducing it to an effective two-qubit one, for which exact results are available. However this approach does not generalise so naturally to the multi-mode case, so we give here an alternative approach by utilising the fact that the entropy of entanglement S_v or negativity $\mathcal{N}$ can be computed directly via the density matrix. From the previous argument we know we can compute the entanglement from Alice's reduced density matrix ρ^A in the coordinate representation. Our first task, therefore, is to evaluate this quantity once Bob has made the measurement of his particle.

We do this by making a further Taylor expansion involving Bob's variables. We define

$$\rho_{n_1 n_2 n_3 n_4} = \frac{\partial^{n_1}}{\partial {q_A}^{n_1}} \frac{\partial^{n_2}}{\partial {q'_A}^{n_2}} \frac{\partial^{n_3}}{\partial {q_B}^{n_3}} \frac{\partial^{n_4}}{\partial {q'_B}^{n_4}} \rho(q_A, q_B; q'_A, q'_B)\Big|_{q_A = q'_A = \overline{q}_A, q_B = q'_B = \overline{q}_B}. \tag{7.1}$$

As we will see, to obtain the first nontrivial term in the solution we need all terms to first order in Alice's coordinates and to second order in Bob's:

$$\begin{aligned}
\rho(q_A, q_B; q'_A, q'_B) &= \rho(\bar{q}_A + x_A, \bar{q}_B + x_B; \bar{q}_A + x'_A, \bar{q}_B + x'_B) \\
&= \rho_{0000} + \rho_{1000} x_A + \rho_{0100} x'_A + \rho_{0010} x_B + \rho_{0001} x'_B \\
&\quad + \frac{1}{2}(\rho_{0020} {x_B}^2 + \rho_{0002} {x'_B}^2) \\
&\quad + \rho_{1100} x_A x'_A + \rho_{1010} x_A x_B + \rho_{1001} x_A x'_B \\
&\quad + \rho_{0110} x'_A x_B + \rho_{0101} x'_A x'_B + \rho_{0011} x_B x'_B \\
&\quad + \frac{1}{2}(\rho_{1020} x_A {x_B}^2 + 2\rho_{1011} x_A x_B x'_B + \rho_{1002} x_A {x'_B}^2 \\
&\quad\quad + \rho_{0120} x'_A {x_B}^2 + 2\rho_{0111} x_{A'} x_B x'_B + \rho_{0102} x'_A {x'_B}^2) \\
&\quad + \mathcal{O}({x_A}^2, {x'_A}^2, {x_B}^3, {x'_B}^3).
\end{aligned} \tag{7.2}$$

Alice's reduced density matrix is then found by writing

$$\begin{aligned}
\rho^A(x_A; x'_A) &= \frac{1}{p} \int_{-b}^{b} \mathrm{d}x_B \, \rho(x_A, x_B; x'_A, x_B) \\
&= \frac{2b}{p} \Big[\rho_{0000} + x_A \rho_{1000} + x'_A \rho_{0100} \Big] + \frac{b^3}{3} \Big[\rho_{0020} + 2\rho_{0011} + \rho_{0002} \\
&\quad + (\rho_{1020} + 2\rho_{1011} + \rho_{1002}) x_A + (\rho_{0120} + 2\rho_{0111} + \rho_{0102}) x'_A \Big] \\
&\quad + \mathcal{O}(b^5, {x_A}^2, {x'_A}^2).
\end{aligned} \tag{7.3}$$

where p is a normalisation constant. By comparison with equation 6.1 and equating powers of x_A and x'_A we can immediately identify the terms which appear in the expression for ϵ (as

defined in equation 6.7), and therefore determine the entanglement:

$$\begin{aligned}
\rho^A_{00} &= \frac{2b}{p}\Big[\rho_{0000} + \frac{b^2}{6}(\rho_{0020} + 2\rho_{0011} + \rho_{0002})\Big] + \mathcal{O}(b^5);\\
\rho^A_{10} &= \frac{2b}{p}\Big[\rho_{1000} + \frac{b^2}{6}(\rho_{1020} + 2\rho_{1011} + \rho_{1002})\Big] + \mathcal{O}(b^5);\\
\rho^A_{01} &= \frac{2b}{p}\Big[\rho_{0100} + \frac{b^2}{6}(\rho_{0120} + 2\rho_{0111} + \rho_{0102})\Big] + \mathcal{O}(b^5);\\
\rho^A_{11} &= \frac{2b}{p}\Big[\rho_{1100} + \frac{b^2}{6}(\rho_{1120} + 2\rho_{1111} + \rho_{1102})\Big] + \mathcal{O}(b^5).
\end{aligned} \tag{7.4}$$

The leading order (b^2) terms in the numerator of the expression for ϵ cancel—this is the reason why we need the density matrix to quadratic order in Bob's coordinates. The cancellation occurs because Alice and Bob (by hypothesis) share a pure state, and so

$$\begin{aligned}
\rho(q_A, q_B; q'_A, q'_B) &= \psi(q_A, q_B)\psi^*(q'_A, q'_B)\\
\Rightarrow \quad \rho_{n_1n_2n_3n_4} &= \frac{\partial^{n_1}}{\partial {q_A}^{n_1}}\frac{\partial^{n_3}}{\partial {q_B}^{n_3}}\psi(q_A, q_B)\Big|_{q_A=\bar{q}_A, q_B=\bar{q}_B}\\
&\qquad \frac{\partial^{n_2}}{\partial {q'_A}^{n_2}}\frac{\partial^{n_4}}{\partial {q'_B}^{n_4}}\psi^*(q'_A, q'_B)\Big|_{q'_A=\bar{q}_A, q'_B=\bar{q}_B}.
\end{aligned} \tag{7.5}$$

We can thus re-arrange the indices in a product of two $\rho_{n_1n_2n_3n_4}$ terms as

$$\rho_{abcd}\rho_{efgh} = \rho_{ebgd}\rho_{afch}, \tag{7.6}$$

so in particular

$$\rho_{1100}\rho_{0000} = \rho_{0100}\rho_{1000}. \tag{7.7}$$

Hence the leading term in the numerator of ϵ is of order b^4, and the overall expression becomes

$$\begin{aligned}
\epsilon &= \frac{a^2b^2}{18\rho^2_{0000}}\Big[\rho_{1100}(\rho_{0020} + 2\rho_{0011} + \rho_{0002}) + \rho_{0000}(\rho_{1120} + 2\rho_{1111} + \rho_{1102})\\
&\qquad -\rho_{1000}(\rho_{0120} + 2\rho_{0111} + \rho_{0102}) - \rho_{0100}(\rho_{1020} + 2\rho_{1011} + \rho_{1002})\Big].
\end{aligned} \tag{7.8}$$

Using equation 7.6 we can simplify this to obtain

$$\frac{\epsilon}{a^2b^2} = \frac{1}{9\rho^2_{0000}}[\rho_{1100}\rho_{0011} + \rho_{0000}\rho_{1111} - \rho_{1000}\rho_{0111} - \rho_{0100}\rho_{1011}] \tag{7.9}$$

$$\begin{aligned}
&= \frac{1}{18\rho^2_{0000}}[2\rho_{1100}\rho_{0011} + 2\rho_{0000}\rho_{1111} - \rho_{1000}\rho_{0111}\\
&\qquad -\rho_{0100}\rho_{1011} - \rho_{0010}\rho_{1101} - \rho_{0001}\rho_{1110}].
\end{aligned} \tag{7.10}$$

The first form (7.9) is slightly more compact, while the second form (7.10) makes it clear that the coordinates of Alice's and Bob's subsystems are treated equivalently, as required. The von

Neumann entropy, and hence the entanglement (since this is still a pure state), is then $S_v = h(\epsilon)$ in equation 3.29 as before.

We know, from the arguments leading to equation 6.12, that the leading correction to this result is $\mathcal{O}(a^4)$, and we should expect from the symmetry between Alice's and Bob's systems that it is also $\mathcal{O}(b^4)$. We have explicitly computed the correction and this is indeed the case: the result is given in Appendix E. The third eigenvalue λ_3 measures the extent of the breakdown of our approach. We note that it is of order a^4b^4, and therefore does not affect the expression for ϵ, which is of order a^2b^2.

7.3 Multimode Systems

7.3.1 General approach

Consider first the case in which only Alice makes preliminary measurements. If Alice's system is two-dimensional (not to be mistaken for a qubit) and she localises the particle so $-a_i \leq x_i \leq +a_i, i \in \{1,2\}$, one can find the eigenvalues of $\rho^A(\mathbf{q}_A, \mathbf{q'}_A)$, where $\mathbf{q}_A = (q_{A,1}, q_{A,2})$ and similarly $\mathbf{q}_B = (q_{B,1}, q_{B,2})$, by a straightforward generalisation of the methods in Section 6.2.1. Once again we find that there are only two non-zero eigenvalues to order a_i^2:

$$\begin{aligned} \lambda_1 &= \sum_i^2 \frac{a_i^2}{3(\bar{\rho}^A)^2}\left(\bar{\rho}^A \frac{\partial^2 \rho^A}{\partial q_{A,i}\partial q'_{A,i}} - \frac{\partial \rho^A}{\partial q_{A,i}}\frac{\partial \rho^A}{\partial q'_{A,i}}\right) + \text{H.T.} \\ \lambda_2 &= 1 - \lambda_1 + \text{H.T.} \end{aligned} \tag{7.11}$$

where i goes over the two spatial dimensions of Alice's subsystems, H.T. stands for higher-order terms[2] and both ρ and its derivatives are to be evaluated with both arguments set to the reference coordinates $\bar{\mathbf{q}}_A = (\bar{q}_{A,1}, \bar{q}_{A,2})$ (and similarly $\bar{\mathbf{q}}_B = (\bar{q}_{B,1}, \bar{q}_{B,2})$):

$$\bar{\rho}^A \equiv \rho^A(\bar{\mathbf{q}}_A; \bar{\mathbf{q}}_A). \tag{7.12}$$

We now argue that this property, of effectively having only two non-zero eigenvalues in the limit of very small measured regions, holds irrespective of the dimensionality of Alice's system, as follows. The entanglement must be invariant under exchange of the axis labels, and under all transformations of the form $a_i \to -a_i$. The only possibilities consistent with these requirements are

$$\lambda_1 = 1 - \sum_i t_i a_i^2; \quad \lambda_2 = \sum_i t_i a_i^2; \quad \lambda_3, \lambda_4 \ldots = 0, \tag{7.13}$$

or

$$\lambda_1 = 1 - \sum_i t_i a_i^2; \quad \lambda_2 = t_1 a_1^2; \quad \lambda_3 = t_2 a_2^2, \ldots, \tag{7.14}$$

[2]Typically different λ's have different higher-order terms. The notation H.T does not imply that the higher-order terms concerned are the same.

where the t_i are arbitrary constants. Furthermore the eigenvalues must reduce to the known forms for one- and two-dimensional systems if all other a_i are set to zero. If we keep a_1 and a_2 non-zero, sending all others to zero, only the first form 7.13 is consistent with equation 7.11. Therefore, the form of the non-zero eigenvalues must be

$$\begin{aligned}\lambda_1 &= \sum_i \frac{a_i^2}{3(\bar{\rho}^A)^2}\left(\bar{\rho}^A\frac{\partial^2\rho^A}{\partial q_{A,i}\partial q'_{A,i}} - \frac{\partial\rho^A}{\partial q_{A,i}}\frac{\partial\rho^A}{\partial q'_{A,i}}\right) + \text{H.T.}\\ \lambda_2 &= 1-\lambda_1+\text{H.T.}\\ \lambda_3 &= 0+\text{H.T.}\end{aligned} \tag{7.15}$$

where i now goes over all the dimensions of Alice's subsystems.

Define

$$\begin{aligned}\rho_{(i,j;n_1n_2n_3n_4)} = \frac{\partial^{n_1}}{\partial {q_{A,i}}^{n_1}}\frac{\partial^{n_2}}{\partial {q'_{A,i}}^{n_2}}\frac{\partial^{n_3}}{\partial {q_{B,j}}^{n_3}}\frac{\partial^{n_4}}{\partial {q'_{B,j}}^{n_4}}\\ \rho(\mathbf{q}_A,\mathbf{q}'_A,\mathbf{q}_B,\mathbf{q}'_B)\Big|_{\mathbf{q}_A=\mathbf{q}'_A=\bar{\mathbf{q}}_A,\mathbf{q}_B=\mathbf{q}'_B=\bar{\mathbf{q}}_B}.\end{aligned} \tag{7.16}$$

where i (j) represents one of available dimensions of Alice's (Bob's) subsystem. If the state $\rho(\mathbf{q}_A,\mathbf{q}'_A,\mathbf{q}_B,\mathbf{q}'_B)$ is pure, by following the same reasoning, we can generalise equation (7.6) to become

$$\rho_{(i,j;n_1n_2n_3n_4)}\rho_{(i,j;n_5n_6n_7n_8)} = \rho_{(i,j;n_5n_2n_7n_4)}\rho_{(i,j;n_1n_6n_3n_8)}. \tag{7.17}$$

From the previous analysis that led to equation 7.4 for a pure two-mode state, we know we can extend equation 7.15 to a pure multi-dimensional bipartite state $\rho(\mathbf{q}_A,\mathbf{q}'_A,\mathbf{q}_B,\mathbf{q}'_B)$ for the case where both parties make preliminary measurements on their particles by making the following substitutions:

$$\begin{aligned}\rho^A_{(i;00)} &= \sum_j\left(\frac{\prod_{j'}2b_{j'}}{p}\right)\left[\rho_{(ij;0000)}+\frac{b_j^2}{6}(\rho_{(ij;0020)}+2\rho_{(ij;0011)}+\rho_{(ij;0002)})\right]+\text{H.T.};\\ \rho^A_{(i;10)} &= \sum_j\left(\frac{\prod_{j'}2b_{j'}}{p}\right)\left[\rho_{(ij;1000)}+\frac{b_j^2}{6}(\rho_{(ij;1020)}+2\rho_{(ij;1011)}+\rho_{(ij;1002)})\right]+\text{H.T.};\\ \rho^A_{(i;01)} &= \sum_j\left(\frac{\prod_{j'}2b_{j'}}{p}\right)\left[\rho_{(ij;0100)}+\frac{b_j^2}{6}(\rho_{(ij;0120)}+2\rho_{(ij;0111)}+\rho_{(ij;0102)})\right]+\text{H.T.};\\ \rho^A_{(i;11)} &= \sum_j\left(\frac{\prod_{j'}2b_{j'}}{p}\right)\left[\rho_{(ij;1100)}+\frac{b_j^2}{6}(\rho_{(ij;1120)}+2\rho_{(ij;1111)}+\rho_{(ij;1102)})\right]+\text{H.T.};\end{aligned} \tag{7.18}$$

where j and j' go over all the dimensions of Bob's subsystem and p is an appropriate normalisation constant.

Therefore, to the lowest order in a and b, λ_1 in equation 7.15 becomes

$$\begin{aligned}\lambda_1 &= \sum_{i,j}\frac{a_i^2 b_j^2}{18{\rho_{(i,j;0000)}}^2}\Big\{\rho_{(i,j;1100)}[\rho_{(i,j;0020)}+2\rho_{(i,j;0011)}+\rho_{(i,j;0002)}]\\ &\quad+\rho_{(i,j;0000)}[\rho_{(i,j;1120)}+2\rho_{(i,j;1111)}+\rho_{(i,j;1102)}]\\ &\quad-\rho_{(i,j;1000)}[\rho_{(i,j;0120)}+2\rho_{(i,j;0111)}+\rho_{(i,j;0102)}]\\ &\quad-\rho_{(i,j;0100)}[\rho_{(i,j;1020)}+2\rho_{(i,j;1011)}+\rho_{(i,j;1002)}]\Big\}.\end{aligned}$$

This can be further simplified by using equation 7.17 to obtain

$$\begin{aligned}\lambda_1 &= \sum_{i,j}\frac{a_i^2 b_j^2}{9{\rho_{(i,j;0000)}}^2}[\rho_{(i,j;1100)}\rho_{(i,j;0011)}+\rho_{(i,j;0000)}\rho_{(i,j;1111)}-\rho_{(i,j;1000)}\rho_{(i,j;0111)}\\ &\quad-\rho_{(i,j;0100)}\rho_{(i,j;1011)}].\end{aligned} \tag{7.19}$$

Again the entanglement is completely determined by $S_v = h(\epsilon)$, where $\epsilon = \lambda_1$ as before.

7.3.2 Concurrence and negativity for general bipartite multi-mode pure states

In a similar way, we can generalise our previous expressions (Section 6.2.2) for the concurrence and negativity of the system after the preliminary measurement has been made.

For an $\mathcal{H}_{n_1}\otimes\mathcal{H}_{n_2}$ ($n_1 \le n_2$) bipartite system, where n_1 and n_2 are the Hilbert space dimension for the two subsystems respectively, the generalised concurrence of a pure quantum state ψ is defined by [CAF05]

$$\mathcal{C}^2(\psi) = 4\sum_{m<n}\lambda_m\lambda_n, \tag{7.20}$$

where $\sqrt{\lambda_m}$ ($m = 1,\ldots,n_1$) are the eigenvalues of the reduced density matrices ρ^A and ρ^B. Additionally, the trace norm of the partial transposed density matrix with respect to Alice's subsystem turns out to be

$$\|\rho^{T_A}\| = (\sum_m\sqrt{\lambda_m})^2. \tag{7.21}$$

From this we can determine the negativity, which is defined in equation 3.34.

As we argued earlier, the reduced density matrix in the discarding ensemble has only two non-zero eigenvalues (λ_1 and λ_2) to the lowest order; even though in general the expressions for negativity and concurrence are different, to order $(a_i^2 b_j^2)$ they are closely related because

$$\begin{aligned}4\sum_{1<2}\lambda_1\lambda_2 &= 4\lambda_1\lambda_2+4\lambda_1\lambda_3+\ldots\\ &\cong 4\lambda_1(1-\lambda_1)\cong 4\lambda_1\end{aligned} \tag{7.22}$$

and

$$\begin{aligned}\Big((\sum_m\sqrt{\lambda_m})^2-1\Big)^2 &= \Big(2\sqrt{\lambda_1\lambda_2}+2\sqrt{\lambda_1\lambda_3}+\ldots\Big)^2\\ &\cong 4\lambda_1,\end{aligned} \tag{7.23}$$

where we have used $\sum_m \lambda_m = 1$. Therefore, we have proved that in the limit of small a_i and b_j, for any multi-mode bipartite pure state ψ,

$$\mathcal{C}(\psi) = 2\mathcal{N}(\psi) = 2\sqrt{\epsilon}. \tag{7.24}$$

Specifically, the squared concurrence is

$$\begin{aligned} \mathcal{C}^2 &= \sum_{ij} \left(\frac{2a_i b_j}{3|\psi|^2}\right)^2 \left|\psi \frac{\partial^2 \psi}{\partial q_{A,i} \partial q_{B,j}} - \frac{\partial \psi}{\partial q_{A,i}} \frac{\partial \psi}{\partial q_{B,j}}\right|^2 \\ &\equiv \sum_{ij} \mathcal{C}_{ij}^2, \end{aligned} \tag{7.25}$$

where i goes over all dimensions of Alice's subsystem and j of Bob's subsystem. $\mathcal{C}_{ij}^2$ is the squared concurrence associated with the degrees of freedom i and j.[3] Note that $\mathcal{C}_{ij} \propto a_i b_j$, consistent with the existence of a well-defined local concurrence density for two-mode systems (equation 6.18).

Note also that the concurrence is made particularly simple by writing

$$\psi = e^{-S}, \tag{7.26}$$

where normalisation can be ensured by adding a constant to S, in which case

$$\mathcal{C}^2 = \sum_{ij} \frac{4a_i^2 b_j^2}{9} \left|\frac{\partial^2 S}{\partial q_{A,i} \partial q_{B,j}}\right|^2. \tag{7.27}$$

From this, we see that if S is quadratic in the coordinates (i.e. the state is a Gaussian), the local entanglement is constant; on the other hand whenever S is a linear function of the coordinates, the local entanglement is zero.

7.3.3 "No-force no-entanglement" theorem

As long as there is no external force acting on the system, we can always find a solution of the eigenstate of a quantum system with a potential V in the free-particle form:

$$\psi \sim e^{\mathrm{i}\sum_i k_i x_i}, \tag{7.28}$$

[3] One may think that it is natural, in some sense, to have linearly increased entanglement as the other mode of the entangled state is taken into account, and hence mistake equation 7.25 for implying that concurrence for the multi-dimensional bipartite systems is the simple addition of entanglement for each dimension of the systems. This is not correct. Even though it is not surprising that the entanglement increases as further coordinates of the system are considered. However, the effect is not linear because each of Alice's coordinates is entangled with *all* of Bob's, and this is exactly why equation 7.25 is written out in terms of the *squared* concurrence so that each mode contributes non-linearly to the total concurrence. This non-linear structure of the local concurrence and negativity is also the main reason why it is difficult to extend our analytical analysis to multi-mode mixed states.

where $\{k_i\}$ can be real or complex and $\sum_i k_i^2/2 = E - V$ (E is energy), such that the boundary conditions are also satisfied. Since in this case the terms in the exponential are a linear function of the coordinates, equation 7.27 tells that there will be no local entanglement. However, if the Schrödinger equation and the boundary conditions require that the eigenstate to be in a superposition of linearly independent free-particle wavefunctions, the eigenstate can still be written in terms of a single exponential but the terms in the exponential will no longer be linear in coordinates, and the local entanglement is then not necessarily zero.

Consider a simple case, a superposition of the *incident* and *reflected* waves in one dimension:

$$\Psi = \xi_1 e^{-\mathrm{i}(k_A q_A + k_B q_B)} + \xi_2 e^{\mathrm{i}(k_A q_A + k_B q_B)}, \tag{7.29}$$

where ξ_1 and ξ_2 are some constants. The local concurrence in this case will be

$$\mathcal{C} = \frac{8\xi_1\xi_2 k_A k_B\, ab}{3(\xi_1^2 + \xi_2^2 + 2\xi_1\xi_2 \cos[2k_A q_A + 2k_B q_B])}. \tag{7.30}$$

Therefore, we conclude that by excluding the effects of the superposition of wavefunctions, the non-superposed eigenstate for the force-free Schrödinger equation, such that the boundary conditions are satisfied, can always be written in the form of equation 7.26 with S being a linear function of coordinates so that there is no local entanglement.

7.3.4 Nodes in the wavefunction

Evidently S in equation 7.26 diverges near nodes of the wavefunction, so that for a fixed a_i and b_j the concurrence given by equation 7.27 also diverges (like $1/|\psi|^2$ as $|\psi| \to 0$). It is important to realize that this diverging quantity refers to the entanglement in the discarding ensemble (i.e., in the sub-ensemble conditional on finding the particles in the chosen measurement region—see equation 4.19), and that even in this ensemble our expression applies only in the limit of very small measurement regions. We now show that the discarding entanglement always remains finite provided we keep within the domain of validity of our approach.

The extent of the domain of validity follows inevitably from our Taylor-series approximations for the wavefunctions (or density operators—see equation 7.5), which are valid only close to the chosen reference point $(\bar{\mathbf{q}}_A, \bar{\mathbf{q}}_B)$. The requirement that the second term in this expansion should be small compared with the first is

$$\left.\frac{\partial\psi}{\partial q_{A,i}}\right|_{\bar{\mathbf{q}}_A,\bar{\mathbf{q}}_B} a_i \ll \psi(\bar{\mathbf{q}}_A, \bar{\mathbf{q}}_B) \quad \Rightarrow \quad a_i \ll \left.\frac{\psi}{\partial\psi/\partial q_{A,i}}\right|_{\bar{\mathbf{q}}_A,\bar{\mathbf{q}}_B} \tag{7.31}$$

and similarly for b_j; therefore, the domain of validity shrinks to zero near a node in ψ. Equivalently, if this condition is not satisfied it leads to the breakdown of the isomorphism of each mode to one qubit described in Section 6.2.2.

One way to understand the behaviour of the entanglement near points where the wavefunction vanishes is to satisfy equation 7.31 by writing the maximum valid region size as

$$a_i^{\mathrm{MAX}} = \sigma \frac{\psi}{\partial\psi/\partial q_{A,i}}\bigg|_{\bar{\mathbf{q}}_A,\bar{\mathbf{q}}_B}, \tag{7.32}$$

where $\sigma \ll 1$ is a small parameter, and similarly for b_j^{MAX}. (We assume here that the derivatives are not also zero near the nodes.) We further define three quantities k_i, k_j, and k_{ij} by

$$\begin{aligned} \frac{\partial^2\psi}{\partial q_{A,i}\partial q_{B,j}}\bigg|_{\bar{\mathbf{q}}_A,\bar{\mathbf{q}}_B} &= k_{ij}\psi(\bar{\mathbf{q}}_A,\bar{\mathbf{q}}_B); \\ \frac{\partial\psi}{\partial q_{A,i}}\bigg|_{\bar{\mathbf{q}}_A,\bar{\mathbf{q}}_B} &= k_i\psi(\bar{\mathbf{q}}_A,\bar{\mathbf{q}}_B); \\ \frac{\partial\psi}{\partial q_{B,j}}\bigg|_{\bar{\mathbf{q}}_A,\bar{\mathbf{q}}_B} &= k_j\psi(\bar{\mathbf{q}}_A,\bar{\mathbf{q}}_B), \end{aligned} \tag{7.33}$$

so $a_i^{\mathrm{MAX}}k_i = b_j^{\mathrm{MAX}}k_j = \sigma$. From equation 7.25, if we choose $a_i = a_i^{\mathrm{MAX}}$, $b_j = b_j^{\mathrm{MAX}}$ near a node where the condition $k_ik_j \gg k_{ij}$ is met, the expression for ϵ reduces to

$$\epsilon_{\mathrm{MAX}} = N_AN_B\frac{\sigma^4}{9}, \tag{7.34}$$

where N_A and N_B are the number of degrees of freedom in Alice's and Bob's subsystems respectively. Therefore ϵ (and hence also the local concurrence and entanglement) is cut off near the node at a finite value that depends on the choice of σ.

7.3.5 Transformation of coordinates

We now discuss the behaviour of our expressions for the local entanglement under various coordinate transformations.

7.3.5.1 Invariance under local transformations

We would expect that the definitions of our local entanglement would remain unchanged if we made a local redefinition of our coordinate axes (possibly accompanied by changes in the measurement region). To see that this is the case, consider the following transformation of Alice's coordinates:

$$\frac{Q_i}{A_i} = \sum_j O_{ij}\frac{q_j}{a_j} \tag{7.35}$$

where O is an orthogonal matrix ($OO^T = \mathbf{1}$) and the sum goes only over the other coordinates of Alice's particle. A_i is to determine the length of the measurement region for new variable Q_i. Note that if $a_j = A_i = a\ \forall i,j$ (i.e. both measurement volumes are hypercubes with the same dimensions)[4] then equation 7.35 reduces to a simple orthogonal transformation of Alice's coordinates.

[4]Equation 7.35 does not assume $a_j = A_i = a\ \forall i,j$; this condition is only introduced to explain that the transformations considered are a generalisation of simple orthogonal transformations on the individual coordinates.

Now

$$a_i \frac{\partial}{\partial q_i} = \sum_j A_j \frac{\partial Q_j}{\partial q_i} \frac{\partial}{\partial Q_j} = \sum_j O_{ij} A_j \frac{\partial}{\partial Q_j}. \tag{7.36}$$

We then have

$$\begin{aligned} \sum_i a_i^2 \frac{\partial^2 \rho}{\partial q_i \partial {q'}_i} &= \sum_{ijk} O_{ij} O_{ik} A_j A_k \frac{\partial^2 \rho}{\partial Q_j \partial {Q'}_k} \\ &= \sum_j A_j^2 \frac{\partial^2 \rho}{\partial Q_j \partial {Q'}_j} \end{aligned} \tag{7.37}$$

and similarly

$$\sum_i a_i^2 \frac{\partial \rho}{\partial q_i} \frac{\partial \rho}{\partial {q'}_i} = \sum_i A_i^2 \frac{\partial \rho}{\partial Q_i} \frac{\partial \rho}{\partial {Q'}_i}. \tag{7.38}$$

Therefore, equation 7.15 is invariant under the generalised orthogonal transformation 7.35. It follows that equation 7.19, and hence the local entanglement, are also invariant under these local transformations.

7.3.5.2 Non-local transformations

We now consider some transformations which mix Alice's and Bob's coordinates—specifically, those that make the system separable. That is to say we look for a new set of coordinates

$$X_k = \sum_i T_{ik} x_i \tag{7.39}$$

such that the wavefunction factors as

$$\psi = \prod_k \psi_k(X_k). \tag{7.40}$$

Note that the sum over i in equation 7.39 runs over all coordinates of the system (both Alice's and Bob's). In this situation it does not make sense to consider any accompanying change in the shape or size of the measurement region, which we continue to define in terms of the original coordinates and to describe by $\{a_i\}$ and $\{b_j\}$.

Therefore,

$$\begin{aligned} \frac{\partial^2 \psi}{\partial x_i \partial x_j} &= \sum_{kk'} T_{ik} T_{jk'} \frac{\partial^2 \psi}{\partial X_k \partial X_{k'}} \\ &= \sum_k T_{ik} T_{jk} \frac{\psi}{\psi_k} \frac{\partial^2 \psi_k}{\partial X_k^2} + \sum_{k \neq k'} T_{ik} T_{jk'} \frac{\psi}{\psi_k \psi_{k'}} \frac{\partial \psi_k}{\partial X_k} \frac{\partial \psi_{k'}}{\partial X_{k'}} \end{aligned} \tag{7.41}$$

and similarly

$$\frac{\partial \psi}{\partial x_i} \frac{\partial \psi}{\partial x_j} = \sum_{kk'} T_{ik} T_{jk'} \frac{\psi^2}{\psi_k \psi_{k'}} \frac{\partial \psi_k}{\partial X_k} \frac{\partial \psi_{k'}}{\partial X_{k'}}. \tag{7.42}$$

It follows from equation 7.25 that

$$\epsilon = \sum_{ij} \frac{(a_i b_j)^2}{9} \left| \sum_k T_{ik} T_{jk} \frac{\psi}{\psi_k} \left[\frac{\partial^2 \psi_k}{\partial X_k^2} - \frac{1}{\psi_k} \left(\frac{\partial \psi_k}{\partial X_k} \right)^2 \right] \right|^2, \tag{7.43}$$

where the second term inside the modulus signs comes from the part of equation 7.42 having $k = k'$. In terms of the logarithms of the separable wavefunctions $S_k = -\log[\psi_k(X_k)]$, we have

$$\epsilon = \sum_{ij} \frac{(a_i b_j)^2}{9} \left| \sum_k T_{ik} T_{jk} \frac{\partial^2 S_k}{\partial X_k^2} \right|^2. \tag{7.44}$$

One important special case of this result is the transformation to normal coordinates in a harmonic system: if the potential can be quadratically expanded about an energy minimum, the transformation to normal coordinates takes the form of equation 7.39 with

$$T_{ik} = \sqrt{m_i} O_{ik}, \tag{7.45}$$

where O is an orthogonal matrix.

7.3.5.3 Relative coordinates

A closely related example is the transformation to centre-of-mass and relative coordinates. (Here we assume that the particles live in the same physical space, and hence that the dimensions N_A and N_B are equal.) If Alice's particle and Bob's particle have masses m_A and m_B respectively, we define $r_i \equiv q_i^A - q_i^B$ and $R_i \equiv (\mu/m_B) q_i^A + (\mu/m_A) q_i^B$ where $\mu \equiv m_A m_B/(m_A + m_B)$ is the reduced mass and i goes over all dimensions of the system ($\{x, y, z\}$ in three-dimensional system, for example).

$$\begin{aligned} \epsilon \;=\; & \sum_{ij} \left(\frac{a_i b_j}{3|\psi|^2} \right)^2 \Big| -(\frac{\mu}{m_B} \frac{\partial \psi}{\partial R_i} + \frac{\partial \psi}{\partial r_i})(\frac{\mu}{m_A} \frac{\partial \psi}{\partial R_j} - \frac{\partial \psi}{\partial r_j}) \\ & + \psi(\frac{\mu}{m_B} \frac{\partial}{\partial R_i} + \frac{\partial}{\partial r_i})(\frac{\mu}{m_A} \frac{\partial}{\partial R_j} - \frac{\partial}{\partial r_j})\psi \Big|^2, \end{aligned} \tag{7.46}$$

where i and j run over all the dimensions of the system.

In many cases, including most importantly the case where there is no external potential, the wave function $\psi(\mathbf{R}, \mathbf{r})$ can be decoupled into a centre-of-mass part $\chi(\mathbf{R})$ and a relative-motion part $\varphi(\mathbf{r})$:

$$\psi(\mathbf{R}, \mathbf{r}) = \chi(\mathbf{R}) \varphi(\mathbf{r}). \tag{7.47}$$

If we write

$$\varphi(\mathbf{r}) = e^{-S_\varphi(\mathbf{r})}, \qquad \chi(\mathbf{R}) = e^{-S_\chi(\mathbf{R})} \tag{7.48}$$

(with normalisation once again enforced by appropriate additive constants in S_φ and S_χ) then the entanglement takes the particularly simple form

$$\epsilon = \sum_{ij} \frac{a_i^2 b_j^2}{9} \left| \frac{\partial^2 S_\varphi(\mathbf{r})}{\partial r_i \partial r_j} + \frac{\mu^2}{m_A m_B} \frac{\partial^2 S_\chi}{\partial R_i \partial R_j} \right|^2 . \tag{7.49}$$

For example, if $\chi(\mathbf{R})$ is a free-particle plane wave $\chi(\mathbf{R}) = e^{i\mathbf{k}_0\mathbf{R}}$, its contribution to the entanglement $\mathcal{E}_D$ is zero; if $\chi(\mathbf{R})$ is a Gaussian wave packet with wave number $\mathbf{k}_0$ and real-space width R_0:

$$\psi(\mathbf{R}, \mathbf{r}) = (\frac{2}{\pi R_0^2})^{1/4} e^{-\mathbf{R}^2/R_0^2} e^{i\mathbf{k}_0\mathbf{R}} \varphi(\mathbf{r}), \tag{7.50}$$

the expression for ϵ becomes

$$\epsilon = \sum_{ij} \frac{a_i^2 b_j^2}{9} \left| \frac{\partial^2 S_\varphi(\mathbf{r})}{\partial r_i \partial r_j} - \frac{2\mu^2}{m_A m_B R_0^2} \delta_{ij} \right|^2 . \tag{7.51}$$

7.4 Examples

In this section we apply our method to some easily soluble examples: first to wavefunctions that (while remaining pure states) are semiclassical in the sense that the potential varies slowly on the scale of the de Broglie wavelength, so WKB methods are applicable, then to energy eigenstates of harmonically-interacting particles in arbitrary dimensionality, and finally to bound states of an electron and proton (i.e. to the hydrogen atom).

7.4.1 The semiclassical case: one-dimensional WKB wavefunctions

Consider two particles moving in one dimension with an interaction potential $V(r)$ that depends only on the relative coordinate. Neglecting centre-of-mass contributions, the entanglement can then be calculated from the relative wavefunction $\varphi(r)$ using equation 7.49. If $V(r)$ is a slowly varying function of r, we can use the WKB method to find $\varphi(r)$.

We consider an interaction with a single potential well (shown schematically in Figure 7.1), so the system moving in a bound state with energy E has just two classical turning points. For the classically allowed region with $E > V$ (region 2 of Figure 7.1), the classical momentum at r is $p(r) = \sqrt{2m(E - V(r))}$ and the corresponding wavefunction of the nth bound state can be expressed as either one of [Zet01]

$$\varphi_2^{WKB}(r) = \frac{2(-1)^n Z}{\sqrt{p(r)}} \sin\left[\frac{1}{\hbar}\int_{r_1}^{r} p(r')\,\mathrm{d}r' + \frac{\pi}{4}\right], \quad r_1 < r < r_2 \tag{7.52}$$

$$= \frac{2Z}{\sqrt{p(r)}} \sin\left[\frac{1}{\hbar}\int_{r}^{r_2} p(r')\,\mathrm{d}r' + \frac{\pi}{4}\right], \quad r_1 < r < r_2 \tag{7.53}$$

where Z is a normalisation constant, so that the local concurrence is

$$\mathcal{C}_2 = \left| \frac{ab}{3\hbar^2 p(r)^2} \left\{ 2\csc^2\left[\frac{1}{\hbar}\int_r^{r_2} p(r')\mathrm{d}r' + \frac{\pi}{4}\right] p(r)^4 + \hbar^2 p(r) \frac{\partial^2 p(r)}{\partial r^2} \right\} - \hbar^2 \left(\frac{\partial p(r)}{\partial r}\right)^2 + 2\hbar \cot\left[\frac{1}{\hbar}\int_r^{r_2} p(r')\mathrm{d}r' + \frac{\pi}{4}\right] p(r)^2 \frac{\partial p(r)}{\partial r} \right|. \tag{7.54}$$

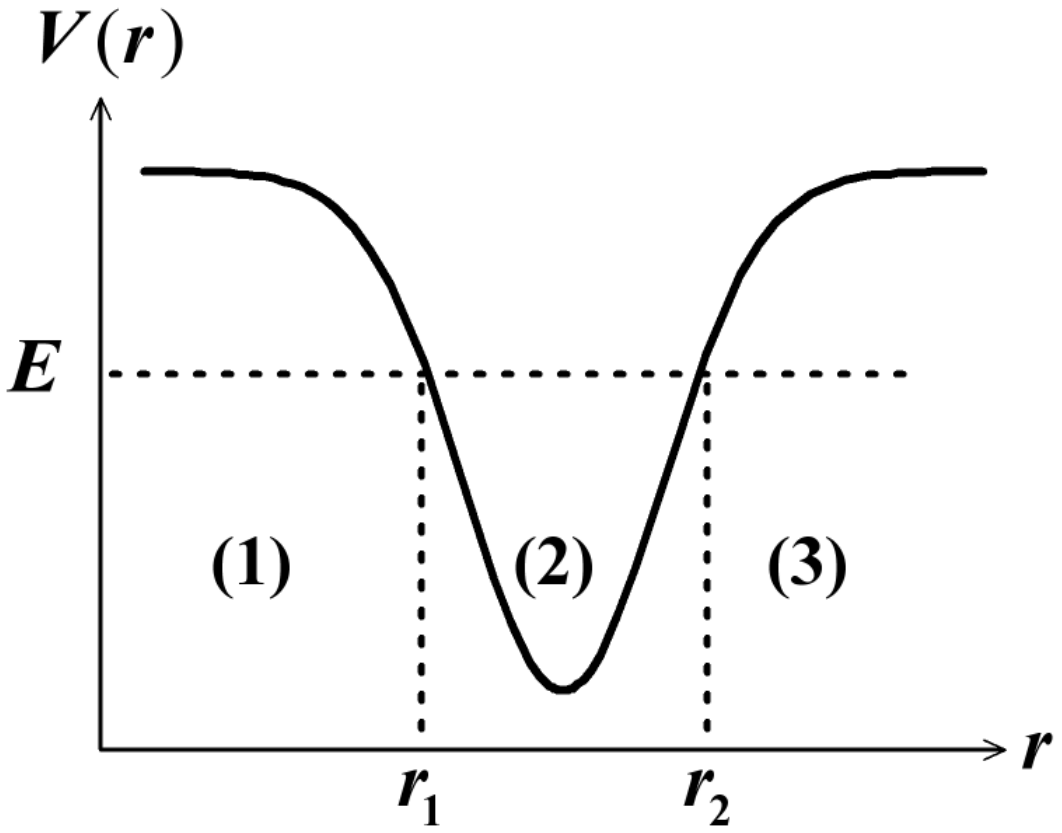

Figure 7.1: Diagram of a potential well illustrating the different regions discussed in the text.

The oscillatory structure of the wavefunction, arising from the interference between right- and left-moving travelling waves, produces nodes at which the entanglement in the discarding ensemble for fixed a and b diverges (but remains finite provided we remain within the domain of validity of equation 7.54—see Section 7.3.4).

Note also that the entanglement contribution from the first term in equation 7.54 is non-zero even where $V(r)$ (and hence $p(r)$) is constant.

For $E < V$ (region 1 and region 3 of Figure 7.1), we express the wavefunction in terms of the local momentum on the inverted potential surface $p(r) = \sqrt{2m(V(r) - E)}$. The wavefunctions are respectively

$$\varphi_1^{WKB}(r) = \frac{(-1)^n A}{\sqrt{|p(r)|}} \exp\left[-\frac{1}{\hbar}\int_r^{r_1} |p(r')|\mathrm{d}r'\right], \quad r < r_1; \tag{7.55}$$

$$\varphi_3^{WKB}(r) = \frac{A}{\sqrt{|p(r)|}} \exp\left[-\frac{1}{\hbar}\int_{r_2}^{r} |p(r')|\mathrm{d}r'\right], \quad r > r_2, \tag{7.56}$$

where n is the number of nodes in Region 2. Correspondingly, the concurrences are

$$\mathcal{C}_1 = \left| \frac{-ab}{3\hbar \left|p(r)\right|^2} \left[2\left|p(r)\right|^2 \frac{\partial \left|p(r)\right|}{\partial r} + \hbar \left(\frac{\partial \left|p(r)\right|}{\partial r} \right)^2 - \hbar \left|p(r)\right| \frac{\partial^2 \left|p(r)\right|}{\partial r^2} \right] \right|; \quad (7.57)$$

$$\mathcal{C}_3 = \left| \frac{ab}{3\hbar \left|p(r)\right|^2} \left[2\left|p(r)\right|^2 \frac{\partial \left|p(r)\right|}{\partial r} - \hbar \left(\frac{\partial \left|p(r)\right|}{\partial r} \right)^2 + \hbar \left|p(r)\right| \frac{\partial^2 \left|p(r)\right|}{\partial r^2} \right] \right|. \quad (7.58)$$

Note that in this case (by contrast to the behaviour in region 2) if there is no *force*, $p(r)$ is constant, and hence there is no entanglement. This is a nice example of the "no-force, no entanglement" theorem (Section 7.3.3). Furthermore, the first terms in equation 7.57 and equation 7.58 are simply proportional to the force on the particle ($\partial \left|p(r)\right| / \partial r$). Later, we will show another example which demonstrates this intriguing relationship between the local entanglement and the force.

It is interesting that the boundaries between these different behaviours of the entanglement correspond to the classical turning points—the WKB solutions themselves are no longer valid close to these turning points, and must be joined according to a connection formula derived from an exact solution to a linearised equation [Zet01].

7.4.2 Multi-dimensional harmonic oscillators

Consider first a system of two one-dimensional harmonic oscillators of masses m_A and m_B, having identical frequencies ω, and coupled by a spring constant K; the Hamiltonian is

$$\hat{H} = \hat{H}_A + \hat{H}_B + \frac{1}{2} K (\hat{X}_A - \hat{X}_B)^2. \quad (7.59)$$

Transforming to centre-of-mass and relative coordinates, the eigenstates are simply

$$\begin{aligned} \psi_{n_R,n_r}(R,r) &= \psi_{n_R}(R)\psi_{n_r}(r) \\ &= \frac{1}{\sqrt{\sqrt{\pi} 2^{n_R} 2^{n_r} n_R! n_r! R_0 r_0}} e^{-R^2/2R_0^2} \\ &\quad e^{-r^2/2r_0^2} H_{n_R}(\frac{R}{R_0}) H_{n_r}(\frac{r}{r_0}), \end{aligned} \quad (7.60)$$

where n_R and n_r label the excitations of each coordinate, $R_0 = \sqrt{\hbar/(M\omega)}$, $r_0 = \sqrt{\hbar/(\mu\sqrt{\omega^2 + K/\mu})}$, and $H_n(x)$ is the Hermite polynomial.

If Alice and Bob each possess an oscillator, the entanglement between their subsystems given by $h(\epsilon)$ can be determined from equation 7.46; for example, for the ground state:

$$\begin{aligned} \epsilon &= \frac{a^2 b^2 (m_A m_B r_0^2 - M^2 R_0^2)^2}{9 M^4 r_0^4 R_0^4} \\ &= \frac{a^2 b^2}{9 M^2 \hbar^2} (m_A m_B \omega - M\mu \sqrt{\frac{K}{\mu} + \omega^2})^2, \end{aligned} \quad (7.61)$$

where $M = m_A + m_B$. Note that the ground state is Gaussian, so ϵ is constant, as expected.

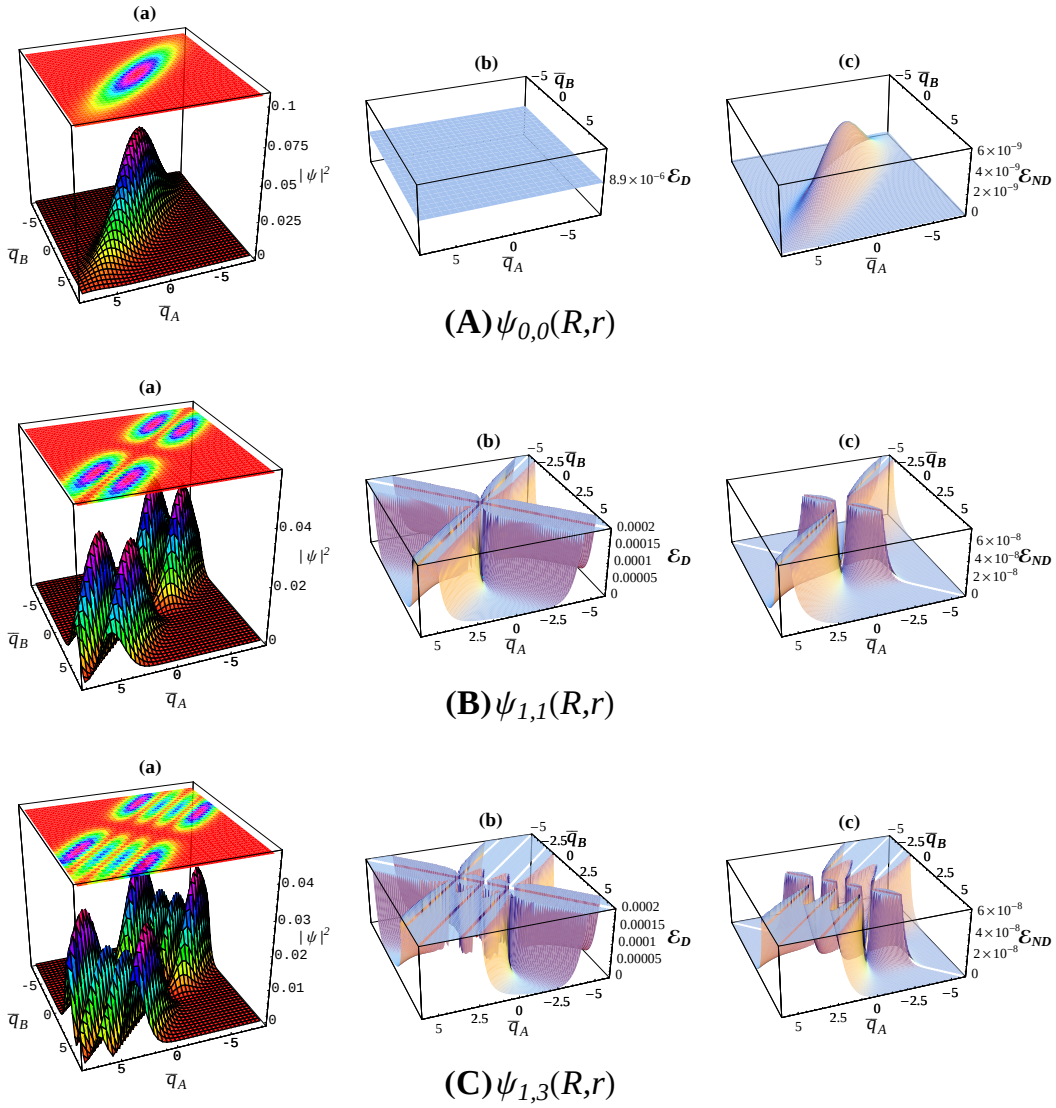

Figure 7.2: Probability density (left plot), local entanglement $\mathcal{E}_D$ in the discarding ensemble (centre plot) and local entanglement $\mathcal{E}_{ND}$ in the nondiscarding ensemble (right plot) for three pure states of the two-oscillator system: (A) $n_R = 0$, $n_r = 0$; (B) $n_R = 1$, $n_r = 1$; (C) $n_R = 1$, $n_r = 3$. The characteristic lengths of the problem are $r_0 = 2$ and $R_0 = 4$ in all plots, and all plots are for $a = b = 0.1$. The cut-off points for plots of $\mathcal{E}_D$ and $\mathcal{E}_{ND}$ are determined from ϵ_{MAX} in equation 7.34 with $\sigma = 0.1$; specifically, $\mathcal{E}_{ND}^{\mathrm{MAX}} = p_{\mathcal{AB}}^{\mathrm{MAX}} h(\epsilon_{\mathrm{MAX}})$, where h is defined in equation 3.29.

In Figure 7.2, we plot the probability distributions and entanglement $\mathcal{E}$ (in the discarding ensemble—centre column, and nondiscarding ensemble—right column) for the ground state and some excited states. Note that the ground state (a) is a Gaussian state so the discarding entanglement is constant and the left and right plots are proportional to one another; this is no longer true for the other (non-Gaussian) states, for which there are also nodes in the wavefunctions. We therefore show the entanglement in both ensembles cut off at the maximum value determined by equation 7.34.

For general multi-dimensional oscillators, the wavefunction becomes a product over the normal modes X_k of one-dimensional harmonic oscillator wavefunctions. The entanglement is determined by these normal-mode wavefunctions through equation 7.44. (Note that in the one-dimensional example considered above, the normal coordinates are the same as the relative and centre-of-mass coordinates.)

7.4.3 The hydrogen atom

We next consider the entanglement between the electron ('Alice's particle') and the proton ('Bob's particle') in a hydrogen atom. For simplicity, the sizes of the measured regions are assumed to be the same for all dimensions $\{x, y, z\}$, i.e. $a_i = a$ and $b_i = b$. First, consider the case where there is no centre-of-mass motion. Instead of directly applying equation 7.49, we transform the coordinates and the equation into to spherical coordinates:

$$\begin{aligned}
\frac{\partial}{\partial r_x} &= \sin\theta\cos\phi\frac{\partial}{\partial r} + \frac{\cos\theta\cos\phi}{r}\frac{\partial}{\partial\theta} - \frac{\csc\theta\sin\phi}{r}\frac{\partial}{\partial\phi} \\
\frac{\partial}{\partial r_y} &= \sin\theta\sin\phi\frac{\partial}{\partial r} + \frac{\cos\theta\sin\phi}{r}\frac{\partial}{\partial\theta} + \frac{\csc\theta\cos\phi}{r}\frac{\partial}{\partial\phi} \\
\frac{\partial}{\partial r_z} &= \cos\theta\frac{\partial}{\partial r} - \frac{\sin\theta}{r}\frac{\partial}{\partial\theta}.
\end{aligned} \tag{7.62}$$

By substituting the most general form of the relative wave function $\varphi_{nlm}(r, \theta, \phi)$ of a hydrogen atom into equation 7.49 after it has been transformed to spherical coordinates, we have ϵ in terms of polar derivatives. The full expression is given in Appendix F.

The ground state is

$$\varphi_{100}(r, \theta, \phi) = (\frac{1}{\pi a_0^3})^{1/2} e^{-r/a_0}, \tag{7.63}$$

where a_0 is the Bohr radius. In this case,

$$\epsilon = 2(\frac{ab}{3a_0 r})^2. \tag{7.64}$$

Interestingly, this expression indicates that the entanglement $\mathcal{E}_D$ for the ground state of a hydrogen atom falls off with distance in exactly the same way as the electrostatic force between

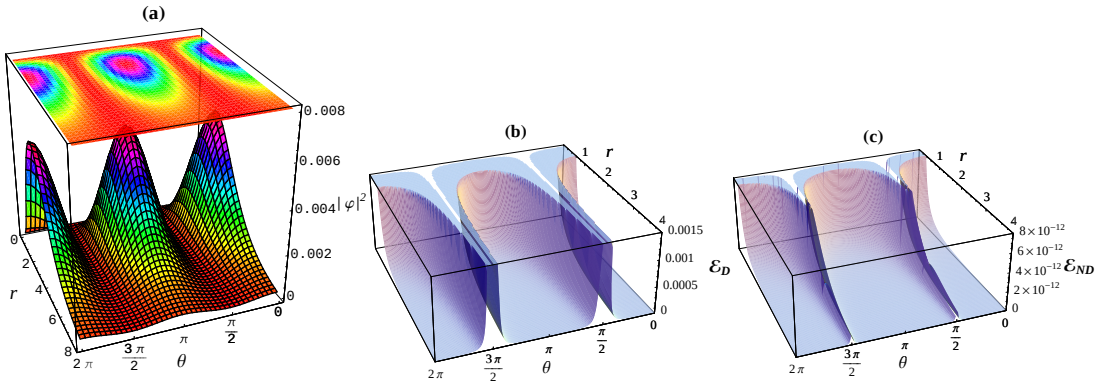

Figure 7.3: Probability density (left plot), local entanglement $\mathcal{E}_D$ in the discarding ensemble (centre plot) and local entanglement $\mathcal{E}_{ND}$ in the nondiscarding ensemble (right plot) for the relative wavefunction $\varphi_{210}(r,\theta,\phi)$ of a hydrogen atom. All plots are for $a = b = 0.1$. The cut-off points for plots of $\mathcal{E}_D$ and $\mathcal{E}_{ND}$ are determined from $\epsilon_{\rm MAX}$ in equation 7.34 with $\sigma = 0.1$; specifically, $\mathcal{E}_{ND}^{\rm MAX} = p_{\mathcal{AB}}^{\rm MAX} h(\epsilon_{\rm MAX})$, where h is defined in equation 3.29.

the electron and the nucleus. Again, this is an example of the "no-force, no entanglement" theorem, and note the similarity between this example and the previous WKB example. The WKB approximation is valid in this limit, and it is not surprising then that in both cases, the dominant terms in the local entanglements are proportional to the force.

If we include a centre-of-mass part to the wave function with a Gaussian form as in equation 7.50, we obtain

$$\begin{aligned}\epsilon &= \frac{2a^2b^2}{9R_0^4a_0^2(m_A+m_B)^4r^2}\Big(R_0^4(m_A+m_B)^4 \\ &\quad -4R_0^2a_0m_Am_B(m_A+m_B)^2r+6a_0^2m_A^2m_B^2r^2\Big).\end{aligned} \tag{7.65}$$

The first term is the component noted previously, decaying in the same way as the atom's internal electrostatic force; in addition there are two new contributions from the localisation of the free-particle wave function. Of these the third term corresponds to the spatially constant entanglement of the gaussian centre-of-mass state.

Excited states of the atom can also be analysed, by substituting the appropriate energy eigenfunction into the expression for ϵ in Appendix F. The excited states have nodes in the wavefunction, which have to be treated as discussed earlier. We show the corresponding probability distribution, and entanglement $\mathcal{E}$ (in the discarding and nondiscarding ensembles) in Figure 7.3.

7.5 Summary

Our approach allows us to analyse the distribution of entanglement after imperfect local position measurements in any smooth bipartite pure state. Equations 7.25 and 7.27 are the main results in this chapter, allowing us to calculate the concurrence in terms of simple derivatives of the wavefunction. Equation 7.43 allows us to express the entanglement in the same local region in terms of an arbitrary linear transformation of the coordinates, and equation 7.49 treats the important case where the motion separates into centre-of-mass and relative coordinates.

The three examples of exactly integrable systems that we have discussed show a number of common features. First, there is generic behaviour near nodes in the wavefunction. There is an apparent divergence in the entanglement in the discarding ensemble for a fixed region size, but this does not mean that large amounts of entanglement can be extracted from the continuous-variable wavefunction once the system has been localised in this region. Our expressions for entanglement are always true only in the limit of small region sizes, and their domain of validity shrinks as we approach a node; the discarding entanglement remains finite so long as we take care always to remain within this domain. Furthermore, when we measure the locations of the particles we are unlikely to find them near a node in the wavefunction, so the probability factor in equation 4.19 further suppresses the nondiscarding entanglement relative to the discarding entanglement.

As the size of the measurement regions increases, our approach starts to break down because more than two eigenvalues of the reduced density matrix become important. We have explicitly computed the extent of this breakdown, giving the lowest-order corrections to our main results in Appendix E.

As pointed out in Section 7.3.3 and Section 7.3.5.3, free-particle wavefunctions do not give rise to any local entanglement, but there may be some local entanglement if the state is in a superposition of linearly independent plain waves. We have shown how our entanglement expressions are transformed when moving to other coordinates (e.g. centre-of-mass and relative coordinates); however, it is important to realize that the entanglement we quantify is still between the original subsystems. The transformation is only done for the convenience of the calculations.

Our results for the WKB wavefunctions and for the hydrogen atom suggest an intriguing link between the interaction force and the local entanglement, but the exact details of the relationship and its generality need to be further explored.

For any bipartite multi-mode pure states, the local concurrence equals twice the corresponding local negativity in the limit of very small sizes, a_i and b_j, of measurement regions.

In addititon, each mode of the entangled state contributes non-linearly to the total concurrence, $\mathcal{C}^2 = \sum_{ij} \mathcal{C}_{ij}^2$. It is therefore not straightforward to extend the previous results for two-mode mixed states to multi-mode ones. Much more work is required in order to gain significant insights in this direction.

Chapter 8

Indistinguishable Particles

8.1 Introduction

So far we have ignored the problem of indistinguishability. In quantum systems, particles are usually indistinguishable (for example, photons) and in many situations, the effects of their quantum statistics will be too significant to be neglected. It is therefore important to extend our analysis to take this into account. and we will apply our approach in this chapter to study the local entanglement of identical particles. We will show that once the identical particles are localised, the localised particles effectively behave as distinguishable particles, and the local entanglement between them can then be analysed as before.

Our local approach described in Chapter 4 involves Alice and Bob each making preliminary measurements on their own interacting particles to localise the particles within region $\mathcal{A}$ and region $\mathcal{B}$ respectively but the Hilbert space of each particle need not be the same, that is, particles can be separately localised in different spatial dimensions. However, identical particles, by definition, cannot have distinct state spaces so now their spatial dimensions must be the same and region $\mathcal{A}$ and region $\mathcal{B}$ have to be part of the same Hilbert space. This is an important distinction from our previous formulation worth bearing in mind throughout the rest of the analysis.

8.2 The Density Operator in the Discarding Ensemble ρ_D

Let Alice and Bob share a state of two identical particles moving in one-dimension. To extend our analysis to systems of indistinguishable particles, we first need to modify the previous definition of the discarding ensemble. Alice makes a preliminary measurement on a region of configuration space around $\bar{q}_{\mathcal{A}}$ to determine whether she can find *any* particle, and similarly Bob makes a measurement to see whether he can find *any* particle in the region around $\bar{q}_{\mathcal{B}}$. This process only grants them knowledge of the number of particles in their possession after measurements but nothing more. Any entanglement between Alice's and Bob's subsystems

must come from the interaction or quantum statistics of the particles. For a given density of particles, the probability of finding more than one in a chosen region can always be made negligibly small by choosing smaller regions so it is reasonable to consider only *the entanglement between Alice's and Bob's subsystems after each successfully finds exactly one particle in their chosen non-overlapping regions*. We therefore define the appropriate discarding ensemble to consider in the case of indistinguishable particles to be the resulting subensemble after all the other instances are discarded.

The projector corresponding to Alice's measurement of finding exactly one particle (coordinate q) in a chosen region $\mathcal{A}$ around $\bar{q}_{\mathcal{A}}$ with width $2a$ of configuration space is

$$\hat{E}_A = \theta_A(q_1)[1-\theta_A(q_2)] + \theta_A(q_2)[1-\theta_A(q_1)], \tag{8.1}$$

where

$$\theta_A(q) = \begin{cases} 1 & \text{if } \bar{q}_{\mathcal{A}} - a < q < \bar{q}_{\mathcal{A}} + a \\ 0 & \text{otherwise} \end{cases}. \tag{8.2}$$

The first part in equation (8.1) represents that Alice successfully finds only Particle 1 (coordinate q_1) in the measured region $\mathcal{A}$ whereas the second part represents that Particle 2 (coordinate q_2) is found; either one can be the outcome but she is unable to tell the identity of the found particle. Similarly, the projector corresponding to Bob's measurement of finding exactly one particle in a chosen region $\mathcal{B}$ around $\bar{q}_{\mathcal{B}}$ with width $2b$ of configuration space is

$$\hat{E}_B = \theta_B(q_1)[1-\theta_B(q_2)] + \theta_B(q_2)[1-\theta_B(q_1)]. \tag{8.3}$$

It is essential that Alice's measured region $\mathcal{A}$ is mutually exclusive to Bob's $\mathcal{B}$, otherwise it becomes meaningless to talk about the entanglement between both parties' subsystems. The density matrix in the discarding ensemble is therefore

$$\begin{aligned} \rho_D &= \frac{\hat{E}_A\hat{E}_B\rho\hat{E}_B\hat{E}_A}{p} \\ &= \frac{1}{p}[\theta_A(q_1)\theta_B(q_2) + \theta_B(q_1)\theta_A(q_2)]\,\rho\,[\theta_A(q_1')\theta_B(q_2') + \theta_B(q_1')\theta_A(q_2')] \end{aligned} \tag{8.4}$$

$$\begin{aligned} \Longrightarrow \quad \rho_D(q_1,q_2;q_1',q_2') &= \frac{1}{p}\rho(q_1\in\mathcal{A}, q_2\in\mathcal{B}; q_1'\in\mathcal{A}, q_2'\in\mathcal{B}) \\ &\quad + \frac{1}{p}\rho(q_1\in\mathcal{A}, q_2\in\mathcal{B}; q_1'\in\mathcal{B}, q_2'\in\mathcal{A}) \\ &\quad + \frac{1}{p}\rho(q_1\in\mathcal{B}, q_2\in\mathcal{A}; q_1'\in\mathcal{A}, q_2'\in\mathcal{B}) \\ &\quad + \frac{1}{p}\rho(q_1\in\mathcal{B}, q_2\in\mathcal{A}; q_1'\in\mathcal{B}, q_2'\in\mathcal{A}), \end{aligned} \tag{8.5}$$

where p is the probability for Alice to find exactly one particle in $\mathcal{A}$ and Bob to find exactly one particle in $\mathbf{B}$. Now we need to consider quantum statistics of identical particles before we can go on to deduce the final form of ρ_D.

8.3 Effects of Quantum Particle Statistics

Quantum particle statistics between an indistinguishable particle and another indistinguishable particle in another "remote" location does not give rise to any measurable consequences with respect to *local* measurements, and hence there is no usable entanglement unless the particles are also interacting in some other way [Per95]. The "remoteness" depends on the quantum measurement concerned, and generally speaking is determined by the length scale of the measuring equipment for that particular measurement. In this context, because the measured regions $\mathcal{A}$ and $\mathcal{B}$ are mutually exclusive, the localised states resulting from both Alice's and Bob's preliminary measurements are "remote" with respect to each other.

However, it is worth noting that if localised indistinguishable particles' wave functions are allowed to overlap spatially, it is no longer necessary to have an interaction in order to produce entanglement. For example, two non-interacting electrons with an inter-electron distance roughly below the inverse Fermi momentum in a Fermi sea are entangled in the spin degrees of freedom simply due to the effects of the Pauli exclusion principle [Ved03, Git05].

Since there should be no spatial overlap between Alice's and Bob's subsystems in the discarding ensemble, it is essential to ensure that our treatment does not make it possible for these "non-interacting" correlations to give rise to any usable entanglement.

The *symmetrisation postulate* stipulates that the state of quantum systems containing N identical particles are either totally symmetric or totally antisymmetric under the interchange of any pairs of particles and that states with mixed symmetry do not exist:

$$\psi(\xi_1, \xi_2, \ldots, \xi_i, \ldots, \xi_j, \ldots, \xi_N) = \pm\psi(\xi_1, \xi_2, \ldots, \xi_j, \ldots, \xi_i, \ldots, \xi_N). \tag{8.6}$$

Furthermore, particles with integral spins (bosons) have symmetric states whereas particles with half-odd-integer spins (fermions) have antisymmetric states so that the plus sign is for bosons and the minus sign for fermions in equation 8.6. To satisfy the symmetrisation postulate, we write the overall density matrix $\rho(q_1, q_2; q_1', q_2')$ as

$$\begin{aligned} \rho(q_1, q_2; q_1', q_2') &= \frac{1}{2}[\varrho(q_1, q_2; q_1', q_2') \pm \varrho(q_2, q_1; q_1', q_2') \\ &\quad + \varrho(q_2, q_1; q_2', q_1') \pm \varrho(q_1, q_2; q_2', q_1')], \end{aligned} \tag{8.7}$$

where ϱ is an auxiliary asymmetric density matrix. Any local measurement that Alice (Bob) can carry out on her (his) unidentified particle in the discarding ensemble is represented by an arbitrary one-particle operator $\hat{A}$ ($\hat{B}$):

$$\hat{A}(1,2) = \hat{\mathsf{a}}(1) + \hat{\mathsf{a}}(2) = \hat{\mathsf{a}} \otimes \mathbb{1} + \mathbb{1} \otimes \hat{\mathsf{a}}; \tag{8.8}$$

$$\hat{B}(1,2) = \hat{\mathsf{b}}(1) + \hat{\mathsf{b}}(2) = \hat{\mathsf{b}} \otimes \mathbb{1} + \mathbb{1} \otimes \hat{\mathsf{b}} \tag{8.9}$$

such that

$$\hat{\mathsf{a}}(1)\theta_B(q_1) = 0; \tag{8.10}$$

$$\hat{\mathsf{a}}(2)\theta_B(q_2) = 0; \tag{8.11}$$

$$\hat{\mathsf{b}}(1)\theta_A(q_1) = 0; \tag{8.12}$$

$$\hat{\mathsf{b}}(2)\theta_A(q_2) = 0, \tag{8.13}$$

where $\hat{\mathsf{a}}(1)$ and $\hat{\mathsf{b}}(1)$ are for Particle 1 whereas $\hat{\mathsf{a}}(2)$ and $\hat{\mathsf{b}}(2)$ are for Particle 2.

The expectation value of Alice's and Bob's local operations on their respective subsystems is therefore

$$\begin{aligned}\mathrm{Tr}[\hat{A}\hat{B}\rho_D] &= \mathrm{Tr}\left[\hat{\mathsf{a}}(1)\hat{\mathsf{b}}(2)\frac{\theta_A(q_1)\theta_B(q_2)\rho(q_1,q_2;q_1',q_2')\theta_A(q_1')\theta_B(q_2')}{p}\right. \\ &\quad \left. + \hat{\mathsf{a}}(2)\hat{\mathsf{b}}(1)\frac{\theta_B(q_1)\theta_A(q_2)\rho(q_1,q_2;q_1',q_2')\theta_B(q_1')\theta_A(q_2')}{p}\right] \\ &= 2\mathrm{Tr}\left[\hat{\mathsf{a}}(1)\hat{\mathsf{b}}(2)\theta_A(q_1)\theta_B(q_2)\frac{\rho(q_1,q_2;q_1',q_2')}{p}\theta_A(q_1')\theta_B(q_2')\right]. \end{aligned} \tag{8.14}$$

By substituting equation (8.7) into this, we obtain

$$\begin{aligned}\mathrm{Tr}[\hat{A}\hat{B}\rho_D] &= \frac{1}{p}\mathrm{Tr}\left[\hat{\mathsf{a}}(1)\hat{\mathsf{b}}(2)\theta_A(q_1)\theta_B(q_2)\{\varrho(q_1,q_2;q_1',q_2') \pm \varrho(q_2,q_1;q_1',q_2')\right. \\ &\quad \left. +\varrho(q_2,q_1;q_2',q_1') \pm \varrho(q_1,q_2;q_2',q_1')\}\theta_A(q_1')\theta_B(q_2')\right]. \end{aligned} \tag{8.15}$$

Note that we can start from any asymmetric density matrix $\varrho(q_1,q_2;q_1',q_2')$ to construct a (anti)symmetrised one $\rho(q_1,q_2;q_1',q_2')$ so we can always choose a $\varrho(q_1,q_2;q_1',q_2')$ such that it is nonzero only when $q_1 \in \mathcal{A}$, $q_2 \in \mathcal{B}$, $q_1' \in \mathcal{A}$ and $q_2' \in \mathcal{B}$. For example, suppose the particles are fermions, and hence the overall density matrix $\rho(q_1,q_2;q_1',q_2') = \Psi(q_1,q_2)\Psi^*(q_1',q_2')$ is antisymmetric. It follows that $\varrho(q_1,q_2;q_1',q_2') = \Phi(q_1,q_2)\Phi^*(q_1',q_2')$ if $\Psi(q_1,q_2) = [\Phi(q_1,q_2) - \Phi(q_2,q_1)]/\sqrt{2}$. By choosing the asymmetric wave function $\Phi(q_1,q_2)$ to be

$$\Phi(q_1,q_2) = \frac{\Psi(q_1,q_2) + S(q_1,q_2)}{2} \tag{8.16}$$

where $S(q_1,q_2)$ is an arbitrary symmetric function such that

$$S(q_1,q_2)\begin{cases} = \Psi(q_1,q_2) & \text{if } q_1 \in \mathcal{A}, q_2 \in \mathcal{B} \\ = -\Psi(q_1,q_2) & \text{if } q_1 \in \mathcal{B}, q_2 \in \mathcal{A} \end{cases}, \tag{8.17}$$

we have the desired $\varrho(q_1,q_2;q_1',q_2')$ that is perfectly valid without any additional assumption or restriction (apart from the symmetrisation postulate) on the form of the joint wave function $\Psi(q_1,q_2)$.

It now becomes clear that we can write equation (8.15) as

$$\mathrm{Tr}[\hat{A}\hat{B}\rho_D] = \frac{1}{p}\mathrm{Tr}[\hat{\mathsf{a}}(1)\hat{\mathsf{b}}(2)\theta_A(q_1)\theta_B(q_2)\varrho(q_1,q_2;q_1',q_2')\theta_A(q_1')\theta_B(q_2')] \tag{8.18}$$

without losing generality in $\rho(q_1,q_2;q_1',q_2')$ so that in the discarding ensemble the expectation value of both Alice's observable $\hat{A}$ and Bob's observable $\hat{B}$ is not affected by the fact that the joint state of the two indistinguishable particles is (anti)symmetrised. It is now clear that once localised, the density matrix in the discarding ensemble ρ_D can be written as

$$\begin{aligned}\rho_D &= \frac{1}{p}\rho(q_1\in\mathcal{A}, q_2\in\mathcal{B}; q_1'\in\mathcal{A}, q_2'\in\mathcal{B}) \\ &= \rho_D(q_\mathcal{A}, q_\mathcal{B}; q_\mathcal{A}', q_\mathcal{B}').\end{aligned} \tag{8.19}$$

8.4 Local Entanglement in the Discarding Ensemble $\mathcal{E}_D$

We have seen that despite the indistinguishability of particles, the localising measurements make both Alice's and Bob's subsystems in the discarding ensemble behave exactly as distinguishable particles so that starting from $\rho_D(q_\mathcal{A}, q_\mathcal{B}; q_\mathcal{A}', q_\mathcal{B}')$, our previous method, described in Chapter 6, to quantify local entanglement in a system of two distinguishable interacting particles is again applicable here.

8.5 Generalisation to Many-Particle Systems

Now consider the system to have many identical particles, and Alice and Bob each try to localise *one* particle in mutually exclusive regions so that we are only interested in the entanglement *between the localised particles*. Again, the discarding ensemble will only consist of cases where each party finds exactly one identical particle in his/her chosen region, and all the other cases will be discarded. Therefore, we can start from the two-particle reduced density matrix $\rho^{(2)}$ instead of the full one $\rho^{(N)}$:

$$\rho^{(2)}(r_1,r_2;r_1',r_2') = \frac{N(N-1)}{2}\int \mathrm{d}^2r_3\ldots\mathrm{d}^2r_N\,\rho^{(N)}(r_1,r_2,\ldots,r_N;r_1',r_2',\ldots,r_N). \tag{8.20}$$

Then, replace $\rho(q_1,q_2;q_1',q_2')$ in equation 8.5, equation 8.7 and equation 8.14 by $\rho^{(2)}(r_1,r_2;r_1',r_2')$, the rest of the argument proceeds exactly the same as the $N=2$ case. Note that the symmetry properties of the two-particle reduced density matrix $\rho^{(2)}$ are the same as those of $\rho(q_1,q_2;q_1',q_2')$ in the $N=2$ case, even though their traces will be different.

8.6 Summary

In contrast to the case of distinguishable particles, the Hilbert space of each identical particle must be the same and entanglement between particles can arise from quantum particle statistics.

By considering the discarding ensemble, where only the cases of Alice and Bob each localising exactly one particle in non-overlapping regions are kept and all the others are thrown away, we can overcome these problems and quantify the usable entanglement between the localised particles. The localisation process effectively makes the localised identical particles "distinguishable" so once localised, the quantification of the entanglement between two localised particles, possibly in a many-particle system, are easily done by following the methods described for the case of distinguishable particles. Consequently, our local approach is equally applicable to systems of either identical or distinguishable particles.

Chapter 9

Conclusions

Quantum entanglement is not just a profound feature of quantum mechanics but it is also a valuable physical resource with massive potential for technological applications, such as quantum computation. However, our understanding of entanglement is still far from complete despite current intense research activities. Like other physical resources, for example, energy, the first step towards exploiting them fully is to know how to quantify correctly. It is therefore not surprising that there has been growing interest in the quantification of entanglement in quantum systems.

There are many reasons to focus on the entanglement of continuous-variable states since the underlying degrees of freedom of physical systems carrying quantum information are frequently continuous, rather than discrete. Much of the effort has been concentrated on Gaussian states, because these are common (especially in quantum optics) as the ground or thermal states of optical modes. Within this framework, many interesting topics have been studied and some significant progress made. However one should remember that non-Gaussian states are also extremely important; this is especially so in condensed-phase systems, where harmonic behaviour in any degree of freedom is likely to be only an approximation. So far, there is little knowledge about how to quantify entanglement in these non-Gaussian states.

This thesis aims to contribute to the active field of research in quantum entanglement by opening up a new direction to study the entanglement of general states, especially continuous-variable, and shows particularly that this leads to the first systematic quantification of the (local) entanglement in arbitrary non-Gaussian states.

The local entanglements, the entanglement in the discarding ensemble $\mathcal{E}_D$ and the (useful) entanglement in the nondiscarding ensemble $\mathcal{E}_{ND}$, are simply related (equation 4.19) so the attention is concentrated on $\mathcal{E}_D$. For any convex entanglement measure with an operational definition, the entanglement in the nondiscarding ensemble is simply $\bar{\mathcal{E}}_D$, the average of the entanglement in the discarding ensemble over all possible partitions. $\bar{\mathcal{E}}_D$ can never exceed the

original full entanglement of the system.

We first apply our local approach, whose formalism is described in Chapter 4, to the study of quantum entanglement in the discrete-variable systems by using a simple spin system, where Alice and Bob share two pairs of spin-1/2 particles, as an example. Both pure and mixed states are analysed, and the results of our local approach in this case are examples of quantum distillation and concentration.

An interesting question "where in continuous configuration space is the entanglement located?" is tackled by applying our local approach to investigate the location dependence of the ground-state entanglement between a pair of coupled harmonic oscillators, one oscillator to each of the two communicating parties Alice and Bob. By studying the variations of the entanglement properties with the size of the preliminary measurement region, we argue that the shared entanglement remaining to Alice and Bob (the local entanglement $\mathcal{E}_D$) provides a natural measure of where in configuration space the entanglement is originally located. The local entanglement saturates to the full (global) entanglement as the measured regions become large, and tends to zero as the regions become small. For a fixed region size, the configuration-space location can be varied in order to give a variable-resolution map of the entanglement distribution. It is shown that the distribution of the entanglement is qualitatively different from the classical correlations between the oscillators, being considerably more extended in configuration space than the joint probability and becoming more and more diffuse as the size of the regions decreases.

In the limiting cases where the sizes of the preliminary measurement regions are extremely small, our local approach provides a straightforward scheme that results in simple expressions for quantification of the local entanglements in general continuous-variable states. Many interesting systems can therefore be investigated and aspects of quantum entanglement characterised. We have thoroughly studied general smooth (including non-Gaussian) bipartite two-mode (mixed) continuous-variable states and multi-mode pure continuous-variable states. Surprisingly, in this limit the description of each mode of a continuous-variable state becomes isomorphic to a single qubit.

Our local approach is particularly simple to implement for pure states, since in this case the state in the discarding ensemble is also a pure state, and hence its entanglement can be simply characterised by the entropy of the reduced density matrices. For pure bipartite states, the expressions for the entropy of entanglement and concurrence are explicitly derived, and the local concurrence is simply twice the local negativity.

For two-mode mixed states, a recipe for numerically computing the local concurrence is

given, and in addition we show that the exact expression for the concurrence can be analytically derived for Gaussian states. We do not succeed in obtaining a closed-form expression for the concurrence of general two-mode states (apart from pure states and rank-2 mixed states); however, the difficulty can be bypassed by using the negativity (or the logarithmic negativity) as the measure of entanglement instead. The local negativity of any two-mode continuous-variable states can be directly computed from equation 6.20; based on the sign of C_1, the negativity can be either proportional to $(ab)^2$ or depends on the "area" (ab) and also on the "shape" (b/a). In comparison, the concurrence is always proportional to (ab). Provided $C_1 \geq 0$, we can define the maximised negativity, which is also always proportional to (ab). This naturally leads to the definitions of the concurrence density and the negativity density. The two local-entanglement densities are plotted as a function of temperature for thermal states of two harmonic oscillators with different coupling strengths to show that for this set of states, those which are entangled from the global point of view are also entangled by our local measures. This is a very interesting feature, which unfortunately is not true in general.

Even though quantum entanglement of a pure state can be fully characterised via the von Neumann entropy, the calculation of this entropy for a high-dimensional system is generally very difficult and will almost always have to be performed numerically. Our results (equations 7.25 and 7.27) enable the local entanglement to be computed directly and explicitly, without the time-consuming numerical evaluation of the global entanglement in a high-dimensional system, once the state of the system is known. As the size of the measurement regions increases, this approach will start to break down; the lowest-order corrections to our main results are given in Appendix E.

Equation 7.43 allows us to express the entanglement in the same local region in terms of an arbitrary linear transformation of the coordinates, and equation 7.49 treats the important case where the motion separates into centre-of-mass and relative coordinates. The transformation of the entanglement expressions to other coordinates can be done for the convenience of the calculations; however, it is important to note that the local entanglement quantified is still between the original subsystems.

The "no-force, no-entanglement" theorem in Section 7.3.3 states that by excluding the effects of the superposition of wavefunctions, the non-superposed eigenstate for the force-free Schrödinger equation, such that the boundary conditions are satisfied, can always be written in the form of equation 7.26 with S being a linear function of coordinates so that there is no local entanglement. Consequently, a free-particle wavefunction does not give rise to any local entanglement.

Three examples of pure continuous-variable states are studied: semiclassical WKB systems, multi-dimensional harmonic oscillators, and a hydrogen atom. We find that generic behaviour occurs near nodes in the wavefunction. There is an apparent divergence in the entanglement in the discarding ensemble $\mathcal{E}_D$ for a fixed region size, but this does not imply that large amounts of entanglement can be extracted once the system has been localised in this region. Our expressions for the local entanglement are always true only in the limit of small region sizes, and their domain of validity shrinks as we approach a node; the entanglement in the discarding ensemble $\mathcal{E}_D$ remains finite within this domain of validity. In addition, the particles are unlikely to be found near a node in the wavefunction, so the probability factor in equation 4.19 further suppresses the entanglement in the nondiscarding ensemble $\mathcal{E}_{ND}$ relative to $\mathcal{E}_D$. The results for the WKB wavefunctions and for the hydrogen atom suggest an intriguing link between the interaction force and the local entanglement, but the exact details of the relationship and its generality need to be further explored.

Quantum particle statistics between an indistinguishable particle and another remote indistinguishable particle does not give rise to any measurable consequences with respect to local measurements so there is no usable entanglement unless the particles are also interacting in some other way. In the case of two interacting indistinguishable particles, by considering the case where Alice and Bob each successfully finds exactly one particle in their chosen non-overlapping measurement regions and defining the discarding ensemble to be the resulting subensemble after all the other possible measurement outcomes are discarded, we show that once the particles are localised, the entanglement in the discarding ensemble can then be quantified in the same way as for distinguishable particles. It is also possible to extend our local approach to a system of many indistinguishable particles, provided that we only consider the entanglement after the particles are localised and reside in non-overlapping regions.

Our local approach to quantum entanglement suffers from the disadvantage that there is no sum rule on the entanglements in the discarding ensemble: the sum of the entanglements from all the sub-regions defined by a given decomposition of configuration space does not yield the full entanglement of the system. Instead, the entanglements from the sub-regions satisfy the inequality in equation 4.25. Further studies will therefore be needed in order to understand in more detail the relationship between the local entanglement and the global entanglement.

It is not straightforward to extend our results analytically to multi-mode mixed-states, not least because the difficulty to derive the closed expression for two-mode mixed states. Despite this failure, our approach should open up a new direction to investigate aspects of quantum entanglement in general bipartite continuous-variable states, especially non-Gaussian ones. Local

entanglement of systems with smooth wavefunctions are fully characterised by our expressions, provided the wavefunction of the system is known. In any case our approach provides a scheme that permits much simpler numerical computation for quantifying entanglement of mixed states via the (logarithmic) negativity than is generally possible from directly computing the full entanglement of the system. We hope our local approach to quantum entanglement will be adopted and explored further by the research community, and hence contribute to the important field of quantum entanglement and its applications.

Appendix A

Entanglement of Formation of a Two-Mode Gaussian Ground State

In the case of only two harmonic oscillators ($N = 2$), the $\mathbf{V}$ matrix for the ground state is simply [AEPW02]

$$\mathbf{V} = \begin{pmatrix} 1+2\alpha & -2\alpha \\ -2\alpha & 1+2\alpha \end{pmatrix} \tag{A.1}$$

so that

$$\mathbf{V}^{\frac{1}{2}} = \frac{1}{2m\omega} \begin{pmatrix} 1+\sqrt{1+4\alpha} & 1-\sqrt{1+4\alpha} \\ 1-\sqrt{1+4\alpha} & 1+\sqrt{1+4\alpha} \end{pmatrix} \tag{A.2}$$

and

$$\mathbf{V}^{-\frac{1}{2}} = \frac{m\omega}{2} \begin{pmatrix} 1+\frac{1}{\sqrt{1+4\alpha}} & 1-\frac{1}{\sqrt{1+4\alpha}} \\ 1-\frac{1}{\sqrt{1+4\alpha}} & 1+\frac{1}{\sqrt{1+4\alpha}} \end{pmatrix}. \tag{A.3}$$

The covariance matrix of a thermal state with some temperature, $T > 0$, is

$$\gamma(\beta) = \frac{1}{2}\left(\frac{\gamma_x(\beta)}{m\omega} \oplus m\omega\gamma_p(\beta)\right), \tag{A.4}$$

where $\beta = 1/T$ and

$$\begin{aligned} \gamma_x(\beta) &= \mathbf{V}^{-1/2}\Big\{\mathbb{1}_2 + 2\Big(e^{\mathbf{V}^{1/2}\beta} - \mathbb{1}_2\Big)^{-1}\Big\} \\ \gamma_p(\beta) &= \mathbf{V}^{1/2}\Big\{\mathbb{1}_2 + 2\Big(e^{\mathbf{V}^{1/2}\beta} - \mathbb{1}_2\Big)^{-1}\Big\}. \end{aligned} \tag{A.5}$$

We then have

$$\begin{aligned} &\gamma(\beta) \\ = \frac{1}{2} &\begin{pmatrix} \frac{1}{m\omega}\Big[\coth(\frac{\beta\omega_1}{2}) + \frac{1}{\sqrt{1+4\alpha}}\coth(\frac{\beta\omega_2}{2})\Big] & \frac{1}{m\omega}\Big[\coth(\frac{\beta\omega_1}{2}) - \frac{1}{\sqrt{1+4\alpha}}\coth(\frac{\beta\omega_2}{2})\Big] \\ \frac{1}{m\omega}\Big[\coth(\frac{\beta\omega_1}{2}) - \frac{1}{\sqrt{1+4\alpha}}\coth(\frac{\beta\omega_2}{2})\Big] & \frac{1}{m\omega}\Big[\coth(\frac{\beta\omega_1}{2}) + \frac{1}{\sqrt{1+4\alpha}}\coth(\frac{\beta\omega_2}{2})\Big] \\ 0 & 0 \\ 0 & 0 \end{pmatrix} \end{aligned} \tag{A.6}$$

$$\begin{pmatrix} 0 & 0 \\ 0 & 0 \\ m\omega\Big[\coth(\frac{\beta\omega_1}{2}) + \sqrt{1+4\alpha}\coth(\frac{\beta\omega_2}{2})\Big] & m\omega\Big[\coth(\frac{\beta\omega_1}{2}) - \sqrt{1+4\alpha}\coth(\frac{\beta\omega_2}{2})\Big] \\ m\omega\Big[\coth(\frac{\beta\omega_1}{2}) - \sqrt{1+4\alpha}\coth(\frac{\beta\omega_2}{2})\Big] & m\omega\Big[\coth(\frac{\beta\omega_1}{2}) + \sqrt{1+4\alpha}\coth(\frac{\beta\omega_2}{2})\Big] \end{pmatrix},$$

where $\omega_j = \omega\sqrt{\eta_j}$, $1 \leq j \leq N$, and η_j are the eigenvalues of $\mathbf{V}$. It follows from equation 5.4 that

$$\mathbf{L} = \frac{1}{4}m\omega \begin{pmatrix} \tanh(\frac{\beta\omega_1}{2}) + \sqrt{1+4\alpha}\tanh(\frac{\beta\omega_2}{2}) & \tanh(\frac{\beta\omega_1}{2}) - \sqrt{1+4\alpha}\tanh(\frac{\beta\omega_2}{2}) \\ \tanh(\frac{\beta\omega_1}{2}) - \sqrt{1+4\alpha}\tanh(\frac{\beta\omega_2}{2}) & \tanh(\frac{\beta\omega_1}{2}) + \sqrt{1+4\alpha}\tanh(\frac{\beta\omega_2}{2}) \end{pmatrix} \tag{A.7}$$

and

$$\begin{aligned} \mathbf{M} \;=\; & \frac{1}{4}m\omega \begin{pmatrix} \coth(\frac{\beta\omega_1}{2}) + \sqrt{1+4\alpha}\coth(\frac{\beta\omega_2}{2}) - \tanh(\frac{\beta\omega_1}{2}) - \sqrt{1+4\alpha}\tanh(\frac{\beta\omega_2}{2}) & \\ \coth(\frac{\beta\omega_1}{2}) - \sqrt{1+4\alpha}\coth(\frac{\beta\omega_2}{2}) - \tanh(\frac{\beta\omega_1}{2}) + \sqrt{1+4\alpha}\tanh(\frac{\beta\omega_2}{2}) & \\ \coth(\frac{\beta\omega_1}{2}) - \sqrt{1+4\alpha}\coth(\frac{\beta\omega_2}{2}) - \tanh(\frac{\beta\omega_1}{2}) + \sqrt{1+4\alpha}\tanh(\frac{\beta\omega_2}{2}) & \\ \coth(\frac{\beta\omega_1}{2}) + \sqrt{1+4\alpha}\coth(\frac{\beta\omega_2}{2}) - \tanh(\frac{\beta\omega_1}{2}) - \sqrt{1+4\alpha}\tanh(\frac{\beta\omega_2}{2}) & \end{pmatrix}. \end{aligned} \tag{A.8}$$

For the pure state, $T = 0$ so $\beta \to \infty$. With $\tanh(\infty) = 1$ and $\coth(\infty) = 1$, the $\mathbf{M}$ matrix becomes zero and the $\mathbf{L}$ matrix is therefore written as in equation 5.6.

From Section 5.2, the density matrix of this two-oscillator system can be expressed as

$$\begin{aligned} \rho(q_1, q_2; q_1', q_2') \;=\; & \frac{2}{\pi}(\det\mathbf{L})^{1/2}\exp\Big[-(q_1L_{11}q_1 + q_1L_{12}q_2 + q_2L_{21}q_1 + q_2L_{22}q_2) \\ & -(q_1'L_{11}q_1' + q_1'L_{11}q_2' + q_2'L_{11}q_1' + q_2'L_{11}q_2') \\ & -\frac{1}{2}(q_1 - q_1')M_{11}(q_1 - q_1') - \frac{1}{2}(q_1 - q_1')M_{12}(q_2 - q_2') \\ & -\frac{1}{2}(q_2 - q_2')M_{21}(q_1 - q_1') - \frac{1}{2}(q_2 - q_2')M_{22}(q_2 - q_2')\Big], \end{aligned} \tag{A.9}$$

normalised to unity. Since only the pure-state entanglement can be quantified by the von Neumann entropy, we will ignore the $\mathbf{M}$ matrix ($\mathbf{M} = 0$) from now on but note that the non-zero $\mathbf{M}$ matrix is used to produce Figure 6.2. The one-particle reduced density matrix can be computed easily; as an example, for Particle 1:

$$\begin{aligned} \rho_1(q_1; q_1') \;&=\; \int_{-\infty}^{\infty} \mathrm{d}q_2\, \rho(q_1, q_2; q_1', q_2) \\ &=\; \sqrt{\frac{2\upsilon_1 - 2\upsilon_2}{\pi}}\exp[-\upsilon_1(q_1^2 + q_1'^2) + 2\upsilon_2 q_1 q_1'], \end{aligned} \tag{A.10}$$

also normalised to unity and where

$$\upsilon_1 = L_{11} - \frac{(L_{12} + L_{21})^2}{8L_{22}} \tag{A.11}$$

and

$$\upsilon_2 = \frac{(L_{12}+L_{21})^2}{8L_{22}}. \tag{A.12}$$

In deriving equation A.10, we have used the technique of "completing the square" (with respect to q_2) so the first-line integration obtains the form of the *error function*, such that terms involving q_2 in the exponential are absorbed into the normalisation constant after integration. This is possible because the error function is defined by

$$\mathrm{erf}[x] = \frac{2}{\sqrt{\pi}}\int_0^x e^{-u^2}\mathrm{d}u, \tag{A.13}$$

and $\mathrm{erf}[\infty] = 1$.

We can diagonalise the one-particle reduced density matrix by utilising Mehler's Hermite polynomial formula,

$$\begin{aligned}\sum_{n=0}^{\infty}\frac{H_n(x)H_n(y)}{n!}(\frac{w}{2})^n\exp\Big[-\frac{1}{2}(x^2+y^2)\Big] &= \exp\Big[\frac{2xyw-(x^2+y^2)w^2}{1-w^2}-\frac{1}{2}(x^2+y^2)\Big]\\ &\quad (1-w^2)^{-\frac{1}{2}}\\ &\propto \exp\Big[-\upsilon_1(q^2+q'^2)+2\upsilon_2 qq'\Big]\end{aligned} \tag{A.14}$$

where $H_n(x)$ is a Hermite polynomial. This is done by introducing a new parameter s so that $q_1 = xs$ and $q_1' = ys$. Also

$$\upsilon_1 s^2 = \frac{w^2}{1-w^2}+\frac{1}{2} \tag{A.15}$$

and

$$\upsilon_2 s^2 = \frac{w}{1-w^2}. \tag{A.16}$$

By solving for w ($0 \leq w \leq 1$):

$$w = \frac{(\upsilon_1 - \sqrt{\upsilon_1^2-\upsilon_2^2})}{\upsilon_2} \tag{A.17}$$

as well as remembering that for diagonalisation we require

$$\rho_1(q_1;q_1') = \sum_n \lambda_n\phi_n(q)\phi_n^*(q') \tag{A.18}$$

with

$$\int |\phi_n(q)|^2\, dq = 1 \tag{A.19}$$

such that

$$\sum_n \lambda_n = 1, \tag{A.20}$$

we thus obtain

$$\phi_n(q)\phi_n^*(q') = \frac{1}{2^n\sqrt{\pi}n!s}\exp\Big[-\frac{(q^2+q'^2)}{2s^2}\Big]H_n(\frac{q}{s})H_n(\frac{q'}{s}) \tag{A.21}$$

and the n-th eigenvalue is

$$\lambda_n = \sqrt{2v_1 - 2v_2}w^n(1-w^2)^{1/2}s. \tag{A.22}$$

Note that

$$s\sqrt{2v_1 - 2v_2} = \sqrt{\frac{1-w}{1+w}} \tag{A.23}$$

from equation A.15 and equation A.16.

The ground state is a pure state so we can directly quantify the ground-state entanglement between the two oscillators by the von Neumann entropy S_v. By substituting equation A.22 into equation 2.31, we obtain:

$$S_v(\rho_1) = -\log_2(1-w) - \frac{w\log_2 w}{(1-w)}. \tag{A.24}$$

This expression is actually true for a harmonic ring consisting of any number of harmonic oscillators, provided that we only consider the ground-state entanglement between *one* oscillator and the rest in the system [1].

Quantifying Entanglement between a Harmonic Oscillator and other $(N-1)$ Oscillators

We can extend the previous argument to consider entanglement between a harmonic oscillator and the other $N-1$ harmonic oscillators in a harmonic ring. As before, we need to find the one-particle reduced density matrix. This can be done by applying the technique of completing the square to terms in the exponential of the full density matrix with respect to the other $(N-1)$ coordinates $\{q_2,q_3,\ldots,q_N\}$ all at once. That is, starting from equation 5.3, we have the following equation:

$$\begin{aligned} &\sum_{j\geq 2}^{N}[(q_1+q_1')L_{1j}q_j + q_jL_{j1}(q_1+q_1')] + \sum_{j,k\geq 2}^{N} 2q_jL_{jk}q_k \\ = &\sum_{j,k\geq 2}^{N} 2(q_j+Q_j)L_{jk}(q_k+Q_k) - \Omega(q_1+q_1')^2. \end{aligned} \tag{A.25}$$

The vector $\underline{Q}$ is found to be

$$\underline{Q} = \begin{pmatrix} Q_2 \\ \vdots \\ Q_N \end{pmatrix} = \frac{1}{4}\mathbf{L}_{N-1}^{-1}(q_1+q_1')\underline{\Lambda} \tag{A.26}$$

[1] Alternatively, the von Neumann entropy can be evaluated for any Gaussian state of any number of modes by computing the symplectic eigenvalues.

where $\mathbf{L}_{N-1}$ is the appropriate part of the $\mathbf{L}$ matrix with $(N-1) \times (N-1)$ elements (i.e. excluding the first row and the first column) and

$$\underline{\Lambda} = \begin{pmatrix} L_{12} + L_{21} \\ L_{13} + L_{31} \\ \vdots \\ L_{1N} + L_{N1} \end{pmatrix}. \tag{A.27}$$

The last term in equation A.25 must satisfy

$$\Omega(q_1 + q_1')^2 = 2 \sum_{j,k \geq 2} Q_j L_{jk} Q_k \tag{A.28}$$

so that

$$\Omega = \frac{1}{8} \underline{\Lambda}^T \mathbf{L}_{N-1}^{-1} \underline{\Lambda}. \tag{A.29}$$

Similar to equation A.10, the υ_1 and υ_2 in the one-particle reduced density matrix of a N-oscillator system are then found to be

$$\upsilon_1 = L_{11} - \Omega \tag{A.30}$$

and

$$\upsilon_2 = \Omega. \tag{A.31}$$

By following the previous argument in the $N = 2$ case, w in equation A.14 and the corresponding von Neumann entropy, as given in equation A.24, can thus be computed.

Appendix B

Local Concurrence of Rank-2 Mixed States

For rank-2 mixed states, there are only two non-zero eigenvalues of $\rho\tilde{\rho}$ to order $(ab)^2$. They are

$$\begin{aligned}
\mu_4 \;=\; & \frac{(ab)^2}{9{\rho_{0000}}^4}\Bigg(-\rho_{0111}\rho_{1000}(\rho_{0000})^2+\rho_{0110}\rho_{1001}(\rho_{0000})^2+\rho_{0101}\rho_{1010}(\rho_{0000})^2- \\
& \rho_{0100}\rho_{1011}(\rho_{0000})^2+\rho_{0011}\rho_{1100}(\rho_{0000})^2-\rho_{0010}\rho_{1101}(\rho_{0000})^2- \\
& \rho_{0001}\rho_{1110}(\rho_{0000})^2+\rho_{1111}(\rho_{0000})^3+\sqrt{2}\Big|\Big({\rho_{0000}}^4(2\rho_{0011}\rho_{0110}\rho_{1001}\rho_{1100}- \\
& 2\rho_{0010}\rho_{0111}\rho_{1001}\rho_{1100}+\rho_{0001}\rho_{0111}\rho_{1010}\rho_{1100}-2\rho_{0001}\rho_{0110}\rho_{1011}\rho_{1100}- \\
& 2\rho_{0011}\rho_{0110}\rho_{1000}\rho_{1101}+2\rho_{0010}\rho_{0111}\rho_{1000}\rho_{1101}+\rho_{0001}\rho_{0110}\rho_{1010}\rho_{1101}- \\
& \rho_{0001}\rho_{0111}\rho_{1000}\rho_{1110}-\rho_{0001}\rho_{0010}\rho_{1101}\rho_{1110}+\rho_{0001}\rho_{0110}\rho_{1000}\rho_{1111}+ \\
& \rho_{0001}\rho_{0010}\rho_{1100}\rho_{1111}+\rho_{0100}(\rho_{0111}\rho_{1001}\rho_{1010}-\rho_{0111}\rho_{1000}\rho_{1011}+ \\
& \rho_{0011}\rho_{1010}\rho_{1101}-\rho_{0010}\rho_{1011}\rho_{1101}-2\rho_{0011}\rho_{1001}\rho_{1110}+2\rho_{0001}\rho_{1011}\rho_{1110}+ \\
& \rho_{0011}\rho_{1000}\rho_{1111}+\rho_{0010}\rho_{1001}\rho_{1111}-2\rho_{0001}\rho_{1010}\rho_{1111})+\rho_{0111}\rho_{1011}\rho_{1100}\rho_{0000}- \\
& 2\rho_{0111}\rho_{1010}\rho_{1101}\rho_{0000}+\rho_{0110}\rho_{1011}\rho_{1101}\rho_{0000}+\rho_{0111}\rho_{1001}\rho_{1110}\rho_{0000}+ \\
& \rho_{0011}\rho_{1101}\rho_{1110}\rho_{0000}-\rho_{0110}\rho_{1001}\rho_{1111}\rho_{0000}-\rho_{0011}\rho_{1100}\rho_{1111}\rho_{0000}+ \\
& \rho_{0101}(-\rho_{0110}\rho_{1001}\rho_{1010}+\rho_{0110}\rho_{1000}\rho_{1011}-\rho_{0011}\rho_{1010}\rho_{1100}+\rho_{0010}\rho_{1011}\rho_{1100}+ \\
& \rho_{0011}\rho_{1000}\rho_{1110}+\rho_{0010}\rho_{1001}\rho_{1110}-2\rho_{0010}\rho_{1000}\rho_{1111}- \\
& 2\rho_{1011}\rho_{1110}\rho_{0000}+2\rho_{1010}\rho_{1111}\rho_{0000}))\Big)^{1/2}\Big|\Bigg) \qquad \text{(B.1)}
\end{aligned}$$

and

$$\begin{aligned}
\mu_3 \;=\; & -\frac{(ab)^2}{9{\rho_{0000}}^4}\Bigg(\rho_{0111}\rho_{1000}(\rho_{0000})^2-\rho_{0110}\rho_{1001}(\rho_{0000})^2-\rho_{0101}\rho_{1010}(\rho_{0000})^2+ \\
& \rho_{0100}\rho_{1011}(\rho_{0000})^2-\rho_{0011}\rho_{1100}(\rho_{0000})^2+\rho_{0010}\rho_{1101}(\rho_{0000})^2+ \\
& \rho_{0001}\rho_{1110}(\rho_{0000})^2-\rho_{1111}(\rho_{0000})^3+\sqrt{2}\Big|\Big({\rho_{0000}}^4(2\rho_{0011}\rho_{0110}\rho_{1001}\rho_{1100}- \\
& 2\rho_{0010}\rho_{0111}\rho_{1001}\rho_{1100}+\rho_{0001}\rho_{0111}\rho_{1010}\rho_{1100}-2\rho_{0001}\rho_{0110}\rho_{1011}\rho_{1100}- \\
& 2\rho_{0011}\rho_{0110}\rho_{1000}\rho_{1101}+2\rho_{0010}\rho_{0111}\rho_{1000}\rho_{1101}+\rho_{0001}\rho_{0110}\rho_{1010}\rho_{1101}-
\end{aligned}$$

$$\rho_{0001}\rho_{0111}\rho_{1000}\rho_{1110} - \rho_{0001}\rho_{0010}\rho_{1101}\rho_{1110} + \rho_{0001}\rho_{0110}\rho_{1000}\rho_{1111} + \rho_{0001}\rho_{0010}\rho_{1100}\rho_{1111} + \rho_{0100}(\rho_{0111}\rho_{1001}\rho_{1010} - \rho_{0111}\rho_{1000}\rho_{1011} + \rho_{0011}\rho_{1010}\rho_{1101} - \rho_{0010}\rho_{1011}\rho_{1101} - 2\rho_{0011}\rho_{1001}\rho_{1110} + 2\rho_{0001}\rho_{1011}\rho_{1110} + \rho_{0011}\rho_{1000}\rho_{1111} + \rho_{0010}\rho_{1001}\rho_{1111} - 2\rho_{0001}\rho_{1010}\rho_{1111}) + \rho_{0111}\rho_{1011}\rho_{1100}\rho_{0000} - 2\rho_{0111}\rho_{1010}\rho_{1101}\rho_{0000} + \rho_{0110}\rho_{1011}\rho_{1101}\rho_{0000} + \rho_{0111}\rho_{1001}\rho_{1110}\rho_{0000} + \rho_{0011}\rho_{1101}\rho_{1110}\rho_{0000} - \rho_{0110}\rho_{1001}\rho_{1111}\rho_{0000} - \rho_{0011}\rho_{1100}\rho_{1111}\rho_{0000} + \rho_{0101}(-\rho_{0110}\rho_{1001}\rho_{1010} + \rho_{0110}\rho_{1000}\rho_{1011} - \rho_{0011}\rho_{1010}\rho_{1100} + \rho_{0010}\rho_{1011}\rho_{1100} + \rho_{0011}\rho_{1000}\rho_{1110} + \rho_{0010}\rho_{1001}\rho_{1110} - 2\rho_{0010}\rho_{1000}\rho_{1111} - 2\rho_{1011}\rho_{1110}\rho_{0000} + 2\rho_{1010}\rho_{1111}\rho_{0000}))\Big)^{1/2}\Big|\Big). \tag{B.2}$$

The local concurrence is then

$$\mathcal{C} = \max\{0, \sqrt{\mu_4} - \sqrt{\mu_3}\}. \tag{B.3}$$

Appendix C

D_1 and D_2 in the Expression of the Local Negativity

Here we want to prove that D_1 in equation 6.21 and D_2 in equation 6.22 are always positive. Let $\tilde{\psi}^i$ be a sub-normalized state and suppose $\sum_i \tilde{\psi}^i(\tilde{\psi}^i)^*$ is a decomposition for the state ρ, not necessarily an optimal one, equation 6.21 becomes:

$$\begin{aligned} D_1 &= \frac{1}{3{\rho_{0000}}^2}\Big(\sum_i \tilde{\psi}^i_{01}(\tilde{\psi}^i_{01})^* \sum_j \tilde{\psi}^j_{00}(\tilde{\psi}^j_{00})^* - \sum_i \tilde{\psi}^i_{00}(\tilde{\psi}^i_{01})^* \sum_j \tilde{\psi}^j_{01}(\tilde{\psi}^j_{00})^*\Big) \\ &= \frac{1}{3{\rho_{0000}}^2}\sum_{ij}(\tilde{\psi}^i_{01}\tilde{\psi}^j_{00} - \tilde{\psi}^j_{01}\tilde{\psi}^i_{00})(\tilde{\psi}^i_{01})^*(\tilde{\psi}^j_{00})^* \\ &= \frac{1}{3{\rho_{0000}}^2}\sum_{i>j}(\tilde{\psi}^i_{01}\tilde{\psi}^j_{00} - \tilde{\psi}^j_{01}\tilde{\psi}^i_{00})(\tilde{\psi}^i_{01}\tilde{\psi}^j_{00} - \tilde{\psi}^j_{01}\tilde{\psi}^i_{00})^* \end{aligned} \tag{C.1}$$

but

$$(\tilde{\psi}^i_{01}\tilde{\psi}^j_{00} - \tilde{\psi}^j_{01}\tilde{\psi}^i_{00})(\tilde{\psi}^i_{01}\tilde{\psi}^j_{00} - \tilde{\psi}^j_{01}\tilde{\psi}^i_{00})^* \geq 0 \tag{C.2}$$

so

$$D_1 \geq 0. \tag{C.3}$$

Similarly,

$$D_2 = \frac{1}{3{\rho_{0000}}^2}\sum_{i>j}(\tilde{\psi}^i_{10}\tilde{\psi}^j_{00} - \tilde{\psi}^j_{10}\tilde{\psi}^i_{00})(\tilde{\psi}^i_{10}\tilde{\psi}^j_{00} - \tilde{\psi}^j_{10}\tilde{\psi}^i_{00})^* \tag{C.4}$$

$$\geq 0 \tag{C.5}$$

Appendix D

Pauli Operators for the Effective Two-Qubit System

We wish to find appropriate Pauli operators for the effective two-qubit system in the representation:

$$\phi_0(x) = \sqrt{\frac{1}{2a}}; \qquad \phi_1(x) = \sqrt{\frac{3}{2a^3}}x \qquad (-a \leq x \leq a). \tag{D.1}$$

From Section 3.1.6, we know the Pauli X- and Y-matrices have elements

$$\hat{X} = \begin{pmatrix} 0 & 1 \\ 1 & 0 \end{pmatrix}; \quad \hat{Y} = \begin{pmatrix} 0 & \mathrm{i} \\ -\mathrm{i} & 0 \end{pmatrix} \tag{D.2}$$

Since these matrices need to connect the states ϕ_0 and ϕ_1, which have opposite parity, they must be odd spatially. Natural choices will be the position operator $\hat{x}$ and the momentum operator $\hat{p}$, but it is essential to make sure that the operators are correctly represented by Hermitian matrices.

First, define another function $\phi_2(x)$, correctly normalized from $-a$ to $+a$ and Gram-Schmidt orthogonalised to both ϕ_0 and ϕ_1:

$$\phi_2(x) = \sqrt{\frac{45}{8a^5}}\left(x^2 - \frac{a^2}{3}\right). \tag{D.3}$$

These basis functions $\{\phi_0, \phi_1, \phi_2\}$ are implicitly assumed to vanish outside the region $-a \leq x \leq a$. It is useful to invert these definitions to obtain the first three powers of x in terms of the orthonormal basis functions:

$$1 = \sqrt{2a}\phi_0; \quad x = \sqrt{\frac{2a^3}{3}}\phi_1; \quad x^2 = \sqrt{\frac{8a^5}{45}}\phi_2 + \frac{\sqrt{2a^5}}{3}\phi_0. \tag{D.4}$$

Consider the action of the position operator $\hat{x}$ on the basis states. We find

$$\hat{x}|0\rangle = \sqrt{\frac{1}{2a}}x = \frac{a}{\sqrt{3}}|1\rangle; \tag{D.5}$$

$$\hat{x}|1\rangle = \sqrt{\frac{3}{2a^3}}x^2 = \sqrt{\frac{3}{2a^3}}\left(\sqrt{\frac{8a^5}{45}}\phi_2 + \frac{\sqrt{2a^5}}{3}\phi_0\right) = \frac{a}{\sqrt{3}}\phi_0 + \mathcal{O}\phi_2. \tag{D.6}$$

Hence, the matrix representation of $\hat{x}$ generated by the set $\{\phi_0, \phi_1\}$ is

$$\hat{x} = \begin{pmatrix} 0 & \frac{a}{\sqrt{3}} \\ \frac{a}{\sqrt{3}} & 0 \end{pmatrix}, \tag{D.7}$$

from which we deduce that the Pauli X-operator is represented by

$$\hat{X} = \frac{\sqrt{3}}{a}\hat{x}. \tag{D.8}$$

Next, we turn our attention to the momentum operator $\hat{p}$. The basis functions vanish outside the measurement region, this leads to dicontinuities in the functions and hence the delta-function contributions to their derivatives. The actions of the operator in the position representation are then

$$\hat{p}|0\rangle = -\mathrm{i}\hbar\frac{\partial}{\partial x}\phi_0 = \mathrm{i}\hbar\sqrt{\frac{1}{2a}}[\delta(x-a) - \delta(x+a)]; \tag{D.9}$$

$$\hat{p}|1\rangle = -\mathrm{i}\hbar\frac{\partial}{\partial x}\phi_1 = -\mathrm{i}\hbar\sqrt{\frac{3}{2a^3}} + \mathrm{i}\hbar\sqrt{\frac{3}{2a}}[\delta(x+a) + \delta(x-a)]. \tag{D.10}$$

The matrix elements are found by integrating over the range from $-a$ to $+a$, remembering that the delta-functions contribute exactly one half each to the integral since they are centred at the end points:

$$\langle 1|\hat{p}|0\rangle = -\mathrm{i}\hbar\int_{-a}^{a}\mathrm{d}x\,\phi_1^*\frac{\partial}{\partial x}\phi_0 = \mathrm{i}\hbar\sqrt{\frac{1}{2a}}\sqrt{\frac{3}{2a}} = +\mathrm{i}\hbar\frac{\sqrt{3}}{2a}; \tag{D.11}$$

$$\langle 0|\hat{p}|1\rangle = -\mathrm{i}\hbar\int_{-a}^{a}\mathrm{d}x\,\phi_0^*\frac{\partial}{\partial x}\phi_1 = -\mathrm{i}\hbar\frac{\sqrt{3}}{a} + \mathrm{i}\hbar\sqrt{\frac{3}{2a}}\sqrt{\frac{1}{2a}} = -\mathrm{i}\hbar\frac{\sqrt{3}}{2a}, \tag{D.12}$$

with $\langle 0|\hat{p}|0\rangle = \langle 1|\hat{p}|1\rangle = 0$ by symmetry. It follows the matrix representation is

$$\hat{p} = \mathrm{i}\hbar\begin{pmatrix} 0 & \frac{-\sqrt{3}}{2a} \\ \frac{\sqrt{3}}{2a} & 0 \end{pmatrix}, \tag{D.13}$$

and

$$\hat{Y} = -\frac{2a}{\sqrt{3}\hbar}\hat{p}. \tag{D.14}$$

Appendix E

Corrections to the Local Entanglement after Two-Party Preliminary Measurements

The third eigenvalue of Alice's reduced density matrix in the discarding ensemble when both parties make preliminary measurements can be found by making the following additional substitutions in equation 6.12:

$$\begin{aligned}
\rho_{20}^{(A)} &= \frac{b}{p}\Big[\rho_{2000} + \frac{b^2}{6}(\rho_{2020} + 2\rho_{2011} + \rho_{2002})\Big] + \mathrm{O}(b^5);\\
\rho_{02}^{(A)} &= \frac{b}{p}\Big[\rho_{0200} + \frac{b^2}{6}(\rho_{0220} + 2\rho_{0211} + \rho_{0202})\Big] + \mathrm{O}(b^5);\\
\rho_{21}^{(A)} &= \frac{b}{p}\Big[\rho_{2100} + \frac{b^2}{6}(\rho_{2120} + 2\rho_{2111} + \rho_{2102})\Big] + \mathrm{O}(b^5);\\
\rho_{12}^{(A)} &= \frac{b}{p}\Big[\rho_{1200} + \frac{b^2}{6}(\rho_{1220} + 2\rho_{1211} + \rho_{1202})\Big] + \mathrm{O}(b^5);\\
\rho_{22}^{(A)} &= \frac{b}{2p}\Big[\rho_{2200} + \frac{b^2}{6}(\rho_{2220} + 2\rho_{2211} + \rho_{2202})\Big] + \mathrm{O}(b^5).
\end{aligned} \tag{E.1}$$

This gives

$$\lambda_3 = \frac{\lambda_3^{nu}}{\lambda_3^{de}}(ab)^4, \tag{E.2}$$

where the denominator is

$$\begin{aligned}
\lambda_3^{de} = 120(&\rho_{0002}\rho_{0100}\rho_{1000} + 2\rho_{0011}\rho_{0100}\rho_{1000}\\
&+\rho_{0020}\rho_{0100}\rho_{1000} + \rho_{0000}\rho_{0102}\rho_{1000}\\
&+2\rho_{0000}\rho_{0111}\rho_{1000} + \rho_{0000}\rho_{0120}\rho_{1000}\\
&+\rho_{0000}\rho_{0100}\rho_{1002} + 2\rho_{0000}\rho_{0100}\rho_{1011}\\
&+\rho_{0000}\rho_{0100}\rho_{1020} - 2\rho_{0000}\rho_{0002}\rho_{1100}\\
&-4\rho_{0000}\rho_{0011}\rho_{1100} - 2\rho_{0000}\rho_{0020}\rho_{1100}\\
&-\rho_{0000}\rho_{0000}\rho_{1102} - 2\rho_{0000}\rho_{0000}\rho_{1111}
\end{aligned}$$

$$-\rho_{0000}\rho_{0000}\rho_{1120}), \tag{E.3}$$

and the numerator is

$$\begin{aligned}
\lambda_3^{nu} \;=\; \frac{1}{54}(&\rho_{0211}\rho_{1120}\rho_{2002} - \rho_{0120}\rho_{1211}\rho_{2002} \\
&-\rho_{0111}\rho_{1220}\rho_{2002} + \rho_{0220}\rho_{1111}\rho_{2002} \\
&+\rho_{0202}\rho_{1120}\rho_{2011} - \rho_{0120}\rho_{1202}\rho_{2011} \\
&-\rho_{0102}\rho_{1220}\rho_{2011} + \rho_{0220}\rho_{1102}\rho_{2011} \\
&-\rho_{0220}\rho_{1011}\rho_{2102} - \rho_{0211}\rho_{1020}\rho_{2102} \\
&+\rho_{0020}\rho_{1211}\rho_{2102} + \rho_{0011}\rho_{1220}\rho_{2102} \\
&-\rho_{0220}\rho_{1002}\rho_{2111} - \rho_{0202}\rho_{1020}\rho_{2111} \\
&+\rho_{0020}\rho_{1202}\rho_{2111} + \rho_{0002}\rho_{1220}\rho_{2111} \\
&-\rho_{0211}\rho_{1002}\rho_{2120} + \rho_{0002}\rho_{1211}\rho_{2120} \\
&+\rho_{0211}\rho_{1000}\rho_{2122} - \rho_{0000}\rho_{1211}\rho_{2122} \\
&+\rho_{0120}\rho_{1011}\rho_{2202} + \rho_{0111}\rho_{1020}\rho_{2202} \\
&-\rho_{0020}\rho_{1111}\rho_{2202} - \rho_{0011}\rho_{1120}\rho_{2202} \\
&+\rho_{0120}\rho_{1002}\rho_{2211} + \rho_{0102}\rho_{1020}\rho_{2211} \\
&-\rho_{0020}\rho_{1102}\rho_{2211} - \rho_{0002}\rho_{1120}\rho_{2211} \\
&+\rho_{0111}\rho_{1002}\rho_{2220} + \rho_{0102}\rho_{1011}\rho_{2220} \\
&-\rho_{0011}\rho_{1102}\rho_{2220} - \rho_{0002}\rho_{1111}\rho_{2220} \\
&-\rho_{0111}\rho_{1000}\rho_{2222} - \rho_{0100}\rho_{1011}\rho_{2222} \\
&+\rho_{0011}\rho_{1100}\rho_{2222} + \rho_{0000}\rho_{1111}\rho_{2222}),
\end{aligned} \tag{E.4}$$

where equation (7.6) is applied to obtain the final form.

Appendix F

The Expression of ϵ in Terms of Polar Derivatives

Define

$$\Psi^{(i,j,k)}[r,\theta,\phi] = \frac{\partial^{i+j+k}}{\partial r^i \partial\theta^j \partial\phi^k}\Psi[r,\theta,\phi] \tag{F.1}$$

for any three-dimensional complex wavefunction $\Psi[r_x, r_y, r_z]$ in relative coordinates (Section 7.3.5.3), expressed in spherical coordinates as $\Psi[r,\theta,\phi]$ (Section 7.4.3) with its complex conjugate being $\Psi^*[r,\theta,\phi]$. Its local entanglement between Alice's and Bob's subsystems in the limit of small region sizes is determined by the von Neumann entropy $S_v = h(\epsilon)$. Assume the region sizes are the same for all dimensions, i.e. $a_i = a$ and $b_i = b$ for $i \in \{x, y, z\}$, ϵ is simply: (the Mathematica output is given to avoid introducing typographical errors.)

$$\begin{array}{l}
\epsilon = \dfrac{a^2 b^2}{9\,(\Psi[r,\theta,\phi]\,\Psi^*[r,\theta,\phi])^2\, r^4} \\
\Big(2\,(-\text{Csc}[\theta]\,(\text{Sin}[\theta]\,\Psi^{(0,1,0)}[r,\theta,\phi] - r\,\text{Cos}[\theta]\,\Psi^{(1,0,0)}[r,\theta,\phi]) \\
\qquad (-\text{Sin}[\phi]\,\Psi^{(0,0,1)}[r,\theta,\phi] + \\
\qquad\quad \text{Cos}[\phi]\,\text{Sin}[\theta]\,(\text{Cos}[\theta]\,\Psi^{(0,1,0)}[r,\theta,\phi] + r\,\text{Sin}[\theta]\,\Psi^{(1,0,0)}[r,\theta,\phi])) + \\
\qquad \Psi[r,\theta,\phi]\,(\text{Cos}[2\theta]\,\text{Cos}[\phi]\,\Psi^{(0,1,0)}[r,\theta,\phi] - \text{Sin}[\phi]\,\Psi^{(0,1,1)}[r,\theta,\phi] + \\
\qquad\quad \text{Cos}[\theta]\,\text{Cos}[\phi]\,\text{Sin}[\theta]\,\Psi^{(0,2,0)}[r,\theta,\phi] + r\,\text{Cos}[\theta]\,\text{Cos}[\phi]\,\text{Sin}[\theta]\,\Psi^{(1,0,0)}[r,\theta,\phi] + \\
\qquad\quad r\,\text{Cot}[\theta]\,\text{Sin}[\phi]\,\Psi^{(1,0,1)}[r,\theta,\phi] - r\,\text{Cos}[\theta]^2\,\text{Cos}[\phi]\,\Psi^{(1,1,0)}[r,\theta,\phi] + \\
\qquad\quad r\,\text{Cos}[\phi]\,\text{Sin}[\theta]^2\,\Psi^{(1,1,0)}[r,\theta,\phi] - r^2\,\text{Cos}[\theta]\,\text{Cos}[\phi]\,\text{Sin}[\theta]\,\Psi^{(2,0,0)}[r,\theta,\phi])) \\
\quad (-\text{Csc}[\theta]\,(\text{Sin}[\theta]\,\Psi^{*(0,1,0)}[r,\theta,\phi] - r\,\text{Cos}[\theta]\,\Psi^{*(1,0,0)}[r,\theta,\phi]) \\
\qquad (-\text{Sin}[\phi]\,\Psi^{*(0,0,1)}[r,\theta,\phi] + \\
\qquad\quad \text{Cos}[\phi]\,\text{Sin}[\theta]\,(\text{Cos}[\theta]\,\Psi^{*(0,1,0)}[r,\theta,\phi] + r\,\text{Sin}[\theta]\,\Psi^{*(1,0,0)}[r,\theta,\phi])) + \\
\qquad \Psi^*[r,\theta,\phi]\,(\text{Cos}[2\theta]\,\text{Cos}[\phi]\,\Psi^{*(0,1,0)}[r,\theta,\phi] - \text{Sin}[\phi]\,\Psi^{*(0,1,1)}[r,\theta,\phi] + \\
\qquad\quad \text{Cos}[\theta]\,\text{Cos}[\phi]\,\text{Sin}[\theta]\,\Psi^{*(0,2,0)}[r,\theta,\phi] + r\,\text{Cos}[\theta]\,\text{Cos}[\phi]\,\text{Sin}[\theta]\,\Psi^{*(1,0,0)}[r,\theta,\phi] + \\
\qquad\quad r\,\text{Cot}[\theta]\,\text{Sin}[\phi]\,\Psi^{*(1,0,1)}[r,\theta,\phi] - r\,\text{Cos}[\theta]^2\,\text{Cos}[\phi]\,\Psi^{*(1,1,0)}[r,\theta,\phi] + \\
\qquad\quad r\,\text{Cos}[\phi]\,\text{Sin}[\theta]^2\,\Psi^{*(1,1,0)}[r,\theta,\phi] - r^2\,\text{Cos}[\theta]\,\text{Cos}[\phi]\,\text{Sin}[\theta]\,\Psi^{*(2,0,0)}[r,\theta,\phi])) + \\
\quad \Big((\text{Csc}[\theta]\,\text{Sin}[\phi]\,\Psi^{(0,0,1)}[r,\theta,\phi] - \\
\qquad\quad \text{Cos}[\phi]\,(\text{Cos}[\theta]\,\Psi^{(0,1,0)}[r,\theta,\phi] + r\,\text{Sin}[\theta]\,\Psi^{(1,0,0)}[r,\theta,\phi]))^2 - \\
\qquad \Psi[r,\theta,\phi]\,(\text{Csc}[\theta]^2\,\text{Sin}[2\phi]\,\Psi^{(0,0,1)}[r,\theta,\phi] + \text{Csc}[\theta]^2\,\text{Sin}[\phi]^2\,\Psi^{(0,0,2)}[r,\theta,\phi] - \\
\qquad\quad \text{Cos}[\phi]^2\,\text{Sin}[2\theta]\,\Psi^{(0,1,0)}[r,\theta,\phi] + \text{Cot}[\theta]\,\text{Sin}[\phi]^2\,\Psi^{(0,1,0)}[r,\theta,\phi] - \\
\qquad\quad \text{Cot}[\theta]\,\text{Sin}[2\phi]\,\Psi^{(0,1,1)}[r,\theta,\phi] + \text{Cos}[\theta]^2\,\text{Cos}[\phi]^2\,\Psi^{(0,2,0)}[r,\theta,\phi] + \\
\qquad\quad r\,\text{Cos}[\theta]^2\,\text{Cos}[\phi]^2\,\Psi^{(1,0,0)}[r,\theta,\phi] + r\,\text{Sin}[\phi]^2\,\Psi^{(1,0,0)}[r,\theta,\phi] - \\
\qquad\quad r\,\text{Sin}[2\phi]\,\Psi^{(1,0,1)}[r,\theta,\phi] + r\,\text{Cos}[\phi]^2\,\text{Sin}[2\theta]\,\Psi^{(1,1,0)}[r,\theta,\phi] + \\
\qquad\quad r^2\,\text{Cos}[\phi]^2\,\text{Sin}[\theta]^2\,\Psi^{(2,0,0)}[r,\theta,\phi])\Big) \\
\quad \Big((\text{Csc}[\theta]\,\text{Sin}[\phi]\,\Psi^{*(0,0,1)}[r,\theta,\phi] - \\
\qquad\quad \text{Cos}[\phi]\,(\text{Cos}[\theta]\,\Psi^{*(0,1,0)}[r,\theta,\phi] + r\,\text{Sin}[\theta]\,\Psi^{*(1,0,0)}[r,\theta,\phi]))^2 -
\end{array}$$

```
    Ψ*[r, θ, ϕ] (Csc[θ]^2 Sin[2 ϕ] Ψ*^(0,0,1)[r, θ, ϕ] + Csc[θ]^2 Sin[ϕ]^2 Ψ*^(0,0,2)[r, θ, ϕ] -
       Cos[ϕ]^2 Sin[2 θ] Ψ*^(0,1,0)[r, θ, ϕ] + Cot[θ] Sin[ϕ]^2 Ψ*^(0,1,0)[r, θ, ϕ] -
       Cot[θ] Sin[2 ϕ] Ψ*^(0,1,1)[r, θ, ϕ] + Cos[θ]^2 Cos[ϕ]^2 Ψ*^(0,2,0)[r, θ, ϕ] +
       r Cos[θ]^2 Cos[ϕ]^2 Ψ*^(1,0,0)[r, θ, ϕ] + r Sin[ϕ]^2 Ψ*^(1,0,0)[r, θ, ϕ] -
       r Sin[2 ϕ] Ψ*^(1,0,1)[r, θ, ϕ] + r Cos[ϕ]^2 Sin[2 θ] Ψ*^(1,1,0)[r, θ, ϕ] +
       r^2 Cos[ϕ]^2 Sin[θ]^2 Ψ*^(2,0,0)[r, θ, ϕ])) +
2 (-Csc[θ] (Sin[θ] Ψ^(0,1,0)[r, θ, ϕ] - r Cos[θ] Ψ^(1,0,0)[r, θ, ϕ])
    (Cos[ϕ] Ψ^(0,0,1)[r, θ, ϕ] + Sin[θ] Sin[ϕ]
       (Cos[θ] Ψ^(0,1,0)[r, θ, ϕ] + r Sin[θ] Ψ^(1,0,0)[r, θ, ϕ])) +
    Ψ[r, θ, ϕ] (Cos[2 θ] Sin[ϕ] Ψ^(0,1,0)[r, θ, ϕ] + Cos[ϕ] Ψ^(0,1,1)[r, θ, ϕ] +
       Cos[θ] Sin[θ] Sin[ϕ] Ψ^(0,2,0)[r, θ, ϕ] + r Cos[θ] Sin[θ] Sin[ϕ] Ψ^(1,0,0)[r, θ, ϕ] -
       r Cos[ϕ] Cot[θ] Ψ^(1,0,1)[r, θ, ϕ] - r Cos[θ]^2 Sin[ϕ] Ψ^(1,1,0)[r, θ, ϕ] +
       r Sin[θ]^2 Sin[ϕ] Ψ^(1,1,0)[r, θ, ϕ] - r^2 Cos[θ] Sin[θ] Sin[ϕ] Ψ^(2,0,0)[r, θ, ϕ]))
  (-Csc[θ] (Sin[θ] Ψ*^(0,1,0)[r, θ, ϕ] - r Cos[θ] Ψ*^(1,0,0)[r, θ, ϕ])
    (Cos[ϕ] Ψ*^(0,0,1)[r, θ, ϕ] +
       Sin[θ] Sin[ϕ] (Cos[θ] Ψ*^(0,1,0)[r, θ, ϕ] + r Sin[θ] Ψ*^(1,0,0)[r, θ, ϕ])) +
    Ψ*[r, θ, ϕ] (Cos[2 θ] Sin[ϕ] Ψ*^(0,1,0)[r, θ, ϕ] + Cos[ϕ] Ψ*^(0,1,1)[r, θ, ϕ] +
       Cos[θ] Sin[θ] Sin[ϕ] Ψ*^(0,2,0)[r, θ, ϕ] + r Cos[θ] Sin[θ] Sin[ϕ] Ψ*^(1,0,0)[r, θ, ϕ] -
       r Cos[ϕ] Cot[θ] Ψ*^(1,0,1)[r, θ, ϕ] - r Cos[θ]^2 Sin[ϕ] Ψ*^(1,1,0)[r, θ, ϕ] +
       r Sin[θ]^2 Sin[ϕ] Ψ*^(1,1,0)[r, θ, ϕ] - r^2 Cos[θ] Sin[θ] Sin[ϕ] Ψ*^(2,0,0)[r, θ, ϕ])) +
2 (-Cos[ϕ] Csc[θ]^2 Sin[ϕ] Ψ^(0,0,1)[r, θ, ϕ]^2 +
    Cos[2 ϕ] Csc[θ] Ψ^(0,0,1)[r, θ, ϕ] (Cos[θ] Ψ^(0,1,0)[r, θ, ϕ] + r Sin[θ] Ψ^(1,0,0)[r, θ, ϕ]) +
    1/2 Sin[2 ϕ] (Cos[θ] Ψ^(0,1,0)[r, θ, ϕ] + r Sin[θ] Ψ^(1,0,0)[r, θ, ϕ])^2 +
    Ψ[r, θ, ϕ] (Cos[2 ϕ] Csc[θ]^2 Ψ^(0,0,1)[r, θ, ϕ] + Cos[ϕ] Csc[θ]^2 Sin[ϕ] Ψ^(0,0,2)[r, θ, ϕ] +
       Cos[ϕ] Cot[θ] Sin[ϕ] Ψ^(0,1,0)[r, θ, ϕ] +
       2 Cos[θ] Cos[ϕ] Sin[θ] Sin[ϕ] Ψ^(0,1,0)[r, θ, ϕ] - Cos[ϕ]^2 Cot[θ] Ψ^(0,1,1)[r, θ, ϕ] +
       Cot[θ] Sin[ϕ]^2 Ψ^(0,1,1)[r, θ, ϕ] - Cos[θ]^2 Cos[ϕ] Sin[ϕ] Ψ^(0,2,0)[r, θ, ϕ] +
       r Cos[ϕ] Sin[ϕ] Ψ^(1,0,0)[r, θ, ϕ] - r Cos[θ]^2 Cos[ϕ] Sin[ϕ] Ψ^(1,0,0)[r, θ, ϕ] -
       r Cos[ϕ]^2 Ψ^(1,0,1)[r, θ, ϕ] + r Sin[ϕ]^2 Ψ^(1,0,1)[r, θ, ϕ] -
       2 r Cos[θ] Cos[ϕ] Sin[θ] Sin[ϕ] Ψ^(1,1,0)[r, θ, ϕ] -
       r^2 Cos[ϕ] Sin[θ]^2 Sin[ϕ] Ψ^(2,0,0)[r, θ, ϕ]))
  (-Cos[ϕ] Csc[θ]^2 Sin[ϕ] Ψ*^(0,0,1)[r, θ, ϕ]^2 +
    Cos[2 ϕ] Csc[θ] Ψ*^(0,0,1)[r, θ, ϕ] (Cos[θ] Ψ*^(0,1,0)[r, θ, ϕ] + r Sin[θ] Ψ*^(1,0,0)[r, θ, ϕ]) +
    1/2 Sin[2 ϕ] (Cos[θ] Ψ*^(0,1,0)[r, θ, ϕ] + r Sin[θ] Ψ*^(1,0,0)[r, θ, ϕ])^2 +
    Ψ*[r, θ, ϕ] (Cos[2 ϕ] Csc[θ]^2 Ψ*^(0,0,1)[r, θ, ϕ] + Cos[ϕ] Csc[θ]^2 Sin[ϕ] Ψ*^(0,0,2)[r, θ, ϕ] +
       Cos[ϕ] Cot[θ] Sin[ϕ] Ψ*^(0,1,0)[r, θ, ϕ] +
       2 Cos[θ] Cos[ϕ] Sin[θ] Sin[ϕ] Ψ*^(0,1,0)[r, θ, ϕ] - Cos[ϕ]^2 Cot[θ] Ψ*^(0,1,1)[r, θ, ϕ] +
       Cot[θ] Sin[ϕ]^2 Ψ*^(0,1,1)[r, θ, ϕ] - Cos[θ]^2 Cos[ϕ] Sin[ϕ] Ψ*^(0,2,0)[r, θ, ϕ] +
       r Cos[ϕ] Sin[ϕ] Ψ*^(1,0,0)[r, θ, ϕ] - r Cos[θ]^2 Cos[ϕ] Sin[ϕ] Ψ*^(1,0,0)[r, θ, ϕ] -
       r Cos[ϕ]^2 Ψ*^(1,0,1)[r, θ, ϕ] + r Sin[ϕ]^2 Ψ*^(1,0,1)[r, θ, ϕ] -
       2 r Cos[θ] Cos[ϕ] Sin[θ] Sin[ϕ] Ψ*^(1,1,0)[r, θ, ϕ] -
       r^2 Cos[ϕ] Sin[θ]^2 Sin[ϕ] Ψ*^(2,0,0)[r, θ, ϕ])) +
  ((Cos[ϕ] Csc[θ] Ψ^(0,0,1)[r, θ, ϕ] +
       Sin[ϕ] (Cos[θ] Ψ^(0,1,0)[r, θ, ϕ] + r Sin[θ] Ψ^(1,0,0)[r, θ, ϕ]))^2 -
    Ψ[r, θ, ϕ] (-Csc[θ]^2 Sin[2 ϕ] Ψ^(0,0,1)[r, θ, ϕ] + Cos[ϕ]^2 Csc[θ]^2 Ψ^(0,0,2)[r, θ, ϕ] +
       Cos[ϕ]^2 Cot[θ] Ψ^(0,1,0)[r, θ, ϕ] - Sin[2 θ] Sin[ϕ]^2 Ψ^(0,1,0)[r, θ, ϕ] +
       Cot[θ] Sin[2 ϕ] Ψ^(0,1,1)[r, θ, ϕ] + Cos[θ]^2 Sin[ϕ]^2 Ψ^(0,2,0)[r, θ, ϕ] +
       r Cos[ϕ]^2 Ψ^(1,0,0)[r, θ, ϕ] + r Cos[θ]^2 Sin[ϕ]^2 Ψ^(1,0,0)[r, θ, ϕ] +
       r Sin[2 ϕ] Ψ^(1,0,1)[r, θ, ϕ] + r Sin[2 θ] Sin[ϕ]^2 Ψ^(1,1,0)[r, θ, ϕ] +
       r^2 Sin[θ]^2 Sin[ϕ]^2 Ψ^(2,0,0)[r, θ, ϕ]))
  ((Cos[ϕ] Csc[θ] Ψ*^(0,0,1)[r, θ, ϕ] +
       Sin[ϕ] (Cos[θ] Ψ*^(0,1,0)[r, θ, ϕ] + r Sin[θ] Ψ*^(1,0,0)[r, θ, ϕ]))^2 -
```

```
    Ψ*[r, θ, ϕ] (-Csc[θ]^2 Sin[2 ϕ] Ψ*^(0,0,1)[r, θ, ϕ] + Cos[ϕ]^2 Csc[θ]^2 Ψ*^(0,0,2)[r, θ, ϕ] +
       Cos[ϕ]^2 Cot[θ] Ψ*^(0,1,0)[r, θ, ϕ] - Sin[2 θ] Sin[ϕ]^2 Ψ*^(0,1,0)[r, θ, ϕ] +
       Cot[θ] Sin[2 ϕ] Ψ*^(0,1,1)[r, θ, ϕ] + Cos[θ]^2 Sin[ϕ]^2 Ψ*^(0,2,0)[r, θ, ϕ] +
       r Cos[ϕ]^2 Ψ*^(1,0,0)[r, θ, ϕ] + r Cos[θ]^2 Sin[ϕ]^2 Ψ*^(1,0,0)[r, θ, ϕ] +
       r Sin[2 ϕ] Ψ*^(1,0,1)[r, θ, ϕ] + r Sin[2 θ] Sin[ϕ]^2 Ψ*^(1,1,0)[r, θ, ϕ] +
       r^2 Sin[θ]^2 Sin[ϕ]^2 Ψ*^(2,0,0)[r, θ, ϕ])) +
  ((Sin[θ] Ψ^(0,1,0)[r, θ, ϕ] - r Cos[θ] Ψ^(1,0,0)[r, θ, ϕ])^2 -
    Ψ[r, θ, ϕ] (Sin[2 θ] Ψ^(0,1,0)[r, θ, ϕ] + Sin[θ]^2 Ψ^(0,2,0)[r, θ, ϕ] +
       r (Sin[θ]^2 Ψ^(1,0,0)[r, θ, ϕ] - Sin[2 θ] Ψ^(1,1,0)[r, θ, ϕ] + r Cos[θ]^2 Ψ^(2,0,0)[r, θ, ϕ])))
  ((Sin[θ] Ψ*^(0,1,0)[r, θ, ϕ] - r Cos[θ] Ψ*^(1,0,0)[r, θ, ϕ])^2 -
    Ψ*[r, θ, ϕ] (Sin[2 θ] Ψ*^(0,1,0)[r, θ, ϕ] + Sin[θ]^2 Ψ*^(0,2,0)[r, θ, ϕ] +
       r (Sin[θ]^2 Ψ*^(1,0,0)[r, θ, ϕ] - Sin[2 θ] Ψ*^(1,1,0)[r, θ, ϕ] +
          r Cos[θ]^2 Ψ*^(2,0,0)[r, θ, ϕ])))
```

This can then be used for the analysis of the local entanglement in a hydrogen atom in Section 7.4.3.

List of Publications

• In press or submitted

1. Local Entanglement of Multidimensional Continuous-Variable Systems
   H.-C. Lin and A. J. Fisher; *Phys. Rev. A*, **78**, 012349, (2008)

2. Entanglement in General Two-mode Continuous-Variable States: Local Approach and Mapping to a Two-Qubit System
   H.-C. Lin and A. J. Fisher; *Phys. Rev. A*, **76**, 042320, (2007)

3. Configuration-Space Location of the Entanglement between Two Subsystems
   H.-C. Lin and A. J. Fisher; *Phys. Rev. A*, **75**, 032330, (2007)

Bibliography

[AB05] G. S. Agarwal and A. Biswas. Inseparability inequalities for higher order moments for bipartite systems. *New J. Phys.*, 7:211, 2005.

[ADMS95] Arvind, B. Dutta, N. Mukunda, and R. Simon. The real symplectic groups in quantum mechanics and optics. *Pramana*, 45:471, 1995.

[AEPW02] K. Audenaert, J. Eisert, M. B. Plenio, and R. F. Werner. Entanglement properties of the harmonic chain. *Phys. Rev. A*, 66:042327, 2002.

[APE03] K. Audenaert, M. B. Plenio, and J. Eisert. Entanglement cost under positive-partial-transpose-preserving operations. *Phys. Rev. Lett.*, 90:027901, 2003.

[ASI04] G. Adesso, A. Serafini, and F. Illuminati. Quantification and scaling of multipartite entanglement in continuous variable systems. *Phys. Rev. Lett.*, 93:220504, 2004.

[ASI06] G. Adesso, A. Serafini, and F. Illuminati. Multipartite entanglement in three-mode Gaussian states of continuous-variable systems: Quantification, sharing structure, and decoherence. *Phys. Rev. A*, 73:032345, 2006.

[AVM01] K. Audenaert, F. Verstraete, and B. De Moor. Variational characterizations of separability and entanglement of formation. *Phys. Rev. A*, 64:052304, 2001.

[BBC$^+$93] C. H. Bennett, G. Brassard, C. Crepeau, R. Jozsa, A. Peres, and W. K. Wootters. Teleporting an unknown quantum state via dual classical and einstein-podolsky-rosen channels. *Phys. Rev. Lett.*, 70:1895, 1993.

[BBP$^+$96] C. H. Bennett, G. Brassard, S. Popescu, B. Schumacher, J. A. Smolin, and W. K. Wootters. Purification of noisy entanglement and faithful teleportation via noisy channels. *Phys. Rev. Lett.*, 76:722, 1996.

[BBPS96] C. H. Bennett, H. J. Bernstein, S. Popescu, and B. Schumacher. Concentrating partial entanglement by local operations. *Phys. Rev. A*, 53:2046, 1996.

[BDF+99] C. H. Bennett, D. P. DiVincenzo, C. A. Fuchs, T. Mor, E. Rains, P. W. Shor, J. A. Smolin, and W. K. Wootters. Quantum nonlocality without entanglement. *Phys. Rev. A*, 59:1070, 1999.

[BDSW96] C. H. Bennett, D. P. DiVincenzo, J. A. Smolin, and W. K. Wootters. Mixed-state entanglement and quantum error correction. *Phys. Rev. A*, 54:3824, 1996.

[BP03] S. L. Braunstein and A. K. Pati. *Quantum Information Theory with Continuous Variables*. Kluwer Academic Press, Dordrecht, 2003.

[BR01] H. J. Briegel and R. Raussendorf. Persistent entanglement in arrays of interacting particles. *Phys. Rev. Lett.*, 86:910, 2001.

[BR04] A. Botero and B. Reznik. Spatial structures and localization of vacuum entanglement in the linear harmonic chain. *Phys. Rev. A*, 70:052329, 2004.

[BvL05] S. L. Braunstein and P. van Loock. Quantum information with continuous variables. *Rev. Mod. Phys.*, 77:531, 2005.

[CAF05] K. Chen, S. Albeverio, and S.-M. Fei. Concurrence of arbitrary dimensional bipartite quantum states. *Phys. Rev. Lett.*, 95:040504, 2005.

[CEPD06] M. Cramer, J. Eisert, M. B. Plenio, and J. Dreissig. An entanglement-area law for general bosonic harmonic lattice systems. *Phys. Rev. A*, 73:012309, 2006.

[CLP07] N. J. Cerf, G. Leuchs, and E. S. Polzik. *Quantum Information With Continuous Variables of Atoms and Light*. Imperial College Press, London, 2007.

[CW04] M. Christandl and A. Winter. "Squashed entanglement": An additive entanglement measure. *J. Math. Phys.*, 45:829, 2004.

[Deu85] D. Deutsch. Quantum theory, the church-turing principle and the universal quantum computer. *Proc. R. Soc. Lond. A*, 400:97, 1985.

[DGCZ00] L.-M. Duan, G. Giedke, J. I. Cirac, and P. Zoller. Inseparability criterion for continuous variable systems. *Phys. Rev. Lett.*, 84:2722, 2000.

[DHR02] M.J. Donald, M. Horodecki, and O. Rudolph. The uniqueness theorem for entanglement measures. *J. Math. Phys.*, 43:4252, 2002.

[EFP+00] J. Eisert, T. Felbinger, P. Papadopoulos, M. B. Plenio, and M. Wilkens. Classical information and distillable entanglement. *Phys. Rev. Lett.*, 84:1611, 2000.

[Eke91] A. K. Ekert. Quantum cryptography based on bell's theorem. *Phys. Rev. Lett.*, 67:661, 1991.

[EP99] J. Eisert and M. B. Plenio. A comparison of entanglement measures. *J. Mod. Optic.*, 46:145, 1999.

[EP02] J. Eisert and M. B. Plenio. Conditions for the local manipulation of Gaussian states. *Phys. Rev. Lett.*, 89:097901, 2002.

[EP03] J. Eisert and M. B. Plenio. Introduction to the basics of entanglement theory in continuous-variable systems. *Int. J. Quant. Inf.*, 1:479, 2003.

[ESP02a] J. Eisert, S. Scheel, and M.B. Plenio. Distilling Gaussian states with Gaussian operations is impossible. *Phys. Rev. Lett.*, 89:137903, 2002.

[ESP02b] J. Eisert, C. Simon, and M. B. Plenio. On the quantification of entanglement in infinite-dimensional quantum systems. *J. Phys. A*, 35:3911, 2002.

[Fiu02] J. Fiurasek. Gaussian transformations and distillation of entangled Gaussian states. *Phys. Rev. Lett.*, 89:137904, 2002.

[GC02] G. Giedke and J. I. Cirac. Characterization of Gaussian operations and distillation of Gaussian states. *Phys. Rev. A*, 66:032316, 2002.

[GDCZ01] G. Giedke, L.-M. Duan, J. I. Cirac, and P. Zoller. Distillability criterion for all bipartite Gaussian states. *Quant. Inf. Comp.*, 1:79, 2001.

[GECP03] G. Giedke, J. Eisert, J. I. Cirac, and M. B. Plenio. Entanglement transformations of pure Gaussian states. *Quant. Inf. Comp.*, 3:211, 2003.

[Git05] J. R. Gittings. *Quantifying Entanglement of Overlapping Indistinguishable Particles*. PhD thesis, University College London, 2005. (Unpublished).

[GKLC01] G. Giedke, B. Kraus, M. Lewenstein, and J. I. Cirac. Separability properties of three-mode Gaussian states. *Phys. Rev. A*, 64:052303, 2001.

[GWK+03] G. Giedke, M. M. Wolf, O. Kruger, R. F. Werner, and J. I. Cirac. Entanglement of formation for symmetric Gaussian states. *Phys. Rev. Lett.*, 91:107901, 2003.

[HAV06] L. Heaney, J. Anders, and V. Vedral. Spatial entanglement of a free bosonic field. *eprint quant-ph/0607069*, 2006.

[HHH96] R. Horodecki, P. Horodecki, and M. Horodecki. Quantum α-entropy inequalities: independent condition for local realism? *Phys. Lett. A*, 210:377, 1996.

[HHH98] M. Horodecki, P. Horodecki, and R. Horodecki. Mixed-state entanglement and distillation: Is there a "bound" entanglement in nature? *Phys. Rev. Lett.*, 80:5239, 1998.

[HHT01] P. M. Hayden, M. Horodecki, and B. M. Terhal. The asymptotic entanglement cost of preparing a quantum state. *J. Phys. A: Math. Gen.*, 34:6891, 2001.

[Hol82] A. S. Holevo. *Probabilistic and Statistical Aspects of Quantum Theory*. North-Holland, Amsterdam, 1982.

[Hor97] P. Horodecki. Separability criterion and inseparable mixed states with positive partial transposition. *Phys. Lett. A*, 232:333, 1997.

[HOSW84] M. Hillery, R. F. O'Connell, M.O. Scully, and E. P. Wigner. Distribution functions in physics: Fundamentals. *Phys. Rep.*, 106:12, 1984.

[HSS03] M. Horodecki, A. Sen, and U. Sen. Rates of asymptotic entanglement transformations for bipartite mixed states: Maximally entangled states are not special. *Phys. Rev. A*, 67:062314, 2003.

[HZ06a] M. Hillery and M. S. Zubairy. Entanglement conditions for two-mode states. *Phys. Rev. Lett.*, 96:050503, 2006.

[HZ06b] M. Hillery and M. S. Zubairy. Entanglement conditions for two-mode states: Applications. *Phys. Rev. A*, 74:032333, 2006.

[JK04] B. Q. Jin and V. E. Korepin. Quantum spin chain, Toeplitz determinants and the Fisher-Hartwig conjecture. *J. Stat. Phys.*, 116:79, 2004.

[JLL00] Y. J. Park J. Lee, M. S. Kim and S. Lee. Partial teleportation of entanglement in a noisy environment. *J. Mod. Opt.*, 47:2151, 2000.

[KC04] B. Kraus and J. I. Cirac. Discrete entanglement distribution with squeezed light. *Phys. Rev. Lett.*, 92:013602, 2004.

[KTSC06] A. Kitagawa, M. Takeoka, M. Sasaki, and A. Chefles. Entanglement evaluation of non-Gaussian states generated by photon subtraction from squeezed states. *Phys. Rev. A*, 73:042310, 2006.

[LF07a] H.-C. Lin and A. J. Fisher. Configuration-space location of the entanglement between two subsystems. *Phys. Rev. A*, 75:032330, 2007.

[LF07b] H.-C. Lin and A. J. Fisher. Entanglement in general two-mode continuous-variable states: Local approach and mapping to a two-qubit system. *Phys. Rev. A*, 76:042320, 2007.

[LF08] H.-C. Lin and A. J. Fisher. Local entanglement of multidimensional continuous-variable systems. *Phys. Rev. A*, 78:012349, 2008.

[LRV04] J. I. Latorre, E. Rico, and G. Vidal. Ground state entanglement in quantum spin chains. *Quantum Inf. Comput.*, 4:48, 2004.

[MBZ06] D. McHugh, V. Buzek, and M. Ziman. When non-Gaussian states are Gaussian: Generalization of nonseparability criterion for continuous variables. *Phys. Rev. A*, 74:050306(R), 2006.

[MD] M. A. Martin-Delgado. Entanglement and concurrence in the BCS state. *e-print quant-ph/0207026*.

[MG04] A. Miranowicz and A. Grudka. Ordering two-qubit states with concurrence and negativity. *Phys. Rev. A*, 70:032326, 2004.

[MPHH] A. Miranowicz, M. Piani, P. Horodecki, and R. Horodecki. Inseparability criteria based on matrices of moments.

[MV00] B. M.Terhal and K. G. H. Vollbrecht. Entanglement of formation for isotropic states. *Phys. Rev. Lett.*, 85:2625, 2000.

[NC00] M. A. Nielsen and I. L. Chuang. *Quantum Computation and Quantum Information*. Cambridge University Press, Cambridge, UK, 2000.

[Nie98] M. A. Nielsen. *Quantum Information Theory*. PhD thesis, University of New Mexico, 1998. (e-print quant-ph/0011036).

[NK06] H. Nha and J. Kim. Entanglement criteria via the uncertainty relations in su(2) and su(1,1) algebras: Detection of non-Gaussian entangled states. *Phys. Rev. A*, 74:012317, 2006.

[OAFF02] A. Osterloh, L. Amico, G. Falci, and R. Fazio. Scaling of entanglement close to a quantum phase transition. *Nature*, 416:608, 2002.

[ON02] T. J. Osborne and M. A. Nielsen. Entanglement in a simple quantum phase transition. *Phys. Rev. A*, 66:032110, 2002.

[OW01] K. M. O'Connor and W. K. Wootters. Entangled rings. *Phys. Rev. A*, 63:052302, 2001.

[PEDC05a] M. B. Plenio, J. Eisert, J. Dreissig, and M. Cramer. Entropy, entanglement, and area: Analytical results for harmonic lattice systems. *Phys.Rev.Lett.*, 94:060503, 2005.

[PEDC05b] M. B. Plenio, J. Eisert, J. Dreissig, and M. Cramer. Entropy, entanglement, and area: Analytical results for harmonic lattice systems. *Phys. Rev. Lett.*, 94:060503, 2005.

[Per95] A. Peres. *Quantum Theory: Concepts and Methods*. Kluwer Academic, Dordrecht, 1995.

[Per96] A. Peres. Separability criterion for density matrices. *Phys. Rev. Lett.*, 77:1413, 1996.

[PHE04] M. A. Plenio, J. Hartley, and J. Eisert. Dynamics and manipulation of entanglement in coupled harmonic systems with many degrees of freedom. *New J. Phys.*, 6:36, 2004.

[Ple05] M. B. Plenio. Logarithmic negativity: A full entanglement monotone that is not convex. *Phys. Rev. Lett.*, 95:090503, 2005.

[PR97] S. Popescu and D. Rohrlich. Thermodynamics and the measure of entanglement. *Phys. Rev. A*, 56:R3319, 1997.

[PSK+04] M. Paternostro, W. Son, M. S. Kim, G. Falci, and G. M. Palma. Dynamical entanglement transfer for quantum-information networks. *Phys. Rev. A*, 70:022320, 2004.

[PV07] M. B. Plenio and S. Virmani. An introduction to entanglement measures. *Quant. Inf. Comp.*, 7:1, 2007.

[Rai99] E.M. Rains. Rigorous treatment of distillable entanglement. *Phys. Rev. A*, 60:173, 1999.

[RR05] R. W. Rendell and A. K. Rajagopal. Entanglement of pure two-mode Gaussian states. *Phys. Rev. A*, 72:012330, 2005.

[Sch01] W. P. Schleich. *Quantum Optics in Phase Space*. Wiley-VCH, Weinheim, 2001.

[Ser06] A. Serafini. Multimode uncertainty relations and separability of continuous variable states. *Phys. Rev. Lett.*, 96:110402, 2006.

[Shi04] M. E. Shirokov. On entropic quantities related to the classical capacity of infinite dimensional quantum channels. *E-print quant-ph/0411091*, 2004.

[Sim00] R. Simon. Peres-Horodecki separability criterion for continuous variable systems. *Phys. Rev. Lett.*, 84:2726, 2000.

[SKLA02] W. Son, M. S. Kim, J. Lee, and D. Ahn. Entanglement transfer from continuous variables to qubits. *J. Mod. Optic.*, 49:1739, 2002.

[SMD94] R. Simon, N. Mukunda, and B. Dutta. Quantum-noise matrix for multimode systems: U(n) invariance, squeezing, and normal forms. *Phys. Rev. A*, 49:1567, 1994.

[SSM87] R. Simon, E. C. G. Sudarshan, and N. Mukunda. Gaussian-Wigner distributions in quantum mechanics and optics. *Phys. Rev. A*, 36:3868, 1987.

[SV05] E. Shchukin and W. Vogel. Inseparability criteria for continuous bipartite quantum states. *Phys. Rev. Lett.*, 95:230502, 2005.

[SV06] E. Shchukin and W. Vogel. Conditions for multipartite continuous-variable entanglement. *Phys. Rev. A*, 74:030302(R), 2006.

[VADM01] F. Verstraete, K. Audenaert, J. Dehaene, and B. De Moor. A comparison of the entanglement measures negativity and concurrence. *J. Phys. A*, 34:10327, 2001.

[VC01] G. Vidal and J. I. Cirac. Irreversibility in asymptotic manipulations of entanglement. *Phys. Rev. Lett.*, 86:5803, 2001.

[Ved03] V. Vedral. Entanglement in the second quantization formalism. *Central Eur. J. Phys.*, 1:289, 2003.

[Ved06] V. Vedral. *Introduction to quantum Information Science*. Oxford University Press, Oxford, 2006.

[Vid00] G. Vidal. Entanglement monotones. *J. Mod. Opt.*, 47:355, 2000.

[vLB00] P. van Loock and S. L. Braunstein. Multipartite entanglement for continuous variables: A quantum teleportation network. *Phys. Rev. Lett.*, 84:3482, 2000.

[VLRK03] G. Vidal, J. I. Latorre, E. Rico, and A. Kitaev. Entanglement in quantum critical phenomena. 90:227902, 2003.

[VP98] V. Vedral and M. B. Plenio. Entanglement measures and purification procedures. *Phys. Rev. A*, 57:1619, 1998.

[VPJK97] V. Vedral, M. B. Plenio, K. Jacobs, and P. L. Knight. Statistical inference, distinguishability of quantum states, and quantum entanglement. *Phys. Rev. A*, 56:4452, 1997.

[VPRK97] V. Vedral, M. B. Plenio, M. A. Rippin, and P. L. Knight. Quantifying entanglement. *Phys. Rev. Lett.*, 78:2275, 1997.

[VW01] K.G.H. Vollbrecht and R.F. Werner. Entanglement measures under symmetry. *Phys. Rev. A*, 64:062307, 2001.

[VW02] G. Vidal and R. F. Werner. Computable measure of entanglement. *Phys. Rev. A*, 65:032314, 2002.

[Wer89] R. F. Werner. Quantum states with Einstein-Podolsky-Rosen correlations admitting a hidden-variable model. *Phys. Rev. A*, 40:4277, 1989.

[WGC06] M. M. Wolf, G. Giedke, and J. I. Cirac. Extremality of Gaussian quantum states. *Phys. Rev. Lett.*, 96:080502, 2006.

[WGK+04] M. M. Wolf, G. Giedke, O. Kruger, R. F. Werner, and J. I. Cirac. Gaussian entanglement of formation. *Phys. Rev. A*, 69:052320, 2004.

[WM94] D.F. Walls and G. J. Milburn. *Quantum Optics*. Springer, Berlin, 1994.

[Woo98a] W. K. Wootters. Entanglement of formation of an arbitrary state of two qubits. *Phys. Rev. Lett.*, 80:2245, 1998.

[Woo98b] W. K. Wootters. Entanglement of formation of an arbitrary state of two qubits. *Phys. Rev. Lett.*, 80(10):2245–2248, Mar 1998.

[Woo98c] W. K. Wootters. Quantum entanglement as a quantifiable resource. *Phil. Trans. Roy. Soc. A*, 356:1717, 1998.

[Woo01] W. K. Wootters. Entanglement of formation and concurrence. *Quantum Inf. Comput.*, 1:27, 2001.

[Woo02a] W. K. Wootters. Entangled chains. *Contemporary Mathematics*, 305:299, 2002.

[Woo02b] W. K. Wootters. Parallel transport in an entangled ring. *J. Math. Phys*, 43:4307, 2002.

[WW01] R. F. Werner and M. M. Wolf. Bound entangled Gaussian states. *Phys. Rev. Lett.*, 86:3658, 2001.

[WZ82] W. K. Wootters and W. H. Zurek. A single quantum cannot be cloned. *Nature*, 299:802, 1982.

[Zet01] N. Zettili. *Quantum Mechanics: Concepts and Applications*. John Wiley, 2001.

[ZHSL98] K. Zyczkowski, P. Horodecki, A. Sanpera, and M. Lewenstein. Volume of the set of separable states. *Phys. Rev. A*, 58:883, 1998.

[ZW02] P. Zanardi and X. Wang. Fermionic entanglement in itinerant systems. *J. Phys. A*, 35:7947, 2002.